

NASA TECHNICAL NOTE



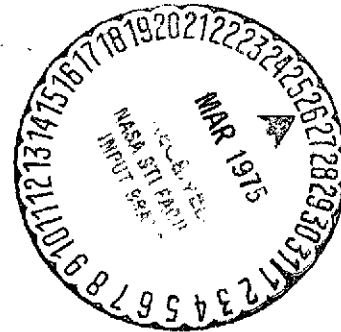
NASA TN D-7863

NASA TN D-7863

(NASA-TN-D-7863) WIND TUNNEL INVESTIGATION
OF AERODYNAMIC LOADS ON A LARGE-SCALE
EXTERNALLY BLOWN FLAP MODEL AND COMPARISON
WITH THEORY (NASA) 99 p HC \$4.75 CSCL 01A

N75-17294

Unclas
H1/02 12354



WIND-TUNNEL INVESTIGATION OF
AERODYNAMIC LOADS ON A LARGE-SCALE
EXTERNALLY BLOWN FLAP MODEL
AND COMPARISON WITH THEORY

Boyd Perry III and George C. Greene

*Langley Research Center
Hampton, Va. 23665*



1. Report No. NASA TN D-7863		2. Government Accession No.		3. Recipient's Catalog No.	
4. Title and Subtitle WIND-TUNNEL INVESTIGATION OF AERODYNAMIC LOADS ON A LARGE-SCALE EXTERNALLY BLOWN FLAP MODEL AND COMPARISON WITH THEORY				5. Report Date March 1975	
				6. Performing Organization Code	
7. Author(s) Boyd Perry III and George C. Greene				8. Performing Organization Report No. L-9854	
				10. Work Unit No. 505-10-41-06	
9. Performing Organization Name and Address NASA Langley Research Center Hampton, Va. 23665				11. Contract or Grant No.	
				13. Type of Report and Period Covered Technical Note	
12. Sponsoring Agency Name and Address National Aeronautics and Space Administration Washington, D.C. 20546				14. Sponsoring Agency Code	
15. Supplementary Notes					
16. Abstract <p>This report presents results from a wind-tunnel investigation of a large-scale externally blown flap model. The model was equipped with four turbofan engines, a triple-slotted flap system, and a T-tail. The wing had a quarter-chord sweep of 25°, an aspect ratio of 7.28, and a taper ratio of 0.4. Aerodynamic loads and load distributions were determined from a total of 564 static pressure orifices located on the upper and lower surfaces of the slat, wing, and flaps. Loads are presented for variations of angle of attack, engine thrust setting, and flap deflection angle. In addition, the experimental results are compared with analytical results calculated by using a potential flow analysis.</p>					
17. Key Words (Suggested by Author(s)) Externally blown flap Propulsive lift STOL			18. Distribution Statement Unclassified - Unlimited Subject Category 02 Aerodynamics		
19. Security Classif. (of this report) Unclassified		20. Security Classif. (of this page) Unclassified		22. Price* \$4.75	
				21. No. of Pages 97	

WIND-TUNNEL INVESTIGATION OF AERODYNAMIC LOADS
ON A LARGE-SCALE EXTERNALLY BLOWN FLAP MODEL
AND COMPARISON WITH THEORY

Boyd Perry III and George C. Greene
Langley Research Center

SUMMARY

This report presents results from a wind-tunnel investigation of a large-scale externally blown flap model. The model was equipped with four turbofan engines, a triple-slotted flap system, and a T-tail. The wing had a quarter-chord sweep of 25° , an aspect ratio of 7.28, and a taper ratio of 0.4. Aerodynamic loads and load distributions were determined from a total of 564 static pressure orifices located on the upper and lower surfaces of the slat, wing, and flaps. Loads are presented for variations of angle of attack, engine thrust setting, and flap deflection angle. In addition, the experimental results are compared with analytical results calculated by using a potential flow analysis.

INTRODUCTION

The objective of short take-off and landing (STOL) aircraft technology is to provide good cruise performance that can be combined with the ability to take off and land on short airstrips. In order to keep the high wing loading necessary for good cruise performance without losing the ability to take off and land in short distances, a lift system which can produce very large lift coefficients is necessary. The externally blown jet-augmented flap (EBF) is one promising concept for achieving the high lift coefficients necessary for STOL operation. In this concept the jet efflux from pod-mounted engines is made to impinge on a large, highly deflected, multiple-slotted flap system. A large amount of lift is generated as the engine wake is deflected by the flap system. The EBF concept is not new (see ref. 1); however, the high exhaust temperatures of early jet engines made its application impractical for commercial aircraft. The development of the high-bypass-ratio turbofan engine with its relatively cool exhaust has revived interest in the EBF concept for STOL aircraft application.

The performance and stability and control aspects of the EBF concept have been investigated extensively. (See refs. 2 to 15 for example.) These results have usually been presented as force and moment coefficients over the range of variables investigated.

These variables include wing sweep and aspect ratio; wing leading-edge treatment; spanwise engine location and engine incidence with respect to the wing; flap span and the number of flap elements; and Reynolds number. Relatively little information has been published which presents the details of the wing and flap load distributions. (See refs. 14, 15, and 16.) The models tested to date have generally been small scale and equipped with compressed-air simulated engines. Such models are satisfactory for determining the gross force and moment characteristics of an EBF configuration, but larger scale models are desirable for measuring detailed pressure distributions at a large number of stations.

The development of analytical methods for predicting EBF performance and loads has closely followed the experimental work; however, these efforts have been hampered somewhat by the lack of detailed experimental data. Lopez and Shen (ref. 17) applied jet flap theory to the EBF with good results by using empirically determined momentum coefficients, turning angles, and spreading factors for the engine wake. Shollenberger (ref. 18) presented a fairly sophisticated method to model a powered-lift configuration which does not require empirical data; however, no results were presented for realistic configurations. Dillenius and others (ref. 19) used a less sophisticated method to model an EBF configuration, again without the need for empirically determined inputs.

This report presents the results of a detailed load investigation on a large-scale EBF model. Wing and flap loads data are presented for parametric variations in angle of attack, flap deflection angle, and engine thrust. In addition, calculated results based on the method in reference 19 are compared with the measured data.

SYMBOLS

Values are given in both SI and U.S. Customary Units. The measurements and calculations were made in U.S. Customary Units.

b span, m (ft)

C_L total lift coefficient of lift system, $\frac{L}{q_\infty S}$

C_p pressure coefficient, $\frac{p - p_\infty}{q_\infty}$

C_μ thrust coefficient, $\frac{T}{q_\infty S}$

c chord, m (ft)

\bar{c}	mean aerodynamic chord, m (ft)
c_l	section lift coefficient, $\frac{l}{q_\infty \bar{c}}$
c_n	section normal-force coefficient, $\int_0^1 \Delta C_p d\left(\frac{x}{\bar{c}}\right)$
L	total lift force of lift system, N (lb)
l	section lift force, N/m (lb/ft)
n	section normal force, N/m (lb/ft)
p	static pressure, N/m ² (lb/ft ²)
p_∞	free-stream static pressure, N/m ² (lb/ft ²)
q_∞	free-stream dynamic pressure, N/m ² (lb/ft ²)
S	wing planform area, m ² (ft ²)
T	gross thrust, N (lb)
x	chordwise coordinate, positive from leading edge to trailing edge, m (ft)
y	spanwise coordinate, measured from center line, m (ft)
\hat{y}	nondimensional spanwise coordinate, $\frac{y}{b/2}$
α	angle of attack, deg
α_u	uncorrected angle of attack, deg
δ	flap deflection angle with respect to wing chord plane, deg

Subscripts:

i	flap number ($i = 1, 2, 3$) (see fig. 3)
id	idealized flap
t	horizontal tail
v	vertical tail
w	wing

Abbreviations:

EBF	externally blown flap
LS	lower surface
STOL	short take-off and landing
US	upper surface

APPARATUS

Model

Figure 1 shows the 11.6-m (38-ft) wing span model mounted in the NASA Ames 12.2- by 24.4-m (40- by 80-ft) Full-Scale Wind Tunnel. The model was equipped with four JT 15D-1 turbofan engines with a nominal bypass ratio of 3.3. Engine spacing and other dimensional data are presented in the three-view drawing in figure 2. The wing was swept back 25° at the quarter-chord line and was equipped with leading-edge slats and full-span, triple-slotted, trailing-edge flaps. The deflection angle of the leading-edge slat was constant at 50° leading edge down. The deflection angles of the flaps were variable. Deflection angles of 15° , 35° , and 55° for the first, second, and third flaps represented a typical landing configuration. Deflection angles of 0° , 20° , and 40° represented a typical take-off configuration. The wing had an aspect ratio of 7.28 and a taper ratio of 0.4.

Figure 3 presents the dimensions of the slat-wing-flap system at an arbitrary span station in terms of the local wing chord and defines the individual airfoil sections. Figure 4 shows the positions of the jet engines and wing-flap system at span stations corre-

sponding to the engine center lines (nondimensional semispan stations at $\hat{y} = 0.256$ and 0.420).

Instrumentation

The slat, wing, and flaps were each instrumented with 10 spanwise stations of static-pressure orifices as shown in figure 5. Note that pressure-station designations and semispan locations are given at the top of the figure. There were 564 pressure orifices in all: 54 on the leading-edge slat, 150 on the wing, and 120 on each of the three flaps. There were variable numbers of orifices in each row. Table I shows the chord-wise position of each orifice on the upper and lower surfaces of the slat, wing, and flaps.

Static-pressure data were measured with a 48-port electrically actuated pressure scanning valve. Table II shows the scanning valve (transducer) pressure ranges.

Wind Tunnel

The tests were conducted in the NASA Ames 12.2- by 24.4-m (40- by 80-ft) Full-Scale Wind Tunnel. Details of the wind tunnel, wind-tunnel instrumentation, and model installation are given in reference 3.

EXPERIMENTAL DATA

Static-pressure data are presented in pressure-coefficient form and are listed in table III for all test conditions investigated in the paper. Static-pressure data from the wing and leading-edge slat were not available for the test conditions corresponding to part (h) of table III.

Section normal-force coefficients were calculated from the pressure-coefficient data in the following manner: At each spanwise station for all lifting surfaces, the pressure coefficients (upper and lower) were plotted as a function of nondimensional local chord. Curves were faired through the plotted points and the curves were integrated graphically to obtain the section normal-force coefficients.

Figure 6 contains sample plots of C_p as a function of x/c and sample curve fairings at stations $\hat{y} = 0.420$ and $\hat{y} = 0.850$ for $\alpha = 7^\circ$, $C_{\mu} = 4.0$, and $\delta = 15^\circ/35^\circ/55^\circ$. This notation for flap deflection angle represents the deflection angles of the first, second, and third flaps, respectively. Nondimensional semispan station $\hat{y} = 0.420$ is along the center line of the outboard engine and station $\hat{y} = 0.850$ is near the tip and well removed from the influence of the engines.

In order to compare the experimental data with the analysis, which will be done in a subsequent section, the form of the experimental data was changed. The experimental

data were transformed from section normal-force coefficients to section lift coefficients. To make the transformation it was assumed that the normal force acting on each lifting surface was equal to the total force acting on that surface. The section lift coefficients for the wing and flaps transformed in this manner are

$$c_{l_w} = c_{n_w} \cos \alpha$$

$$c_{l_i} = c_{n_i} \cos (\alpha + \delta_i)$$

where i represents either flap 1, flap 2, or flap 3.

To obtain the lift coefficient of the slat-wing-flap system, a spanwise integration was necessary. Section lift coefficients were multiplied by free-stream dynamic pressure q_∞ and the local chord c to yield a spanwise lift distribution. The spanwise lift distribution was integrated along the semispan, the result multiplied by 2 (to include the contributions from both semispans), and then divided by the product of q_∞ and wing planform area S

$$C_L = \frac{2}{q_\infty S} \left[\int_0^{b/2} c_{l_w} c_w(y) q_\infty dy + \sum_{i=1}^3 \int_0^{b/2} c_{l_i} c_i(y) q_\infty dy \right]$$

To present the data in a form consistent with reference 3, the correction for wall interference in the wind tunnel described in that report was applied. The correction involves adjusting the angle of attack as follows:

$$\alpha = \alpha_u + 0.4175 C_L$$

ANALYSIS

Several methods (refs. 17 to 19) have been developed for analyzing the aerodynamic characteristics of powered-lift STOL aircraft. These methods vary greatly in level of sophistication and, therefore, in potential application. One relatively unsophisticated method (ref. 19) is publicly available as a well-documented computer program. For a given configuration, only geometry and engine static thrust information are required as program inputs. Therefore, providing it yields reasonably good results, this program would have a wide range of applications in preliminary design. The availability of detailed data on a large-scale EBF model provided the opportunity to assess the ability of the program to predict the distribution as well as total lift on a realistic powered-lift configuration.

In the method described in reference 19, potential flow models are used to represent the wing-flap lifting surfaces and the engine wake. The lifting surfaces are represented by a horseshoe vortex lattice and the engine wake by an expanding vortex ring model. A flow chart of the program is shown in figure 7.

The program predicts the interference between the lifting surfaces and the engine wakes and iterates to arrive at the predicted longitudinal aerodynamic characteristics. The influence of the wing-flap on the jet wake is the deflection of the wake center line. Thus, the iteration locates the predicted wake center-line position. The vortex-lattice lifting-surface program is configured to calculate the induced velocity field at specified points near the lifting surfaces. The induced velocities are used to estimate the deflection of the engine wake center line for input in the engine wake program. The engine wake program is then used to calculate interference velocities at the vortex-lattice control points for input in the lifting surface program. The procedure is repeated until the engine wake center-line position remains essentially constant.

The vortex-lattice portion of the program models a wing with multiple flaps as two lifting surfaces: a wing and a single highly cambered flap. For this study, each lifting surface is partitioned into trapezoidal panels as shown in figure 8. The model used in this investigation was partitioned into 5 chordwise by 20 spanwise panels on the wing and the same arrangement of panels on the flap. The paneling on both the wing and the flap is denser (more panels per unit area) behind the engines than it is inboard and outboard of the engines. This arrangement permits a more accurate definition of the spanwise lift distributions in the regions behind the engines.

In addition to the preceding procedure, the engine wake portion of the program was run with two variations on the suggested procedure to investigate the effects of parameters in the engine wake model. The procedure of reference 19 assumes that the engine wake remains circular and spreads as a circular incompressible turbulent jet in the absence of the lifting surfaces. The engine wake is allowed to deflect (but not deform) due to the presence of the lifting surfaces; however, the equations of reference 19 limit the wake deflection to small angles. This limitation causes the wake to pass through, rather than under, the highly deflected flap used in this study. The first alternate procedure consists of changing the effective diameter and spreading rate to approximate better the actual engine wake measurements presented in reference 3. The second alternate procedure goes one step further and removes the small angle deflection limitation. This change allows large deflections of the engine wake center line so that the wake passes under, rather than through, the flap.

RESULTS AND DISCUSSION

This section of the paper will be presented in two parts: a presentation of the experimental data and a comparison of the data with analytical results.

Experimental Data

Figures 9 and 10 contain plots of section normal-force coefficient as a function of nondimensional semispan position for the slat, wing, and flaps and figure 11 contains the same information for the flaps only. Figure 9 presents data for variations in angle of attack. Figure 10 presents data for variations in thrust coefficient. Figures 11 and 12 present data for variations in flap deflection angles. The tick marks on the horizontal axis in figures 9 to 12 correspond to the locations of the engine center line.

Before discussing the figures individually, a general remark should be made. The most striking features of the curves are the dips in the plots of c_n as a function of \hat{y} for the slat and the peaks in the plots of c_n as a function of \hat{y} for the flaps. These features are due to the presence of the engines and they occur about the engine center lines. The dips in the plots of c_n as a function of \hat{y} for the slat occur because there are breaks in slat as shown in figure 5. The peaks in the flap curves occur because the high velocity jet exhaust impinges on the flap system directly behind the engines.

Angle-of-attack variation. - Figures 9(a) to 9(e) contain plots of section normal-force coefficient as a function of nondimensional semispan position for the slat, wing, and flaps. The thrust coefficient C_μ was 4.0, the flap deflection angles were $15^\circ/35^\circ/55^\circ$, and the slat deflection angle was 50° . The three curves correspond to angles of attack of 6.5° , 18.5° , and 26.5° .

The normal-force coefficients (or more simply, the loads) on the leading-edge slat (fig. 9(a)) increase, as expected, with angle of attack as do the wing loads near the tip (fig. 9(b)). Because the slat and outboard portion of the wing were fairly well removed from the influence of the engine exhaust, they behaved like typical aerodynamic surfaces with variation in angle of attack. However, the flap loads shown in figures 9(c) to 9(e) do not show this trend. Although there are small differences in the spanwise flap loads with variations in angle of attack (i.e., changes in c_n near the tip on the order of 2 or 3 out of 50), the major contribution to flap loads was the engine exhaust. Peak normal-force coefficients for the flaps behind the engines are on the order of 50. Keep in mind when comparing section normal-force coefficients for different flap elements that the definition of section normal-force coefficient contains the local chord in the denominator. Thus one flap with a larger normal-force coefficient than another flap does not necessarily have a larger section normal force.

Power setting variation.- Figures 10(a) to 10(e) contain plots of section normal-force coefficient as a function of nondimensional semispan position for the slat, wing, and flaps. The uncorrected angle of attack was 16° , the flap deflection angles were $15^\circ/35^\circ/55^\circ$, and the slat deflection angle was 50° . The three curves correspond to thrust coefficients C_μ of 0, 2.2, and 4.0. Uncorrected angles of attack are used in figure 10 because identical corrected angles of attack for the three thrust coefficients do not exist.

The loads on each lifting surface increased with increasing thrust coefficient. The large flap loads (figs. 10(c) to 10(e)) resulted from the higher velocity exhaust impinging on the flap lower surfaces. Peak power-on flap loads were approximately an order of magnitude larger than both the power-off loads and the loads outboard near the tip. For the first, second, and third flaps the peak power-on loads are factors of 14, 30, and 40 larger than the power-off loads.

Flap deflection angle variation.- Figures 11(a) to 11(c) contain plots of section normal-force coefficient as a function of nondimensional semispan position for each of the three flaps. The corresponding data for the slat and wing are not available. The uncorrected angle of attack was 16° , the slat deflection angle was 50° , and C_μ was 4.0. Uncorrected angles of attack are used in figure 11 because identical corrected angles of attack for the two flap settings do not exist. The two curves correspond to flap deflection angles of $0^\circ/20^\circ/40^\circ$ and $15^\circ/35^\circ/55^\circ$.

The data indicate that, for all three flaps, the loads are higher at the higher deflection angles. Again for the take-off configuration ($\delta = 0^\circ/20^\circ/40^\circ$), the peak loads on the second and third flaps are about 2 to 3 times as large as the peak loads on the first flap. Since the first flap in the take-off configuration is not deflected ($\delta_1 = 0^\circ$), it acted essentially like an extension of the wing. Except for peaks behind the engines, the first-flap loads (fig. 11(a)) for the take-off configuration were of the same order as the wing loads (fig. 9(b)) at the same thrust setting.

Flap loads.- Figure 12 presents the information given in figure 11 in a different manner. Figure 11 compared the normal-force coefficients on flap 1, flap 2, and flap 3 for changes in flap deflection angle. Figure 12(a) compares the normal forces on flap 1 with the normal forces on flaps 2 and 3 for the landing configuration. Figure 12(b) presents similar data for the take-off configuration. The test conditions were $C_\mu = 4.0$, $\alpha = 19.0^\circ$ for the landing configuration, and $\alpha = 18.0^\circ$ for the take-off configuration.

From figure 12(a) the first and second flaps experience the highest loads near the tip and it appears that the same trend would exist in figure 12(b). Typical values for first and second flap loads in this region are approximately 300 N/m (20 lb/ft) and for the third flap 150 N/m (10 lb/ft). Examining chordwise pressure-distribution data

revealed that the high incidence angle of the third flap with respect to the flow resulted in flow separation and therefore lower loads. The second and third flap experienced loads 3 to 5 times as large as loads on the first flap in the regions of exhaust impingement. The third flap experienced the highest loads with a maximum peak load of over 6000 N/m (425 lb/ft) behind the outboard engine for the landing configuration.

Lift comparisons. - Comparisons of the lift curves from the present study and from reference 3 are shown in figure 13. The circle symbols represent the total lift coefficients of the wing-flap lift system from the pressure-coefficient data. The diamond symbols represent the total lift of the entire wind-tunnel model (tail off) from reference 3. In order to compare one configuration with the other, additional components had to be added to the wing-flap lift coefficients obtained in the present study. These components are as follows: The contribution from the slat; the contributions from the fuselage and the nacelles; and the contribution of engine thrust in the lift direction. The slat contribution was obtained from pressure data presented in this report. The contributions from the fuselage and nacelles were calculated by using slender-body theory (ref. 20). Aerodynamic interference effects were not taken into account. The contribution from engine thrust was calculated by taking the component of engine thrust in the lift direction. When these components are added to the lift coefficients of the wing-flap system, the resulting data (square symbols in fig. 13) are consistent with the data of reference 3. In fact, they are within 5 percent of each other.

A result which is indicated from the information presented in figure 13 is that the wing and flap contribute less and less to the total lift as angle of attack increases. Fuselage and nacelle lift and the component of engine thrust in the lift direction contribute a larger portion to the total lift at the high angles of attack.

Analytical Results and Comparisons

The analytical results obtained by using the procedure described in reference 19 and two modifications to that procedure are presented in this section and compared with the experimental data. The alternate procedures were described in the "Analysis" section of the paper and will be briefly outlined here: In alternate procedure 1, data from reference 3 were used to improve the engine wake calculation in the method of reference 19. In alternate procedure 2, engine wake data were used and, in addition, the small angle limitation was removed from the engine wake center-line equations to allow the engine wake center line to pass under, rather than through, the flap system. The results presented in reference 19 were based on one iteration of the program. In the present study, additional iterations were attempted to see if the solution had converged. After four iterations the solution using the procedure of reference 19 had not converged. For consistency the alternate procedures were each run for four iterations; however, the

fourth iteration proved unnecessary for alternate procedure 2 which converged very rapidly.

For each procedure the following figures will be presented: a typical engine wake center-line variation for each iteration, comparison of the distributions of the experimental and analytical spanwise section lift coefficients, and comparison of the experimental and analytical lift curves. The section and total lift coefficients, both experimental and analytical, are based on aerodynamic contributions from the wing and flaps only.

The analytical and experimental comparisons are presented for two values of thrust coefficient ($C_{\mu} = 2.2$ and 4.0) and three angles of attack (nominally, $\alpha_u = 4^\circ$, 16° , and 24°). A thrust coefficient of 4.0 corresponds to a relatively high engine power setting which, for the landing flap configuration, might be experienced during an aborted landing approach. A thrust coefficient of 2.2 represents a more typical approach power setting.

The analytical results were calculated at angles of attack of 4° , 16° , and 24° , which correspond to the uncorrected experimental angles of attack. The corrected experimental angles of attack are each approximately 2° higher. Because the spanwise load distribution was relatively insensitive to angle of attack, it was assumed that the experimental results could be compared directly with the results calculated at the uncorrected angles of attack.

Basic procedure. - The results of the analysis using the method of reference 19 are shown in figures 14 to 16. Figure 14 shows a typical variation of an engine wake center-line position for four iterations of the program. Notice that the center line "passes through" the flap element for all iterations.

The comparison of analytical and experimental total lift coefficients as a function of angle of attack is shown in figure 15. The comparison at the lowest angle of attack is within about 10 percent, but gets progressively worse with increasing angle of attack. Although the changes in the wake center-line position from iteration to iteration were small, the spanwise lift distribution and the total lift changed as much as 10 percent. The reason for this large effect on the predicted loads is the following: the influence of the ring vortices representing the engine wake on a wing or flap control point varies inversely with distance. When the engine wake passes through a lifting surface, as it does in the basic procedure, a number of control points are either within or very close to the engine wake. Small changes in the engine wake position can therefore result in relatively large changes in the distance between some of the control points and the engine wake. The resulting local loading changes may be completely out of proportion to the wake position change.

Figure 16 contains comparison of the experimental and analytical spanwise variations of section lift coefficient. For both thrust settings and all angles of attack, the basic procedure overpredicted the loads on the wing by a factor of about 3 and underpredicted the peak loads on the flap by a factor of about 3. However, there was good agreement in predicting the wing distribution inboard and outboard of the engines and, although underpredicted, the peak flap loads occurred at the correct spanwise positions. This underprediction occurs, at least partially, because the wake spreading with these engines is significantly different than that predicted for an incompressible, turbulent jet.

Alternate procedure 1. - Figure 17 shows a typical variation of an engine wake center-line position for four iterations. As in the basic procedure, the center line "passes through" the flap.

A comparison of the analytical and experimental lift curves for $C_{\mu} = 4.0$ is presented in figure 18. The experimental and analytical results agree within 10 to 15 percent except at high angles of attack where flow separation reduces the experimental lift coefficient. The lift-curve slope appears to be overpredicted even at low angles of attack, however, additional data would be necessary to quantify the comparison.

Figure 19 contains comparisons of experimental and analytical spanwise variations of section lift coefficient. For both the wing and the flap the analytical spanwise distributions agree reasonably well with the experimentally determined distributions except at the highest angle of attack. By making the engine wake smaller in diameter, the analytically predicted peak loads on the wing have been eliminated. By creating in the engine wake a higher velocity (the result of making it smaller while conserving momentum), the flap loads have the proper magnitude and spanwise distribution.

Alternate procedure 2. - Figure 20 shows a typical variation of an engine wake center-line position for three iterations. Removing the small angle approximation from the equations for the engine wake center line allowed the center line to pass under the flap. The points on the center line which are parallel to the flap are approximately one radius away from the flap. The total lift curves presented in figure 21 show that this procedure consistently underpredicts the total wing and flap lift. With the engine wake passing beneath the flap, very little of the wake momentum is impressed on the flap system. The difference between the experimental and analytical lift coefficients can be approximated by $\Delta C_L = C_{\mu} \sin \delta_{id}$ which represents the wake reaction force. The spanwise lift distributions shown in figure 22 indicate that the underprediction of total lift results from underpredicting both wing and flap lift.

CONCLUDING REMARKS

The results of a wind-tunnel investigation of the aerodynamic loads and load distributions on a large-scale EBF model have been presented. The experimental results indicated high local loads exist where the engine exhaust impinges on the flap system. The magnitude of these loads is highly dependent on the engine thrust level and flap deflection angle. Angle-of-attack effects are relatively small. The peak power-on loads on the flap system are about an order of magnitude greater than the power-off loads.

The experimental data were compared with analytical results based on the analysis procedure described in NASA CR-2358 (ref. 19). This procedure overpredicted the wing loading and underpredicted the flap loading, primarily because the engine wake was not adequately represented. An alternate procedure, based on engine wake measurements, which used a smaller radius, higher velocity (constant momentum) wake gave lift coefficients within 10 to 15 percent of the experimental data. In both of these mathematical models, the engine wake center line always passes through the flap system. In each case the loading was sensitive to the position of the engine wake. To ease the sensitivity to wake position, a third procedure, also based on experimental wake data, was tried which allowed the engine wake center line to pass beneath the flaps. This resulted in very little wake momentum being impressed on the flap system and a consistent underprediction of the lift.

It was found that empirical adjustments in the engine wake calculation were required in any modification to the basic procedure for predicting the detailed loadings. With proper wake modeling the procedure gives reasonably good results and could be a useful tool for preliminary design of STOL aircraft structures. Therefore it is believed that improvements are warranted in the engine wake calculation procedure.

Langley Research Center,
National Aeronautics and Space Administration,
Hampton, Va., January 16, 1975.

REFERENCES

1. Campbell, John P.; and Johnson, Joseph L., Jr.: Wind-Tunnel Investigation of an External-Flow Jet-Augmented Slotted Flap Suitable for Application to Airplanes With Pod-Mounted Jet Engines. NACA TN 3898, 1956.
2. Hughes, Donald L.: Pressures and Temperatures on the Lower Surfaces of an Externally Blown Flap System During Full-Scale Ground Tests. NASA TN D-7138, 1973.
3. Aoyagi, Kiyoshi; Falarski, Michael D.; and Koenig, David G.: Wind-Tunnel Investigation of a Large-Scale 25° Swept-Wing Jet Transport Model With an External Blowing Triple-Slotted Flap. NASA TM X-62197, 1973.
4. Aoyagi, Kiyoshi; Hall, Leo P.; and Falarski, Michael D.: Wind-Tunnel Investigation of a Large-Scale 35° Swept-Wing Jet Transport Model With an External Blowing Triple-Slotted Flap. NASA TM X-2600, 1972.
5. Perry, D. H. (With appendix by D. N. Foster): A Review of Some Published Data on the External-Flow Jet-Augmented Flap. Tech. Rep. 70240, British R.A.E., Sept. 1970.
6. Roe, Marshall H.: Air Force STOL Tactical Aircraft Investigation: Evaluation of Externally Blown Flaps. [Preprint] 730914, Soc. Automot. Eng., Oct. 1973.
7. Heald, Ervin R.: External Blowing Flap Technology on the USAF/McDonnell Douglas YC-15 (AMST) Program. [Preprint] 730915, Soc. Automot. Eng., Oct. 1973.
8. Vogler, Raymond D.: Wind-Tunnel Investigation of a Four-Engine Externally Blowing Jet-Flap STOL Airplane Model. NASA TN D-7034, 1970.
9. Freeman, Delma C., Jr.; Parlett, Lysle P.; and Henderson, Robert L.: Wind-Tunnel Investigation of a Jet Transport Airplane Configuration With an External-Flow Jet Flap and Inboard Pod-Mounted Engines. NASA TN D-7004, 1970.
10. Smith, Charles C., Jr.: Effect of Engine Position and High-Lift Devices on Aerodynamic Characteristics of an External-Flow Jet-Flap STOL Model. NASA TN D-6222, 1971.
11. Parlett, Lysle P.; Smith, Charles C., Jr.; and Megrail, James L.: Wind-Tunnel Investigation of Effects of Variations in Reynolds Number and Leading-Edge Treatment on the Aerodynamic Characteristics of an Externally Blown Jet-Flap Configuration. NASA TN D-7194, 1973.
12. Parlett, Lysle P.; and Shivers, James P.: Wind-Tunnel Investigation of an STOL Aircraft Configuration Equipped With an External-Flow Jet Flap. NASA TN D-5364, 1969.

13. Parlett, Lysle P.; Freeman, Delma C., Jr.; and Smith, Charles C., Jr.: Wind-Tunnel Investigation of a Jet Transport Airplane Configuration With High Thrust-Weight Ratio and an External-Flow Jet Flap. NASA TN D-6058, 1970.
14. Smith, Charles C., Jr.: Effect of Wing Aspect Ratio and Flap Span on Aerodynamic Characteristics of an Externally Blown Jet-Flap STOL Model. NASA TN D-7205, 1973.
15. Wickens, R. H.: Lifting Characteristics and Spanwise Aerodynamic Load Distribution of an External Flow Jet Flap. Canadian Aeronaut. & Space J., vol. 18, no. 9, Nov. 1972, pp. 291-293.
16. Greene, George C.; and Perry, Boyd, III: Aerodynamic Loads Measurements on Externally Blown Flap STOL Models. STOL Technology, NASA SP-320, 1972, pp. 121-130.
17. Lopez, M. L.; and Shen, C. C.: Recent Developments in Jet Flap Theory and Its Application to STOL Aerodynamic Analysis. AIAA Paper No. 71-578, June 1971.
18. Shollenberger, C. A.: A Three-Dimensional Wing/Jet Interaction Analysis Including Jet Distortion Influences. AIAA Paper No. 73-655, July 1973.
19. Dillenius, Marnix F. E.; Mendenhall, Michael R.; and Spangler, S. B.: Calculation of the Longitudinal Aerodynamic Characteristics of STOL Aircraft With Externally-Blown Jet-Augmented Flaps. NASA CR-2358, 1974.
20. Anon.: USAF Stability and Control Datcom. Contracts AF 33(616)-6460, AF 33(615)-1605, F33615-67-C-1156, F33615-68-C-1260, and F33615-70-C-1087, McDonnell Douglas Corp., Oct. 1960. (Revised Sept. 1970.)

TABLE I. - LOCAL CHORDWISE LOCATIONS OF STATIC-PRESSURE ORIFICES

[Stations refer to fig. 5]

Leading-edge slat, stations 1, 4, 5, 8, 9, 10 -		Wing, all stations -		Flaps			
				Stations 1, 5, 9, 10 -		Stations 2, 3, 4, 6, 7, 8 -	
US	LS	US	LS	US	LS	US	LS
0.01c	0.03c	0.01c	0.03c	0.01c	0.03c	0.01c	0.03c
.10c	.15c	.04c	.08c	.10c	.15c	.04c	.08c
.25c	.35c	.10c	.15c	.25c	.35c	.10c	.15c
.45c	.70c	.17c	.35c	.45c	.70c	.17c	.35c
.75c		.25c	.50c	.75c		.25c	.70c
		.35c	.70c			.35c	
		.45c				.45c	
		.60c				.60c	
		.70c				.75c	

TABLE II.- RANGES OF STATIC-PRESSURE TRANSDUCERS

[Stations refer to fig. 5]

Component	US		LS	
	N/m ²	psi	N/m ²	psi
Leading-edge slat, all stations	±5.17	±0.75	±1.72	±0.25
Wing, all stations	±5.17	±.75	±1.72	±.25
Flaps, stations 1 to 8	±34.47	±5.00	±17.24	±2.50
Flaps, stations 9 and 10	±6.89	±1.00	±6.89	±1.00

TABLE III. - PRESSURE COEFFICIENTS ON SLAT, WING,
AND FLAPS

(a) $C_{\mu} = 4.0$; $\alpha = 6.1^{\circ}$; $\delta = 15^{\circ}/35^{\circ}/55^{\circ}$

x/c	Pressure coefficients at $\frac{y}{b/2}$ of -									
	0.160	0.226	0.256	0.316	0.350	0.420	0.450	0.490	0.650	0.850
Slat										
US										
0.01	-0.216			0.185	-1.821			-2.286	-2.165	-2.795
.10	-1.535			-1.133	-2.566			-3.614	-2.967	-3.254
.25	-2.222			-1.764	-2.795			-4.680	-3.426	-3.655
.45	-2.108			-2.050	-2.566			-5.292	-3.426	-3.999
.75	-1.821			-1.821	-2.165			-5.292	.070	-2.566
LS										
.03	.471			.128	.529			-2.439	.643	5.343
.15	.299			.242	.586			-2.541	.843	.643
.35	.586			.013	.586			-2.133	.586	.586
.70	.529			-.446	.185			-2.082	.843	.529
Wing										
US										
0.01	-3.197	-4.687	-0.044	-4.114	-4.343	-0.044	0.013	-8.552	-2.452	-7.610
.04	-3.025	-4.114	-.102	-3.426	-3.712	.013	-.044	-7.380	-7.266	-5.718
.10	-2.566	-2.509	-.044	-3.025	-3.139	.013	-.044	-6.667	-5.260	-4.400
.17	-2.337	-2.108	-.044	-3.025	-3.139	-.044	-.044	-2.592	-3.426	-.044
.25	-1.936	-1.821	-.044	-2.452	-2.623	-.044	-2.623	-5.699	-2.967	-3.197
.35	-1.936	-1.936	-2.394	-2.452	-2.452	-.044	-3.082	-5.801	-3.483	-3.197
.45	-1.936	-1.936	-1.878	-2.452	-2.394	-2.337	-2.795	-5.699	-3.197	-2.853
.60	-1.764	-1.993	-.044	-2.566	-2.509	-2.623	-2.910	-5.699	-3.254	-3.025
.75	-1.993	-2.623	-2.853	-2.795	-2.853	-3.197	-3.254	-5.903	-3.426	-1.706
LS										
.03	.873	1.102	-2.337	.643	.529	.013	-.044	-1.980	.701	.586
.08	.758	-.044	-.102	.873	.643	.013	-.044	-1.675	.414	.701
.15	.815	1.216	-.044	11.590	.758	-.044	-.044	-1.777	.815	.586
.35	.586	.070	.013	.930	.815	1.503	.471	-2.031	.070	.471
.50	.529	-.044	-1.019	.357	.930	-.446	.013	-1.929	.070	.357
.70	.357	.185	2.248	1.790	2.477	1.446	1.045	-1.216	.070	.357

ORIGINAL PAGE IS
OF POOR QUALITY

TABLE III.- PRESSURE COEFFICIENTS ON SLAT, WING,
AND FLAPS - Continued

(a) $C_{\mu} = 4.0$; $\alpha = 6.1^{\circ}$; $\delta = 15^{\circ}/35^{\circ}/55^{\circ}$ - Concluded

x/c	Pressure coefficients at $\frac{y}{b/2}$ of -									
	0.160	0.226	0.256	0.316	0.350	0.420	0.450	0.490	0.650	0.850
Flap 1										
US										
0.01	-2.151	-2.130	-7.824	-3.381	2.418	-7.889	-9.532	-3.485	-3.999	-2.050
.04		-4.214	-7.824	-3.381		-12.112	-7.556	-3.867		
.10	-2.385	-5.256	-7.824	-4.214	-3.999	-12.112	-7.556	-5.395	-5.184	-2.280
.17		-5.777	-7.824	-5.048		-12.715	-7.556	-6.159		
.25	-4.491	-6.819	-7.824	-5.882	-5.184	-12.715	-7.951	-6.159	-6.765	-2.280
.35		-7.340	-7.824	-6.298		-12.715	-7.951	-7.688		
.45	-4.725	-7.340	-7.824	-6.715	-5.975	-12.715	-7.951	-7.688	-7.161	-1.592
.60		-6.298	-7.005	-5.882		-11.509	-6.370	-6.159		
.75	-3.555	-3.693	-2.912	-5.048	-4.394	-9.699	-5.184	-4.259	-5.580	-7.89
LS										
.03	.188	.996	9.370	-.463	-.837	-2.459	3.511	1.482	-.046	.357
.08		3.080	8.960	1.204		5.987	6.278	1.864		
.15	.422	4.122	8.960	2.872	1.535	12.020	7.069	2.246	-.046	.414
.35	.422	4.643	8.960	.371	4.302	15.640	7.859	2.629	-.046	.299
.70	.422	7.769	11.826	7.457	5.883	19.863	9.835	5.303	-.046	.242
Flap 2										
US										
0.01	-1.450	-2.651	-5.777	0.788	-0.837	-2.459	-5.184	1.100	-2.418	-2.280
.04		-5.256	-7.415	-.463		-7.286	-5.580	-1.192		
.10	-3.321	-6.819	-8.643	76.649	-5.184	-13.318	-9.137	-6.159	-4.394	81.053
.17		-8.382	-9.871	-7.549		-16.335	-9.532	-8.070		
.25	-5.660	-8.382	96.567	-7.549	-6.370	-16.335	-9.928	-8.834	-6.370	-5.145
.35		-8.382	-11.099	-7.549		-16.335	-9.928	-9.598		
.45	-5.660	-7.861	-9.462	-7.549	-5.975	-16.335	-9.928	-8.834	-6.370	-4.515
.60		-4.214	-6.187	-5.882		-10.302	-4.394	-5.395		
.75	-4.023	-3.172	-4.959	-4.631	-3.999	-7.889	-3.999	-4.249	-3.999	71.826
LS										
.03	.422	12.980	23.698	6.206	2.721	27.705	15.369	4.921	-.046	.242
.08		12.980	24.517	7.874		17.449	17.345	.336		
.15	.422	13.501	22.470	8.707	3.116	31.325	17.345	6.067	-.046	.414
.35	.890	18.711	24.926	12.459	8.650	39.168	18.531	8.742	-.046	.299
.70	.422	24.963	29.838	19.545	6.278	45.201	20.112	14.855	-.046	.242
Flap 3										
US										
0.01	-2.619	-32.871	-43.440	-4.214	-1.232	47.103	-24.157	-1.192	-2.022	-2.050
.04		-8.382	-10.280	-1.296		-9.095	-9.137	-1.574		
.10	-3.789	-7.861	-9.871	-5.882	-4.789	-15.732	-10.718	-5.395	-3.208	-2.280
.17		-7.861	-9.871	-7.549		-18.748	-11.113	-6.924		
.25	-5.894	-8.382	-9.871	-7.549	-6.370	-16.938	-9.928	-6.924	-3.603	-2.280
.35		-8.382	-9.871	-8.799		-14.525	-7.951	-6.159		
.45	-5.192	-6.819	-9.87	-7.549	-3.208	-11.509	-6.765	-4.631	-3.208	-1.592
.60		-2.651	-4.549	-3.797		-9.699	-4.394	-4.249		
.75	-4.023	1.517	-4.549	-3.381	-1.232	-6.682	-3.603	-2.721	-2.418	-7.89
LS										
.03	2.527	37.468	48.670	4.956	5.883	68.126	30.784	14.855	.349	.357
.08		33.300	47.032	16.210		70.539	30.784	10.652		
.15	2.059	29.131	40.892	14.126	9.440	68.729	29.203	10.270	.349	.414
.35	1.591	.000	.000	.000	15.764	.000	.000	.000	.349	.299
.70	1.591	.000	.000	.000	14.579	.000	.000	.000	.349	.242

ORIGINAL PAGE IS
OF POOR QUALITY

TABLE III. - PRESSURE COEFFICIENTS ON SLAT, WING,
AND FLAPS - Continued

(b) $C_{\mu} = 4.0$; $\alpha = 17.9^\circ$; $\delta = 15^\circ/35^\circ/55^\circ$

x/c	Pressure coefficients at $\frac{y}{b/2}$ of, -									
	0.180	0.226	0.256	0.316	0.350	0.420	0.450	0.490	0.650	0.850
Slat										
US										
0.01	-8.396			-5.021	-11.371			-7.773	-14.231	-16.233
.10	-7.767			-5.650	-7.538			-8.332	-10.398	-10.570
.25	-6.823			-5.822	-6.280			-8.638	-8.625	-9.254
.45	-4.735			-4.220	-4.335			-8.078	-7.424	-8.339
.75	-3.191			-3.362	-4.277			-7.468	.070	-5.364
LS										
.03	-.045			.699	-1.703			-1.621	-3.248	6.648
.15	1.100			.585	.871			-1.722	-3.419	.699
.35	.985			.070	.814			-1.773	.928	.814
.70	.642			-.788	.013			-1.875	.985	.699
Wing										
US										
0.01	-5.250	-5.193	-0.102	-6.222	-6.165	-0.045	0.070	-11.383	-1.589	-12.515
.04	-4.220	-4.335	-.102	-4.849	-4.506	-.045	-.045	-9.858	-11.256	-8.796
.10	-3.362	-3.763	-.045	-3.820	-3.591	-.045	.013	-8.485	-8.339	-6.623
.17	-2.733	-2.390	-.102	-3.591	-3.191	-.045	-.045	-2.536	-5.250	-.045
.25	-2.333	-2.104	-.045	-2.905	-2.561	-.045	-3.648	-6.502	-4.163	-4.449
.35	-2.333	-2.161	-2.504	-2.676	-2.561	-.045	-3.362	-6.451	-4.277	-4.163
.45	-2.218	-2.047	-1.989	-2.619	-2.390	-2.905	-2.962	-5.994	-3.820	-3.763
.60	-1.818	-1.932	-.045	-2.733	-2.504	-2.676	-3.019	-5.841	-3.877	-3.877
.75	-1.703	-2.447	-2.504	-2.504	-2.504	-2.905	-3.191	-5.994	-3.763	-2.161
LS										
.03	.814	1.958	-2.333	1.157	.413	-.045	-.045	-2.434	.699	.585
.08	1.157	1.042	-.045	1.557	.699	-.045	-.045	-1.570	.413	.814
.15	1.214	1.443	-.045	14.142	1.328	-.045	-.045	-1.519	1.042	.814
.35	.985	-.388	-.045	1.443	1.157	2.758	1.100	-1.367	.013	.699
.50	.814	-.045	-.045	1.500	2.244	1.042	.985	-1.265	.013	.585
.70	.756	.699	2.244	2.644	3.216	2.816	1.614	-.604	.013	.528

TABLE III.- PRESSURE COEFFICIENTS ON SLAT, WING,
AND FLAPS - Continued

(b) $C_{\mu} = 4.0$; $\alpha = 17.9^\circ$; $\delta = 150/350/550$ - Concluded

x/c	Pressure coefficients at $\frac{y}{b/2}$ of -									
	0.160	0.226	0.256	0.316	0.350	0.420	0.450	0.490	0.650	0.850
Flap 1										
US										
0.01	-1.914	-2.646	-6.175	-3.374	-2.808	-5.465	-8.725	-2.715	-4.386	-3.820
.04		-4.206	-6.175	-3.790		-10.282	-7.541	-3.478		
.10	2.147	-5.246	-5.766	-4.206	-3.991	-10.282	-6.753	-5.004	-5.964	-5.708
.17		-6.286	-6.175	-5.038		-9.680	-6.753	-5.766		
.25	-3.782	-6.806	-6.583	-5.454	-4.780	-9.680	-6.753	-5.766	-6.753	-6.566
.35		-7.846	-6.583	-6.702		-9.680	-6.753	-6.910		
.45	-4.249	-7.326	-6.583	-6.286	-4.780	-10.282	-6.358	-6.529	-7.147	-7.366
.60		-5.766	-5.766	-5.038		-9.680	-5.569	-5.385		
.75	-3.081	-3.686	-2.498	-4.622	-3.202	-8.476	-4.386	-3.478	-5.964	-5.078
LS										
.03	-.280	.994	8.534	-.046	-1.230	-4.261	3.110	2.242	-.441	.184
.08		3.594	8.534	1.202		3.567	5.871	3.005		
.15	.421	3.074	8.534	3.282	2.715	8.384	6.266	3.767	.348	.470
.35	.654	5.154	8.943	-.046	6.266	12.599	7.449	3.767	.348	.470
.70	.654	7.234	10.577	9.690	7.055	16.814	9.816	6.437	.348	.356
Flap 3										
US										
0.01	-1.447	-2.646	-6.175	-3.374	-2.809	-5.465	-8.725	-2.715	-4.386	-2.619
.04		-3.886	-6.175	-3.790		-10.282	-7.541	-3.478		
.10	-3.081	-6.286	-5.766	-4.206	-3.991	-10.282	-6.753	-5.004	-5.964	78.551
.17		-7.846	-6.175	-5.038		-9.680	-6.753	-5.766		
.25	-4.949	-7.846	-6.583	-5.454	-4.780	-9.680	-6.753	-5.766	-6.753	-5.708
.35		-7.846	-6.583	-6.702		-9.680	-6.753	-6.910		
.45	-4.949	-7.326	-6.583	-6.286	-4.780	-10.282	-6.358	-6.529	-7.147	-5.193
.60		-4.206	-5.766	-5.038		-9.680	-5.569	-5.385		
.75	-3.081	-3.166	-2.498	-4.622	-3.202	-8.476	-4.386	-3.478	-5.964	71.401
LS										
.03	.421	11.914	8.534	-.046	-1.230	-4.261	3.110	2.242	-.441	.299
.08		11.914	8.534	1.202		3.567	5.871	3.005		
.15	.888	12.434	8.534	3.282	2.715	8.384	6.266	3.767	.348	.528
.35	1.121	17.115	8.943	-.046	6.266	12.599	7.449	3.767	.348	.528
.70	-.046	22.385	10.577	8.690	7.055	16.814	9.816	6.437	.348	.470
Flap 3										
US										
0.01	-3.548	-33.327	-43.765	-3.790	-2.808	-42.195	-26.477	-2.715	-2.413	-2.561
.04		-8.366	-9.852	-1.294		-10.384	-9.908	-1.571		
.10	-3.782	-7.326	-8.626	-5.454	-3.991	-15.099	-10.697	-4.622	-3.202	-2.676
.17		-7.326	-9.035	-7.118		-16.304	-10.303	-5.766		
.25	-4.949	-8.366	-9.035	-7.118	-4.780	-14.497	-7.936	-5.766	-3.597	-2.962
.35		-8.366	-8.626	-8.782		-12.691	-6.753	-4.622		
.45	-4.249	-7.326	-8.218	-7.118	-2.019	-9.680	-5.964	-3.860	-3.597	-2.104
.60		-3.166	-3.723	-3.790		-7.874	-3.991	-3.478		
.75	-3.081	.994	-3.723	-3.790	-.441	-6.669	-3.202	-1.953	-2.413	-1.246
LS										
.03	3.923	34.795	48.984	4.946	7.055	60.769	31.908	17.115	.348	.356
.08		31.675	46.124	16.595		64.984	32.303	13.683		
.15	2.055	26.475	39.178	14.931	10.605	64.984	31.119	12.920	.348	.470
.35	1.822	.000	.000	.000	14.550	.000	.000	.000	.348	.413
.70	1.822	.000	.000	.000	12.972	.000	.000	.000	.348	.299

TABLE III. - PRESSURE COEFFICIENTS ON SLAT, WING,
AND FLAPS - Continued

(c) $C_{\mu} = 4.0$; $\alpha = 25.3^{\circ}$; $\delta = 15^{\circ}/35^{\circ}/55^{\circ}$

x/c	Pressure coefficients at $\frac{y}{b/2}$ of -									
	0.160	0.226	0.256	0.316	0.350	0.420	0.450	0.490	0.650	0.850
Slat										
US										
0.01	-7.866			-7.359	-13.325			-13.199	-26.324	-29.869
.10	-3.420			-5.896	-7.022			-11.849	-16.982	-16.814
.25	-2.970			-5.334	-4.940			-11.399	-12.931	-13.887
.45	-3.251			-3.871	-5.052			-9.648	-10.04	-10.961
.75	-3.195			-3.533	-3.195			-8.447	.069	-7.134
LS										
.03	-.494			.406	-3.251			-2.695	-8.654	7.328
.15	1.250			.575	.857			-1.444	-8.766	.350
.35	-1.338			.069	.969			-1.645	1.419	.969
.70	-.832			-.550	.406			-1.645	1.025	.857
Wing										
US										
0.01	-5.615	-3.195	-0.044	-5.165	-5.221	-0.044	-0.044	-11.349	-3.026	-14.900
.04	-3.533	-2.520	-.044	-3.139	-3.702	-.044	-.100	-9.898	-13.550	-10.286
.10	-3.083	-2.914	-.044	-3.083	-3.533	-.044	-.044	-8.347	-9.329	-7.585
.17	-2.407	-2.407	-.044	-2.801	-3.308	-.044	-.044	-2.545	-6.403	-.044
.25	-1.901	-2.632	-.100	-2.351	-3.083	-.100	-3.702	-6.046	-4.377	-4.883
.35	-2.239	-1.957	-1.957	-2.239	-3.026	-.044	-2.914	-5.946	-4.377	-4.490
.45	-1.845	-1.394	-2.070	-2.182	-2.576	-2.858	-2.632	-5.346	-3.702	-3.871
.60	-1.394	-1.845	-.044	-2.126	-2.126	-2.520	-2.407	-5.096	-3.364	-3.758
.75	-1.338	-1.901	-1.901	-1.788	-2.126	-2.351	-2.351	-5.096	-3.251	-2.239
LS										
.03	.913	1.476	-1.732	1.588	.350	-.044	-.044	-2.095	.744	.406
.08	1.138	.519	-.044	1.982	1.025	.012	-.044	-1.494	.969	.744
.15	1.250	1.701	-.100	15.488	1.644	-.044	-.044	-1.595	1.138	.857
.35	1.025	-.438	.012	1.532	.969	2.714	1.194	-1.044	-.044	.800
.50	.631	-.044	-.213	2.263	2.432	1.082	1.419	-.944	.069	.631
.70	.519	1.138	1.982	3.164	3.164	3.107	1.701	.056	.069	.575

TABLE III - PRESSURE COEFFICIENTS ON SLAT, WING,
AND FLAPS - Continued

(c) $C_{\mu} = 4.0$; $\alpha = 25.3^{\circ}$; $\delta = 15^{\circ}/35^{\circ}/55^{\circ}$ - Concluded

x/c	Pressure coefficients at $\frac{y}{b/2}$ of -									
	0.180	0.226	0.256	0.316	0.350	0.420	0.450	0.490	0.650	0.850
Flap 1										
US										
0.01	-1.424	-2.092	-6.075	-3.320	-2.763	-3.008	-7.032	-1.922	-3.539	-3.646
.04		-3.627	-6.075	-2.911		-7.747	-6.256	-2.672		
.10	-1.424	-4.139	-5.673	-3.320	-3.151	-7.747	-5.091	-3.798	-4.703	-5.165
.17		-4.650	-5.673	-3.729		-7.747	-5.091	-3.798		
.25	-2.573	-4.650	-5.673	-4.548	-3.539	-7.747	-4.703	-3.798	-5.479	-6.290
.35		-4.650	-5.673	-4.957		-7.747	-4.703	-4.548		
.45	-2.573	-4.139	-5.272	-4.957	-3.151	-7.747	-4.315	-4.173	-5.479	-6.234
.60		-4.139	-4.468	-3.729		-7.747	-3.539	-3.047		
.75	-2.343	-2.604	-2.458	-3.729	-1.987	-7.154	-3.539	-2.672	-4.315	-4.433
LS										
.03	-.276	.977	7.591	-.865	-.822	-7.154	1.118	1.830	-.434	.125
.08		4.047	7.993	1.591		2.323	4.611	2.580		
.15	.184	4.047	7.993	3.637	3.835	6.470	6.163	3.330	.342	.575
.35	.413	5.581	8.395	.363	6.940	11.801	6.940	3.706	.342	.575
.70	.643	8.139	10.807	8.549	7.328	16.540	9.656	5.957	.342	.519
Flap 2										
US										
0.01	-1.195	-1.069	-4.468	2.410	-0.046	-1.231	-4.703	1.830	-1.598	-2.126
.04		-3.116	-5.673	.772		-4.193	-4.315	-.046		
.10	-2.802	-4.650	-6.075	65.436	-3.151	-8.339	-6.644	-3.798	-3.539	76.489
.17		-6.185	-6.477	-5.367		-10.116	-6.644	-4.923		
.25	-3.491	-6.185	77.934	-5.367	-3.539	-10.709	-6.644	-4.923	-4.315	-5.052
.35		-6.185	-7.683	-5.367		-10.709	-6.256	-5.298		
.45	-3.491	-5.162	-6.075	-5.367	-3.151	-10.116	-6.256	-4.548	-4.315	-4.377
.60		-2.604	-3.664	-4.139		-7.154	-2.763	-2.297		
.75	-2.573	-1.581	-3.262	-2.502	-1.210	-5.377	-2.763	-1.922	-2.763	70.693
LS										
.03	.873	10.186	21.660	6.502	4.223	14.171	12.761	5.206	.342	.406
.08		12.232	26.483	8.958		14.763	15.866	.704		
.15	.643	12.232	20.856	10.186	5.387	26.610	15.866	7.457	.342	.575
.35	1.562	18.836	23.267	13.050	10.044	33.126	18.194	10.083	.730	.575
.70	-.276	21.440	26.885	18.371	7.328	37.865	20.523	15.711	.730	.575
Flap 3										
US										
0.01	-3.262	-29.206	-41.448	-2.502	-3.539	-43.881	-27.601	-3.798	-1.598	-2.745
.04		-7.208	-8.889	-.865		-11.893	-9.748	-1.547		
.10	-3.032	-6.697	-7.683	-4.139	-3.151	-13.670	-9.748	-4.173	-2.375	-3.083
.17		-6.697	-8.085	-5.776		-14.855	-9.360	-4.923		
.25	-3.491	-6.697	-8.085	-5.776	-3.927	-13.078	-7.420	-4.923	-2.375	-3.477
.35		-6.697	-7.683	-7.413		-10.116	-6.256	-3.798		
.45	-3.262	-5.673	-6.879	-5.367	-.046	-7.747	-4.703	-3.047	-2.375	-2.689
.60		-1.581	-3.262	-2.911		-7.154	-3.151	-2.672		
.75	-2.343	1.489	-3.262	-2.911	1.118	-5.377	-3.151	-1.922	-1.598	-1.563
LS										
.03	3.859	34.742	48.591	5.684	8.492	56.820	32.166	17.211	.730	.350
.08		29.626	44.169	15.506		61.559	33.718	14.585		
.15	1.791	25.533	37.738	13.869	11.209	60.967	31.778	13.835	.730	.575
.35	2.021	.000	.000	.000	13.925	.000	.000	.000	.730	.519
.70	1.791	.000	.000	.000	11.597	.000	.000	.000	.730	.463

TABLE III. - PRESSURE COEFFICIENTS ON SLAT, WING,
AND FLAPS - Continued

(d) $C_{\mu} = 2.2$; $\alpha = 6.0^\circ$; $\delta = 15^\circ/35^\circ/55^\circ$

x/c	Pressure coefficients at $\frac{y}{b/2}$ of -									
	0.160	0.226	0.256	0.316	0.350	0.420	0.450	0.490	0.650	0.850
Slat										
US										
0.01	-0.045			0.245	-2.360			-2.154	-1.260	-1.995
.10	-1.376			-1.260	-2.881			-3.544	-2.418	-2.881
.25	-2.013			-1.724	-3.113			-4.470	-2.939	-3.286
.45	-1.955			-1.897	-2.823			-4.933	-3.228	-3.807
.75	-1.724			-1.666	-2.360			-4.933	.013	-2.997
LS										
.03	.418			.071	.187			-2.566	.708	5.107
.15	.302			.476	.071			-2.463	.650	.476
.35	.592			.129	.187			-2.154	.534	.534
.70	.566			-.276	-.219			-2.103	.592	.418
Wing										
US										
0.01	-2.939	-5.081	-0.045	-3.865	-4.386	-0.219	-0.161	-8.123	0.071	-7.338
.04	-2.765	-3.460	-.161	-3.228	-3.749	-.161	-.219	-6.940	-6.759	-5.428
.10	-2.360	-2.592	-.103	-2.708	-3.402	-.219	-.161	-6.476	-4.965	-4.213
.17	-2.244	-2.071	-.103	-2.765	-3.286	-.161	-.219	-2.566	-3.402	-.045
.25	-1.839	-1.839	-.103	-2.244	-2.765	-.219	-2.650	-5.550	-2.708	-2.997
.35	-1.839	-1.955	-2.360	-2.187	-2.708	-.161	-2.997	-5.602	-3.113	-2.997
.45	-1.781	-1.781	-1.897	-2.187	-2.650	-2.302	-2.823	-5.396	-2.881	-2.708
.60	-1.724	-1.839	-.103	-2.360	-2.592	-2.650	-2.823	-5.447	-3.055	-2.823
.75	-1.781	-2.418	-2.592	-2.476	-2.823	-3.055	-3.171	-5.499	-3.055	-2.823
LS										
.03	.823	.823	-2.244	.766	.245	-.161	-.161	-1.897	.766	.534
.08	.881	.129	-.045	.766	.302	-.161	-.276	-1.743	.360	.534
.15	.766	1.055	-.103	20.099	.418	-.219	-.219	-1.691	.708	.534
.35	.476	.013	-.045	.534	.592	1.344	.360	-1.949	.071	.360
.50	.534	-.103	-.103	.708	.245	-.045	.418	-1.897	.071	.302
.70	.534	.360	1.229	1.460	1.344	.592	.708	-1.794	.013	.360

TABLE III. - PRESSURE COEFFICIENTS ON SLAT, WING,
AND FLAPS - Continued

(d) $C_{\mu} = 2.2$; $\alpha = 6.0^{\circ}$; $\delta = 15^{\circ}/35^{\circ}/55^{\circ}$ - Concluded

x/c	Pressure coefficients at $\frac{y}{b/2}$ of -									
	0.160	0.226	0.256	0.316	0.350	0.420	0.450	0.490	0.650	0.850
Flap 1										
US										
0.01	-1.917	-2.232	-4.738	-3.298	-1.969	-3.813	-6.046	-2.950	-3.343	-2.823
.04		-3.623	-5.350	-2.911		-5.559	-5.892	-3.322		
.10	-2.853	-4.220	-5.248	-3.763	-3.200	-8.866	-5.277	-4.513	-4.493	-4.502
.17		-5.015	-5.758	-4.228		-11.072	-6.046	-4.885		
.25	-3.788	-5.611	-6.370	-5.079	-4.584	-12.725	-6.123	-5.183	-5.413	-5.254
.35		-6.406	-6.370	-5.467		-14.379	-6.815	-6.300		
.45	-3.788	-6.008	-5.860	-5.234	-4.815	-16.083	-6.354	-6.300	-5.796	-5.833
.60		-4.816	-4.738	-4.305		-15.482	-5.123	-5.034		
.75	-3.086	-3.524	-3.208	-3.763	-3.508	-15.482	-3.969	-3.843	-3.956	-4.039
LS										
.03	.188	.749	5.564	.031	-.200	-10.520	2.108	.698	.107	.071
.08		2.240	5.870	1.503		-3.354	4.492	1.220		
.15	.422	2.041	5.156	2.122	1.031	2.159	4.877	1.443	.567	.302
.35	.422	2.836	6.176	.186	3.108	7.121	5.415	1.815	.567	.245
.70	.422	4.923	7.706	4.910	3.723	11.531	6.339	3.081	.567	.129
Flap 2										
US										
0.01	-0.514	-1.537	-4.024	0.419	-1.969	-3.813	-3.123	0.177	-1.656	-2.129
.04		-3.922	-5.350	-1.362		-5.559	-4.123	-1.386		
.10	-2.853	-5.213	-6.166	39.292	-3.200	-8.866	-7.123	-4.736	-3.649	70.227
.17		-6.406	-7.288	-5.931		-11.072	-7.123	-8.151		
.25	-4.256	-6.803	43.099	-5.854	-4.584	-12.725	-7.431	-6.970	-4.876	-4.560
.35		-6.704	-7.390	-5.776		-14.379	-7.584	-7.640		
.45	-4.490	-6.207	-6.268	-5.776	-4.815	-16.033	-6.969	-6.449	-4.416	-4.213
.60		-3.623	-3.922	-4.073		-15.482	-3.277	-4.215		
.75	-3.086	-2.828	-3.106	-2.989	-3.508	-15.482	-2.815	-3.322	-2.576	70.632
LS										
.03	.422	7.705	14.234	3.826	.200	-10.520	9.262	3.155	.337	.302
.08		7.904	29.840	5.142		-3.354	10.492	.326		
.15	.422	7.904	12.296	5.607	1.031	2.159	10.185	3.751	.567	.302
.35	.656	11.183	15.152	7.775	3.108	7.121	11.877	5.389	.644	.245
.70	.188	14.760	17.090	11.570	3.723	11.531	12.877	9.260	.644	.245
Flap 3										
US										
0.01	-2.151	-18.032	-20.854	-3.066	-1.661	-13.277	-10.431	-2.428	-1.656	-1.781
.04		-6.008	-5.554	-1.595		-19.341	-5.200	-2.056		
.10	-2.619	-5.213	-5.248	-3.918	-3.431	-20.995	-7.123	-4.290	-2.346	-2.071
.17		-5.213	-6.472	-5.234		-22.648	-7.354	-4.960		
.25	-4.022	-6.108	-6.370	-5.157	-4.508	-22.097	-6.200	-5.034	-2.653	-2.071
.35		-6.008	-6.064	-5.699		-22.097	-5.354	-4.290		
.45	-4.022	-5.114	-5.554	-4.460	-2.354	-20.443	-4.200	-3.471	-2.193	-1.492
.60		-2.232	-2.596	-2.137		-17.687	-3.123	-2.950		
.75	-3.086	-.940	-2.494	-1.905	-.969	-17.136	-1.969	-2.205	-1.273	-.797
LS										
.03	1.591	21.915	25.352	4.136	3.800	37.992	17.339	10.005	.721	.245
.08		18.338	23.312	9.866		52.877	16.646	7.473		
.15	1.591	15.854	20.558	8.550	6.108	56.736	15.569	7.027	.721	.302
.35	1.357	.000	.000	.000	9.339	.000	.000	.000	.644	.245
.70	1.357	.000	.000	.000	8.646	.000	.000	.000	.567	.129

ORIGINAL PAGE IS
OF POOR QUALITY

TABLE III. - PRESSURE COEFFICIENTS ON SLAT, WING,
AND FLAPS - Continued

(e) $C_{\mu} = 2.2$; $\alpha = 17.9^\circ$; $\delta = 15^\circ/35^\circ/55^\circ$

x/c	Pressure coefficients at $\frac{y}{b/2}$ of -									
	0.160	0.226	0.256	0.316	0.350	0.420	0.450	0.490	0.650	0.850
Slat										
US										
0.01	-7.276			-5.020	-11.788			-6.524	-12.367	-13.986
.10	-6.758			-5.599	-7.739			-7.604	-9.127	-9.474
.25	-5.888			-5.309	-6.466			-8.015	-7.855	-8.375
.45	-4.384			-3.921	-4.557			-7.758	-6.871	-7.450
.75	-2.996			-3.285	-4.673			-7.038	.012	-5.483
LS										
.03	.244			.649	-2.706			-1.639	-2.417	5.103
.15	1.054			.880	.475			-1.896	-2.475	.591
.35	.971			.070	.591			-1.845	.764	.707
.70	.591			-.566	-.219			-1.948	.880	.649
Wing										
US										
0.01	-4.615	-5.252	-0.103	-5.830	-5.888	-0.219	-0.219	-10.638	-0.797	-11.557
.04	-3.921	-3.921	-.103	-4.615	-4.789	-.219	-.219	-8.941	-10.400	-8.202
.10	-3.169	-3.285	-.103	-3.458	-3.863	-.219	-.219	-8.015	-7.508	-6.177
.17	-2.706	-2.359	-.103	-3.111	-3.458	-.161	-.277	-2.565	-5.194	-.045
.25	-2.128	-2.070	-.103	-2.475	-2.938	-.219	-3.400	-6.164	-3.748	-4.095
.35	-1.954	-1.954	-2.533	-2.186	-2.533	-.219	-3.169	-5.959	-3.921	-3.805
.45	-1.781	-1.781	-1.781	-2.128	-2.706	-2.648	-2.938	-5.650	-3.400	-3.400
.60	-1.549	-1.665	-.045	-2.186	-2.533	-2.533	-2.764	-5.496	-3.343	-3.400
.75	-1.492	-2.070	-2.186	-2.012	-2.533	-2.591	-2.764	-5.342	-3.285	-3.285
LS										
.03	.880	1.459	-2.128	1.748	.128	-.161	-.161	-2.051	.360	.533
.08	.996	.591	-.103	1.864	.880	-.161	-.219	-1.691	.475	.764
.15	1.112	1.459	-.103	19.680	1.227	-.219	-.219	-1.434	.880	.764
.35	.822	.186	.128	.938	.591	1.748	.302	-1.485	.070	.533
.50	.764	-.161	.012	1.227	.996	.591	.822	-1.537	.128	.475
.70	.649	.533	1.632	2.153	1.690	1.227	.938	-.868	.128	.417

TABLE III. - PRESSURE COEFFICIENTS ON SLAT, WING,
AND FLAPS - Continued

(c) $C_{\mu} = 2.2$; $\alpha = 17.9^{\circ}$; $\delta = 15^{\circ}/35^{\circ}/55^{\circ}$ - Concluded

x/c	Pressure coefficients at $\frac{y}{b/2}$ of -									
	0.160	0.226	0.256	0.316	0.350	0.420	0.450	0.490	0.650	0.850
Flap 1										
US										
0.01	-1.682	-1.734	-4.837	-3.219	-2.737	-4.361	-5.043	-2.799	-3.494	-3.574
.04		-2.727	-5.041	-2.832		-5.004	-5.043	-3.245		
.10	-1.682	-3.323	-4.837	-3.451	-3.198	-8.861	-4.658	-4.212	-4.566	-5.194
.17		-4.217	-4.837	-3.761		-9.963	-5.196	-4.659		
.25	-2.617	-4.713	-5.346	-4.534	-4.043	-11.615	-5.196	-4.808	-5.486	-6.004
.35		-5.210	-5.346	-5.076		-12.717	-5.581	-5.700		
.45	-2.851	-5.111	-4.837	-4.767	-4.197	-14.370	-5.196	-5.552	-5.716	-6.524
.60		-4.118	-3.818	-3.761		-14.370	-3.967	-4.287		
.75	-2.150	-2.727	-2.594	-3.219	-2.890	-14.370	-3.121	-3.245	-3.954	-4.442
LS										
.03	-.046	.153	6.783	.186	.723	-10.514	2.414	.921	.031	.186
.08		2.039	6.070	2.198		-3.352	4.413	1.665		
.15	.655	2.437	5.662	2.972	1.953	1.607	4.797	1.963	.720	.360
.35	.655	3.728	6.376	.264	3.874	6.014	5.258	2.260	.720	.360
.70	.655	5.019	8.007	5.294	3.951	8.769	6.483	3.525	.720	.186
Flap 2										
US										
0.01	0.421	-0.840	-2.900	0.960	-0.277	4.361	-2.198	1.591	-1.732	-2.301
.04		-2.231	-4.531	-.433		.505	-3.275	-1.013		
.10	-2.383	-3.919	-5.041	38.415	-3.736	-5.555	-6.042	-4.138	-3.647	67.635
.17		-5.011	-6.060	-4.999		-9.412	-5.888	-5.403		
.25	-3.318	-5.607	39.402	-4.999	-4.274	-11.615	-5.811	-5.998	-4.720	-5.136
.35		-5.607	-6.162	-4.999		-13.268	-5.965	-6.519		
.45	-3.552	-5.011	-4.939	-5.076	-3.813	-14.921	-5.350	-5.403	-4.260	-4.615
.60		-2.827	-3.002	-3.451		-14.921	-2.275	-3.320		
.75	-2.383	-2.032	-2.289	-2.368	-2.045	-14.370	-2.045	-2.650	-2.421	68.676
LS										
.03	.655	6.012	13.409	4.288	2.875	2.709	9.332	3.674	.414	.302
.08		7.700	29.005	5.913		7.667	10.255	.475		
.15	.889	8.594	12.084	6.377	2.798	13.176	10.178	4.864	.720	.360
.35	1.123	10.679	14.123	8.312	5.719	20.338	11.331	6.501	.797	.360
.70	.188	12.963	16.161	11.639	4.105	25.847	13.022	9.924	.797	.302
Flap 3										
US										
0.01	-1.215	-16.332	-17.884	-1.439	-4.043	-8.310	-10.731	-3.617	-1.655	-2.128
.04		-4.515	-4.225	-.975		-16.023	-4.889	-2.129		
.10	-1.916	-4.217	-4.225	-3.528	-3.198	-17.675	-6.119	-3.915	-2.268	-2.359
.17		-4.118	-5.448	-4.921		-18.777	-6.119	-4.510		
.25	-2.617	-5.011	-5.346	-4.921	-3.659	-18.226	-4.986	-4.510	-2.574	-2.301
.35		-5.210	-4.939	-5.618		-18.226	-4.043	-3.617		
.45	-2.617	-4.416	-4.735	-4.225	-1.814	-17.675	-3.198	-3.022	-2.038	-1.665
.60		-1.933	-2.085	-2.290		-16.023	-2.275	-2.576		
.75	-2.383	-.940	-2.085	-2.058	-.738	-14.921	-1.660	-1.757	-1.195	-1.029
LS										
.03	2.291	20.113	24.316	3.282	4.566	23.093	17.250	11.114	.873	.244
.08		16.538	21.258	9.782		38.518	17.097	9.328		
.15	1.123	13.361	18.608	8.312	6.488	43.477	16.482	9.105	.873	.360
.35	1.123	.000	.000	.000	8.717	.000	.000	.000	.873	.244
.70	1.123	.000	.000	.000	7.411	.000	.000	.000	.720	.186

TABLE III. - PRESSURE COEFFICIENTS ON SLAT, WING,
AND FLAPS - Continued

(f) $C_{\mu} = 0$; $\alpha = 5.0^\circ$; $\delta = 15^\circ/35^\circ/55^\circ$

x/c	Pressure coefficients at $\frac{y}{b/2}$ of -									
	0.160	0.226	0.256	0.316	0.350	0.420	0.450	0.490	0.650	0.850
Slat										
US										
0.01	0.735			0.319	0.497			-1.829	0.735	0.735
.10	.319			-.097	-.335			-2.357	.022	-.038
.25	-.276			-.395	-.692			-2.992	-.632	-.870
.45	-.632			-.751	-.930			-3.573	-1.227	-1.525
.75	-.632			-.811	-.930			-3.732	.141	-1.465
LS										
.03	.022			.379	-.097			-2.780	.022	-2.892
.15	.022			.260	.081			-2.621	.081	.260
.35	.200			.260	.497			-2.463	.022	.260
.70	.081			.081	.379			-2.516	.200	.676
Wing										
US										
0.01	-1.644	-2.952	0.081	-2.060	-2.417	-0.157	-0.157	-5.899	-0.573	-4.201
.04	-1.644	-2.119	.081	-1.762	-2.119	-.157	-.097	-5.106	-3.903	-3.190
.10	-1.525	-1.822	.081	-1.584	-1.703	-.097	-.157	-4.896	-2.773	-2.476
.17	-1.406	-1.108	.022	-1.584	-1.644	-.157	-.157	-2.621	-2.236	.081
.25	-1.108	-1.049	.022	-1.168	-1.227	-.157	-1.762	-4.207	-1.703	-1.762
.35	-1.108	-1.108	-1.287	-1.108	-1.227	-.097	-1.822	-4.260	-1.762	-1.703
.45	-.989	-.930	-.811	-1.108	-1.168	-1.287	-1.525	-4.049	-1.525	-1.525
.60	-.930	-.930	.081	-1.049	-1.049	-1.406	-1.525	-3.943	-1.525	-1.703
.75	-.751	-.889	-1.108	-.989	-1.049	-1.346	-1.406	-3.784	-1.465	-1.762
LS										
.03	.795	.557	-1.049	.557	.914	-.157	-.157	-1.829	.914	.735
.08	.735	.438	.081	.616	.081	-.097	-.157	-1.934	.141	.735
.15	.557	.497	.081	3.293	.379	-.157	-.097	-2.093	.735	.557
.35	.379	.319		.616	.557	.200	.022	-2.199	.141	.497
.50	.379	.081	.022	.616	.438	.260	-.157	-2.199	.200	.438
.70	.497	.616	.914	.616	.676	.379	.795	-2.040	.141	.497

TABLE III. - PRESSURE COEFFICIENTS ON SLAT, WING,
AND FLAPS - Continued

(f) $C_{\mu} = 0$; $\alpha = 5.0^{\circ}$; $\delta = 15^{\circ}/35^{\circ}/55^{\circ}$ - Concluded

x/c	Pressure coefficients at $\frac{y}{b/2}$ of -									
	0.160	0.226	0.256	0.316	0.350	0.420	0.450	0.490	0.650	0.850
Flap 1										
US										
0.01	-1.247	-1.080	-0.998	-1.010	-1.239	-1.466	-1.179	-1.084	-1.632	-1.941
.04		-1.239	-1.116	-1.171		-1.585	-1.502	-1.403		
.10	-1.167	-1.558	-1.473	-1.493	-1.717	-1.940	10.797	-1.643	-2.425	-3.011
.17		-1.876	-1.830	-1.734		-2.058	-2.069	-1.802		
.25	-1.488	-2.115	-2.068	-2.055	-1.876	-2.176	-1.745	-1.802	-3.059	-3.368
.35		-2.353	-2.187	-2.136		-2.295	-2.392	-1.882		
.45	-2.048	-2.115	-2.187	-2.136	-1.876	-2.295	-2.231	-1.722	-3.297	-3.784
.60		-1.717	-1.949	-1.653		-1.821	-1.664	-1.403		
.75	-1.167	-1.239	-1.592	-1.493	-1.478	-1.466	-1.098	-.924	-2.028	-2.357
LS										
.03	.675	.113	-.046	.034	.272	.427	.440	.673	.192	.557
.08		.591	-.046	.034		.546	11.848	.673		
.15	.675	.511	-.046	.034	.272	.546	2.624	.593	.588	.616
.35	.675	.431	.073	-.046	.272	.546	.440	.593	.588	.557
.70	.675	.431	.073	.034	.272	.427	.520	.593	.588	.438
Flap 2										
US										
0.01	0.595	-0.364	-0.165	-0.367	-0.205	-0.283	-0.127	0.513	-0.680	-0.930
.04		-.762	-.641	-.689		-.756	-.531	-.445		
.10	-1.247	-1.160	-1.235	36.602	-1.239	-1.348	-1.179	-1.084	-1.790	55.747
.17		-1.558	-1.473	-1.332		-1.585	-1.421	-1.243		
.25	-1.328	-1.637	11.254	-1.332	-1.319	-1.703	-1.502	-1.164	-2.346	-2.773
.35		-1.637	-1.711	-1.251		-1.703	-1.502	-1.084		
.45	-1.328	-1.478	-1.592	-1.010	-1.319	-1.703	-1.421	-1.084	-2.108	-2.536
.60		-.921	-1.235	-.930		-1.111	-.855	-.764		
.75	-.927	-.046	-1.116	-.930	-1.160	-.874	-.693	-.685	-.998	57.293
LS										
.03	.755	.591	.073	.034	.193	.309	.520	.673	.588	.616
.08		.034	12.681	.034		.309	.601	.194		
.15	.675	.591	.430	.034	.193	.309	.520	.593	.668	.616
.35	.675	.591	.430	.115	.272	.427	.601	.593	.747	.616
.70	.675	.591	.430	.115	.272	.427	.601	.593	.668	.616
Flap 3										
US										
0.01	-0.446	-0.921	-0.760	-0.609	-1.160	-0.756	-0.774	-0.764	-0.601	-0.989
.04		-.603	-.760	-.609		-10.934	-.693	-.764		
.10	-.527	-.603	-.760	-.609	-1.160	-.993	-.774	-.924	-.839	-1.168
.17		-.603	-.760	-.609		-.993	-.936	-.924		
.25	-.687	-.603	-.760	-.609	-1.080	-.993	-.855	-.844	-1.077	-1.168
.35		-.603	-.879	-.609		-.874	-.855	-.764		
.45	-1.007	-.603	-.879	-.609	-1.001	-.874	-.774	-.685	-.839	-.811
.60		-.603	-.760	-.609		-.756	-.612	-.605		
.75	-.767	-.384	-.641	-.609	-.842	-.401	-.370	-.525	-.284	-.335
LS										
.03	.755	.591	.073	-1.573	-.046	.427	43.405	.593	.747	.676
.08		.591	.073	.115		.427	.520	.593		
.15	.675	.591	.073	.115	.113	.546	.520	.593	.668	.557
.35	.675	.591	.073	.115	.272	8.949	.035	.513	.588	.497
.70	.515	.511	.192	.115	.272	.427	.440	.353	.509	.497

TABLE III. - PRESSURE COEFFICIENTS ON SLAT, WING,
AND FLAPS - Continued

(g) $C_{\mu} = 0$; $\alpha = 17^{\circ}$; $\delta = 15^{\circ}/35^{\circ}/55^{\circ}$

x/c	Pressure coefficients at $\frac{y}{b/2}$ of -									
	0.160	0.225	0.256	0.316	0.350	0.420	0.450	0.490	0.650	0.850
Slat										
US										
0.01	-1.515			-3.656	-2.800			-2.711	-1.698	-2.861
.10	-2.616			-1.882	-2.616			-4.017	-2.616	-3.412
.25	-2.738			-1.515	-2.677			-4.234	-2.555	-3.350
.45	-2.494			-1.147	-1.943			-4.180	-2.677	-3.595
.75	-1.821			-1.453	-1.515			-4.234	.015	-2.861
LS										
.03	.749			-2.310	.749			-2.276	.688	-3.412
.15	.505			.382	.566			-2.331	.688	.566
.35	.688			.260	.688			-2.331	.627	.566
.70	.627			-.046	.321			-2.059	.566	.505
Wing										
US										
0.01	-3.167	-2.616	0.015	-3.534	-3.228	-0.230	-0.168	-4.724	-0.903	-6.655
.04	-2.661	-2.310	.015	-2.371	-2.555	-.168	-.168	-4.941	-5.247	-4.758
.10	-2.127	-2.310	.015	-1.882	-2.310	-.230	-.168	-4.833	-3.779	-3.656
.17	-1.821	-1.821	.015	-1.453	-1.392	-.230	-.168	-2.657	-2.677	.015
.25	-1.392	-1.209	.015	-1.209	-1.270	-.168	-1.025	-3.745	-1.821	-2.371
.35	-.964	-1.147	-1.147	-1.025	-.903	-.168	-.842	-3.636	-1.698	-2.249
.45	-1.209	-.903	-.719	-.842	-.964	-1.086	-1.086	-3.582	-1.331	-1.821
.60	-.964	-.780	.015	-.842	-1.47	-1.821	-1.147	-3.582	-1.147	-1.882
.75	-.780	-.903	-1.025	-.658	-.903	-1.025	-1.025	-3.473	-1.209	-2.065
LS										
.03	.872	.811	-.903	.505	.872	-.168	-.230	-2.276	.811	.688
.08	.872	.627	.076	.994	-.413	-.230	-.168	-2.113	.138	.688
.15	.749	.566	.015	1.912	.688	-.230	-.168	-2.004	.749	.627
.35	.505	.505	.627	.749	.566	.443	.505	-2.004	.076	.566
.50	.505	.076	.443	.688	.505	.382	.505	-2.113	.076	.443
.70	.505	.566	.566	.749	.627	.382	.443	-2.059	.015	.505

TABLE III. - PRESSURE COEFFICIENTS ON SLAT, WING,
AND FLAPS - Continued

(g) $C_{\mu} = 0$; $\alpha = 17^{\circ}$; $\delta = 15^{\circ}/35^{\circ}/55^{\circ}$ - Concluded

x/c	Pressure coefficients at $\frac{y}{b/2}$ of -									
	0.160	0.226	0.256	0.316	0.350	0.420	0.450	0.490	0.650	0.850
Flap 1										
US										
0.01	-1.035	-0.946	-0.903	-0.873	-1.274	-1.020	-0.878	-0.785	-1.025	-1.759
.04		-1.110	-1.025	-.955		-1.020	-.878	-.867		
.10	-.870	-1.274	-1.147	-1.286	-1.601	-1.264	6.198	-1.360	-1.678	-2.922
.17		-1.683	-1.514	-1.700		-1.507	-1.378	-1.360	-	
.25	-1.282	-1.765	-1.759	-1.865	-1.519	-1.385	-1.378	-1.360	-1.678	-3.473
.35		-1.847	-1.759	-1.782		-1.385	-1.295	-1.442		
.45	-1.859	-1.601	-1.759	-1.782	-1.519	-1.385	-1.128	-1.114	-2.167	-3.676
.60		-1.192	-1.514	-1.452		-1.020	-.878	-.867		
.75	-1.035	-.946	-1.147	-1.204	-1.356	-1.020	-.878	-.949	-1.351	-2.249
LS										
.03	.778	.200	.321	.202	.118	.563	.703	.693	.607	.382
.08		.773	.444	.202		.563	8.196	.693		
.15	.778	.855	.444	.202	.200	.563	2.535	.693	.688	.382
.35	.778	.773	.444	.037	.200	.563	.537	.611	.688	.382
.70	.696	.691	.444	.202	.200	.563	.620	.611	.607	.321
Flap 2										
US										
0.01	0.696	-0.128	-0.046	-0.129	-0.291	-0.046	-0.046	0.611	-0.127	-1.147
.04		-.537	-.535	-.459		-.533	-.379	-.292		
.10	-1.200	-1.110	-1.147	33.527	-1.438	-1.264	-1.128	-1.196	-1.188	55.700
.17		-1.356	-1.270	-1.204		-1.385	-1.045	-1.032		
.25	-1.200	-1.274	9.378	-1.286	-1.438	-1.264	-1.128	-1.196	-1.514	-2.677
.35		-1.519	-1.637	-1.286		-1.264	-1.045	-1.114		
.45	-1.200	-1.356	-1.637	-1.286	-1.438	-1.264	-.962	-.949	-1.514	-2.371
.60		-.946	-1.147	-1.121		-.898	-.629	-.703		
.75	-.952	-.046	-1.147	-1.121	-1.274	-.898	-.545	-.703	-.699	58.453
LS										
.03	.861	.855	.444	.285	.200	.563	.703	.693	.770	.505
.08		.036	10.846	.285		.441	.703	.201		
.15	.778	.773	.811	.285	.200	.563	.703	.611	.688	.505
.35	.778	.773	.811	.285	.200	.563	.703	.611	.688	.505
.70	.778	.773	.811	.285	.200	.563	.703	.611	.688	.443
Flap 3										
US										
0.01	-0.870	-1.028	-1.025	-0.873	-1.601	-0.898	-0.712	-0.703	-0.454	-1.025
.04		-.619	-1.025	-.873		-10.031	-.629	-.703		
.10	-.870	-.619	-1.025	-.955	-1.356	-1.020	-.712	-.785	-.699	-1.147
.17		-.619	-1.147	-1.121		-1.142	-.962	-1.032		
.25	-.870	-.701	-1.147	-1.121	-1.356	-1.142	-.878	-.785	-.862	-1.209
.35		-.701	-1.147	-1.121		-1.020	-.712	-.703		
.45	-.870	-.865	-1.147	-1.121	-1.274	-.898	-.795	-.867	-.699	-.842
.60		-.537	-1.025	-.955		-.898	-.629	-.785		
.75	-.870	-.537	-.903	-.955	-1.192	-.777	-.545	-.621	-.372	-.413
LS										
.03	.861	.773	.444	-2.113	.282	.563	32.590	.693	.770	.505
.08		.773	.444	.285		.563	.620	.611		
.15	.778	.773	.444	.285	.200	.563	.620	.611	.688	.505
.35	.778	.773	.444	.285	.200	6.652	.037	.529	.607	.443
.70	.778	.773	.444	.285	.118	.319	.370	.365	.444	.382

TABLE III. - PRESSURE COEFFICIENTS ON SLAT, WING,
AND FLAPS - Continued

(h) $C_{\mu} = 4.0$; $\alpha = 18^{\circ}$; $\delta = 0^{\circ}/20^{\circ}/40^{\circ}$

x/c	Pressure coefficients at $\frac{y}{b/2}$ of -									
	0.160	0.226	0.256	0.316	0.350	0.420	0.450	0.490	0.650	0.850
Slat										
US										
0.01	----			----	----				----	----
.10	----			----	----				----	----
.25	----			----	----				----	----
.45	----			----	----				----	----
.75	----			----	----				----	----
LS										
.03	----			----	----				----	----
.15	----			----	----				----	----
.35	----			----	----				----	----
.70	----			----	----				----	----
Wing										
US										
0.01	----	----	----	----	----	----	----	----	----	----
.04	----	----	----	----	----	----	----	----	----	----
.10	----	----	----	----	----	----	----	----	----	----
.17	----	----	----	----	----	----	----	----	----	----
.25	----	----	----	----	----	----	----	----	----	----
.35	----	----	----	----	----	----	----	----	----	----
.45	----	----	----	----	----	----	----	----	----	----
.60	----	----	----	----	----	----	----	----	----	----
.75	----	----	----	----	----	----	----	----	----	----
LS										
.03	----	----	----	----	----	----	----	----	----	----
.08	----	----	----	----	----	----	----	----	----	----
.15	----	----	----	----	----	----	----	----	----	----
.35	----	----	----	----	----	----	----	----	----	----
.50	----	----	----	----	----	----	----	----	----	----
.70	----	----	----	----	----	----	----	----	----	----

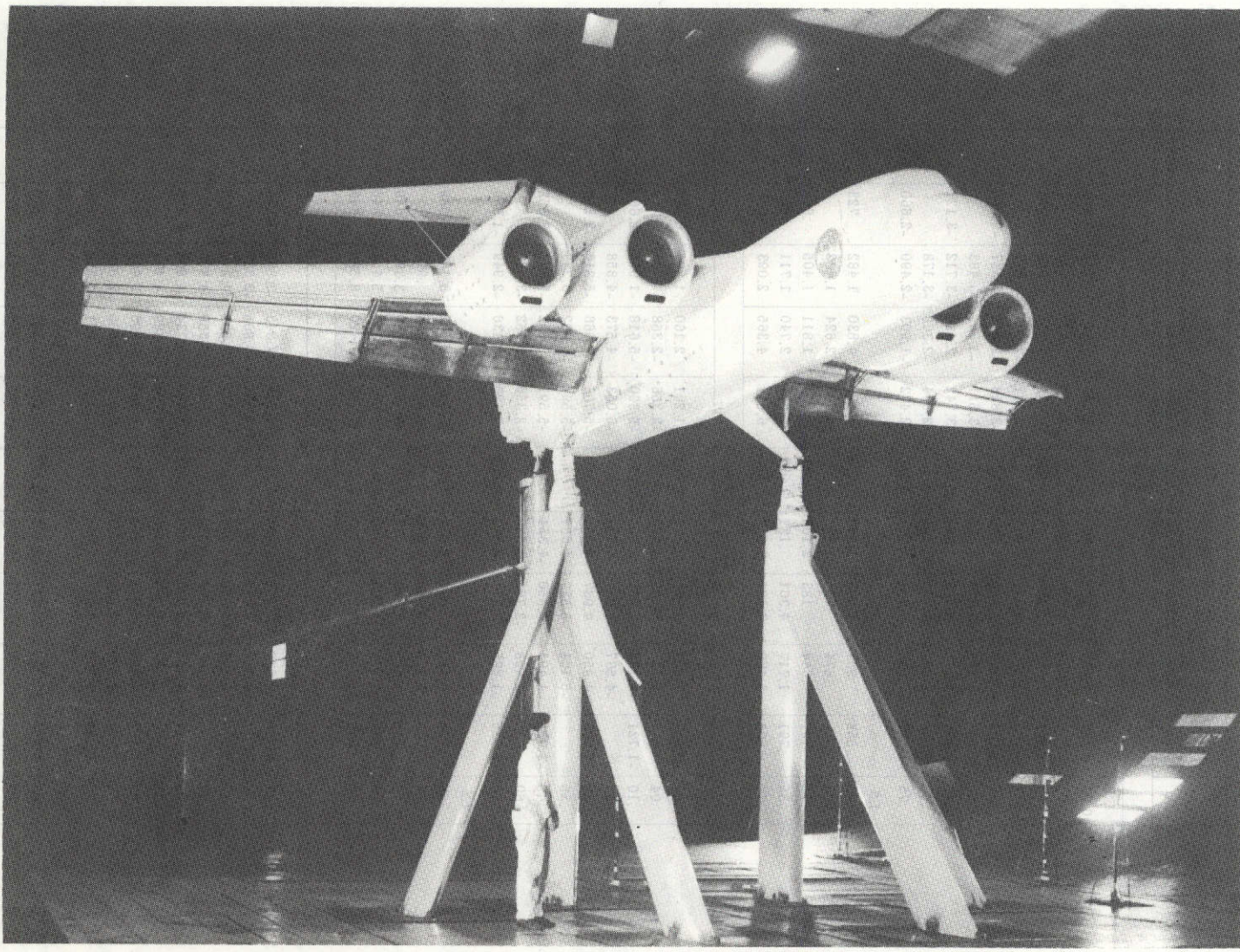
ORIGINAL PAGE IS
OF POOR QUALITY

TABLE III. - PRESSURE COEFFICIENTS ON SLAT, WING,
AND FLAPS - Concluded

(h) $C_{\mu} = 4.0$; $\alpha = 18^{\circ}$; $\delta = 0^{\circ}/20^{\circ}/40^{\circ}$ - Concluded

x/c	Pressure coefficients at $\frac{y}{b/2}$ of -									
	0.160	0.226	0.256	0.316	0.350	0.420	0.450	0.490	0.650	0.850
Flap 1										
US										
0.01	0.182	1.487	2.471	0.860	-0.162	-0.277	1.347	1.100	-0.046	
.04		1.027	1.670	.634		.185	.418	.718		
.10	-.351	.031	.297	.181	-.162	-.739	-.742	-.657	-1.276	
.17		-1.272	-1.991	-1.066		-2.241	-2.484	-1.879		
.25	-1.569	-2.192	-3.020	-2.085	-1.323	-2.818	-2.948	-2.337	-2.660	
.35		-3.285	-3.478	-3.105		-3.511	-3.761	-3.483		
.45	-2.178	-3.341	-3.478	-3.331	-2.368	-3.742	-2.484	-3.712	-3.121	
.60		-2.881	-3.020	-2.991		-2.934	-2.368	-3.178		
.75	-1.569	-1.885	-.961	-2.651	-2.252	-2.472	-1.903	-2.490	-2.660	
LS										
.03	.868	.337	4.072	1.653	.070	6.423	4.830	1.482	.723	
.08		.874	.755	1.993		4.690	2.624	1.482		
.15	.791	.644	.183	2.106	1.115	3.766	1.811	1.405	.646	
.35	.791	1.717	4.301	.181	2.972	5.614	2.740	1.711	.646	
.70	.563	3.479	7.504	3.919	3.553	6.654	4.365	2.093	.646	
Flap 2										
US										
0.01	0.487	1.257	0.526	0.634	-1.091	-1.201	2.160	1.864	-0.969	
.04		-1.425	-3.249	-.499		-2.356	-2.368	-.733		
.10	-1.721	-3.188	-4.850	-2.651	-2.948	-5.360	-5.618	-1.956	-2.660	
.17		-4.567	-5.994	-4.124		-6.053	-4.573	-4.858		
.25	-2.863	-4.950	4.987	-4.351	-3.180	-5.706	-5.966	-5.316	-3.506	
.35		-5.104	-5.537	-4.351		-5.591	-6.082	-6.233		
.45	-3.015	-4.491	-4.850	-4.351	-3.180	-5.591	-5.502	-5.393	-3.352	
.60		-2.498	-2.791	-3.558		-2.356	-2.252	-3.483		
.75	-2.025	-1.885	-2.334	-2.538	-2.252	-2.125	-2.136	-2.949	-1.968	
LS										
.03	.715	5.242	12.994	5.052	2.044	13.007	10.402	3.162	.569	
.08		4.475	9.448	5.505		10.697	7.964	.947		
.15	.715	4.475	6.360	6.071	4.017	9.773	7.500	3.391	.646	
.35	.868	7.617	13.223	7.770	6.919	13.585	11.330	5.454	.646	
.70	.868	11.142	16.311	10.716	6.107	17.166	13.420	8.585	.646	
Flap 3										
US										
0.01	-2.939	-13.610	-23.495	-3.331	-4.225	-18.528	-17.343	-3.865	-1.276	
.04		-4.107	-6.452	-1.972		-7.554	-6.895	-2.337		
.10	-2.178	-4.107	-4.850	-3.784	-3.180	-6.977	-7.592	-4.247	-1.968	
.17		-4.107	-5.994	-5.030		-7.092	-7.359	-4.858		
.25	-3.244	-4.107	-5.537	-5.030	-3.412	-5.591	-5.734	-4.858	-2.122	
.35		-4.184	-5.193	-5.710		-4.204	-4.689	-4.171		
.45	-2.787	-4.184	-5.079	-4.691	-2.948	-3.280	-3.993	-3.407	-1.814	
.60		-1.579	-1.876	-2.651		-2.818	-2.600	-2.872		
.75	-1.721	-1.809	-1.876	-2.085	-.975	-1.779	-1.671	-1.879	-1.199	
LS										
.03	1.857	17.349	29.123	12.642	6.223	28.139	23.287	10.571	.646	
.08		15.970	27.521	11.509		25.367	21.894	8.051		
.15	1.324	16.507	25.462	10.489	7.848	23.865	20.153	7.745	.723	
.35	1.477	14.667	22.488	9.017	9.357	21.902	-.046	7.287	1.415	
.70	1.553	10.836	16.426	7.431	9.241	17.512	13.768	6.217	.569	

10	1.423	10.438	1.423	9.341	11.213	12.168	9.311	282
20	1.415	10.438	1.423	9.341	11.213	12.168	9.311	282
30	1.415	10.438	1.423	9.341	11.213	12.168	9.311	282

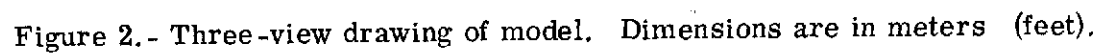


(9) $C_D = 4.0$; $q = 180$; $\delta = 0$; 300 ft/s - Concluding

WIND TUNNEL - Concluding

TABLE II - PRESSURE COEFFICIENTS ON 274' MODEL

Figure 1.- Photograph of test model mounted in wind tunnel.



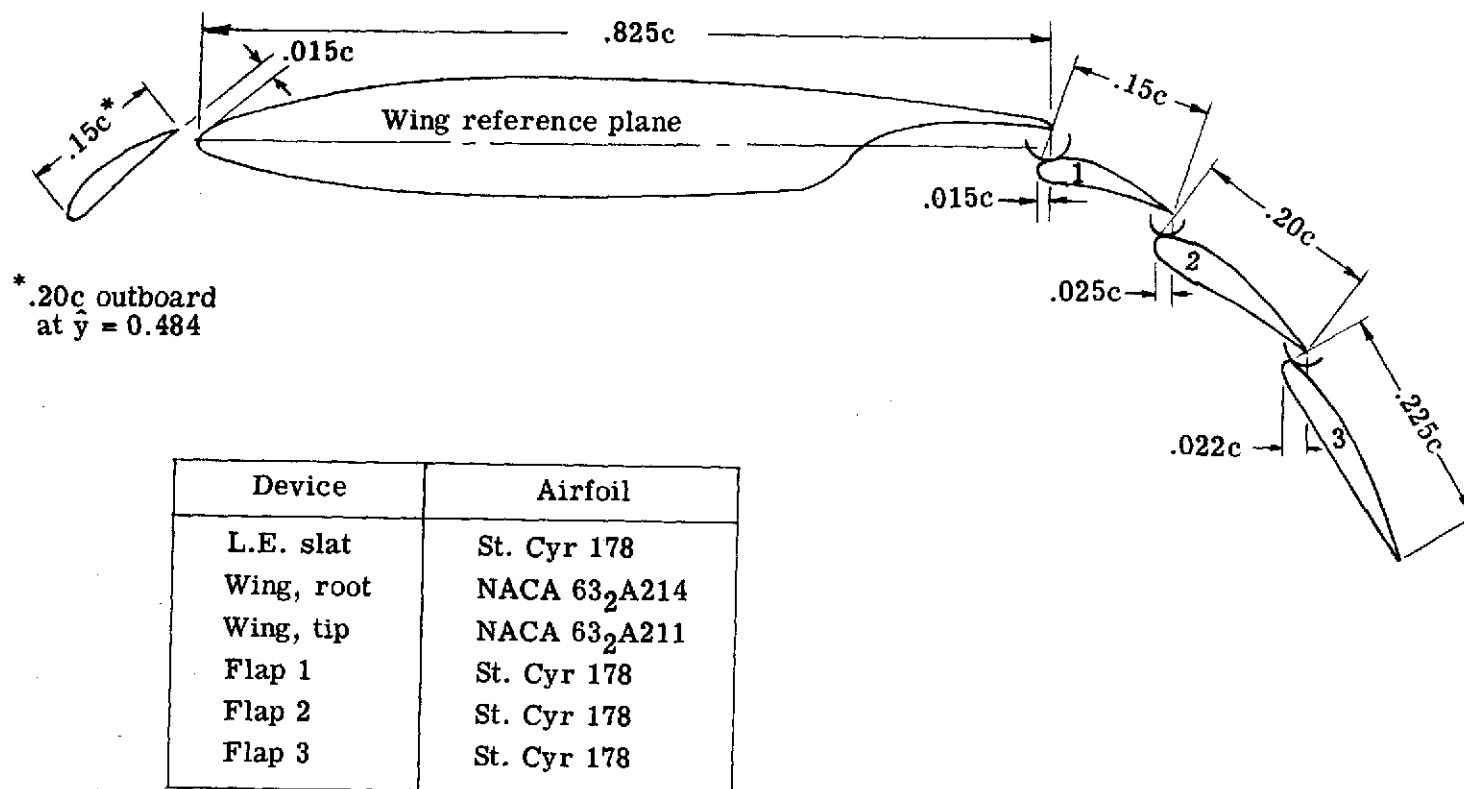


Figure 3.- Cross section of slat-wing-flap system.

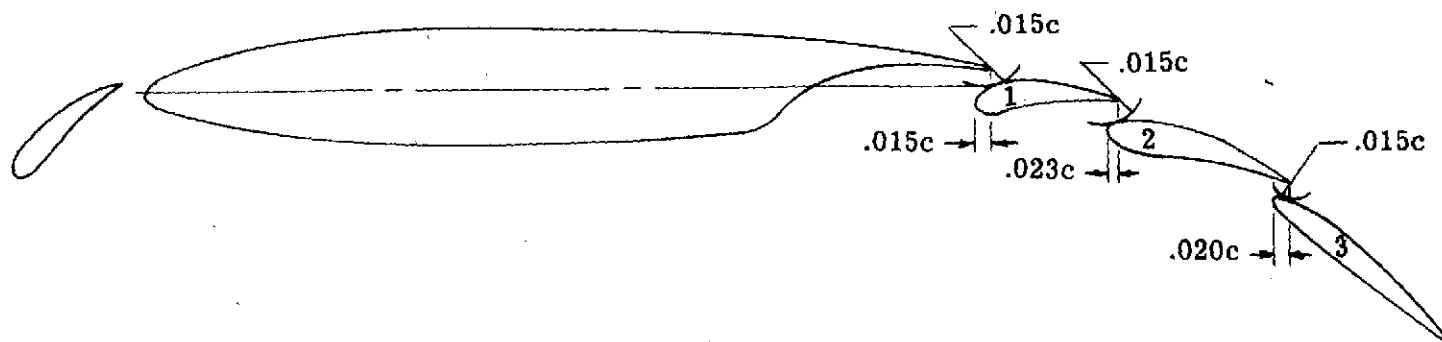
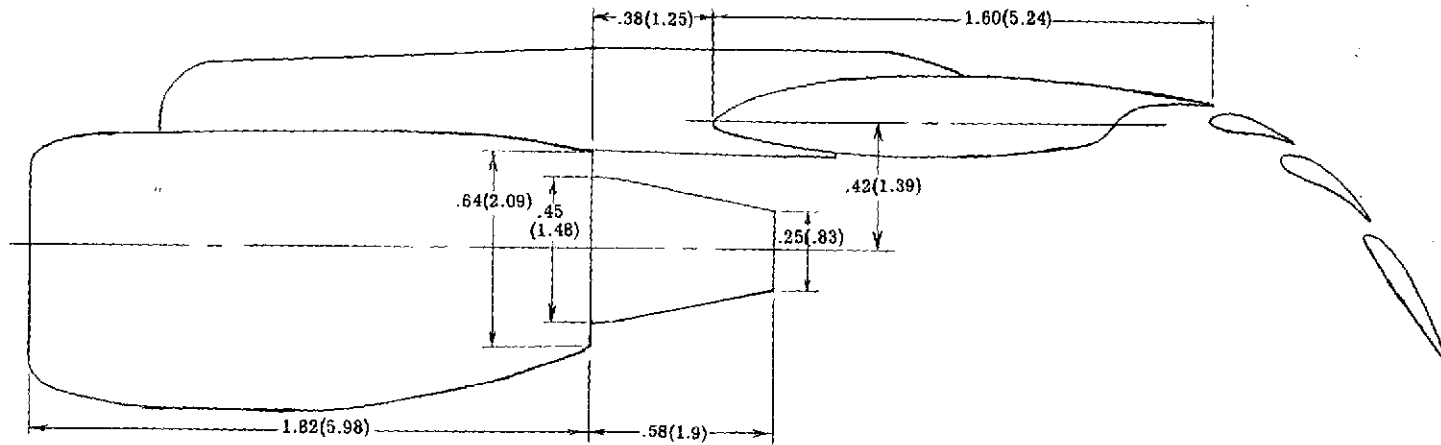
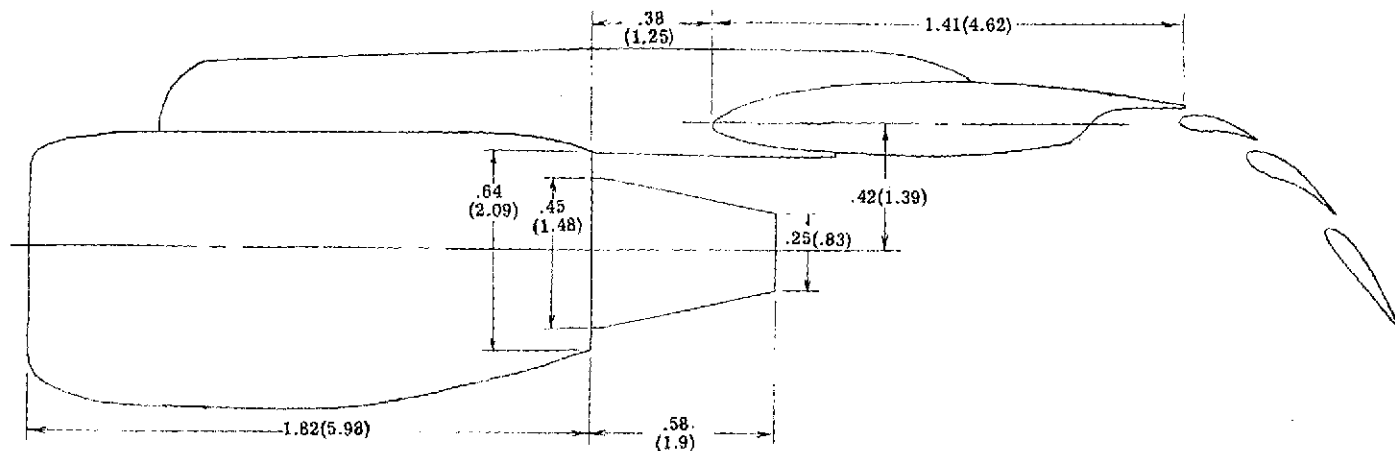


Figure 3.- Concluded.



(a) Inboard engine. $\hat{y} = 0.256$.



(b) Outboard engine. $\hat{y} = 0.420$.

Figure 4. - Relative positions of inboard and outboard engines and flap system. Dimensions are in meters (feet).

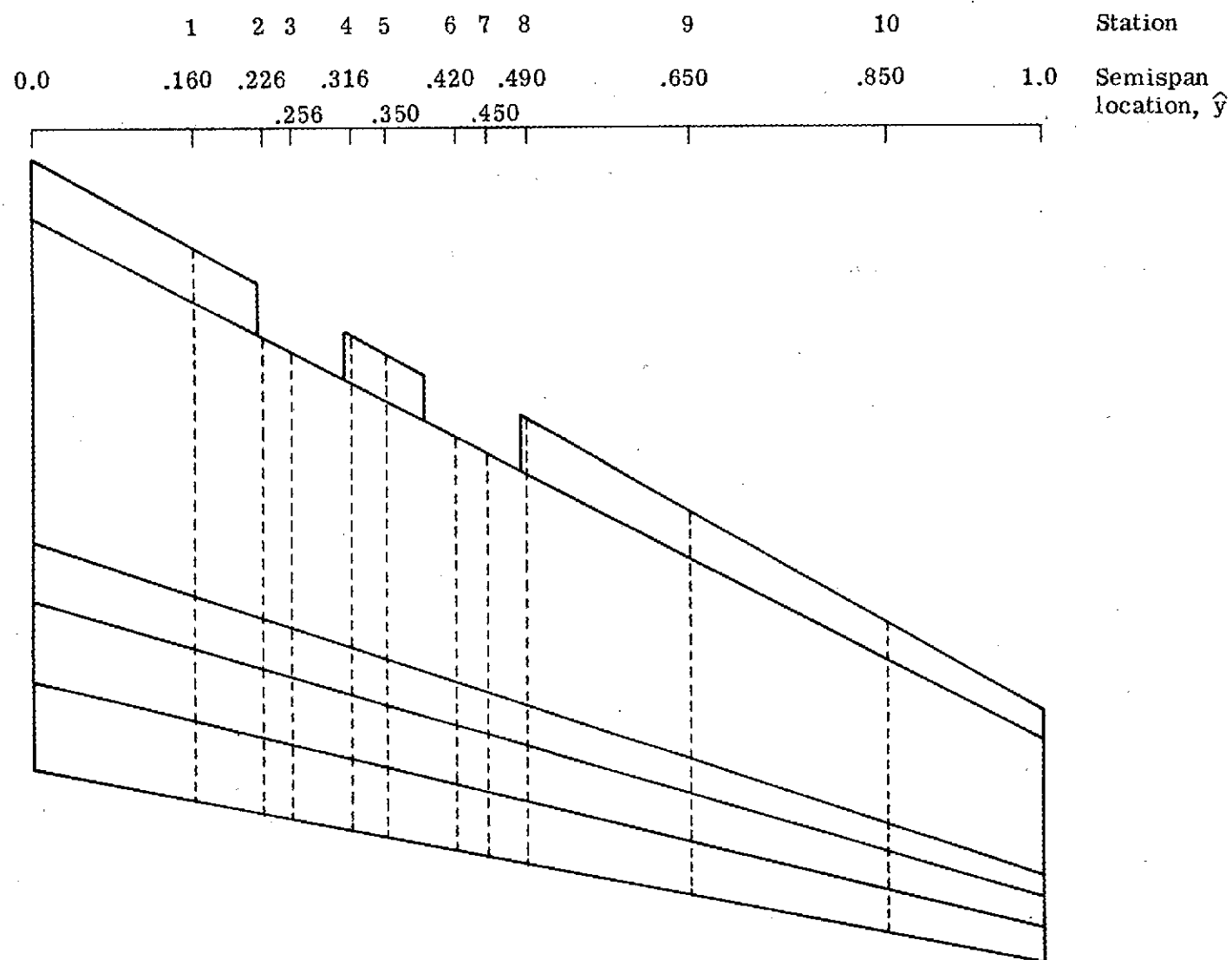
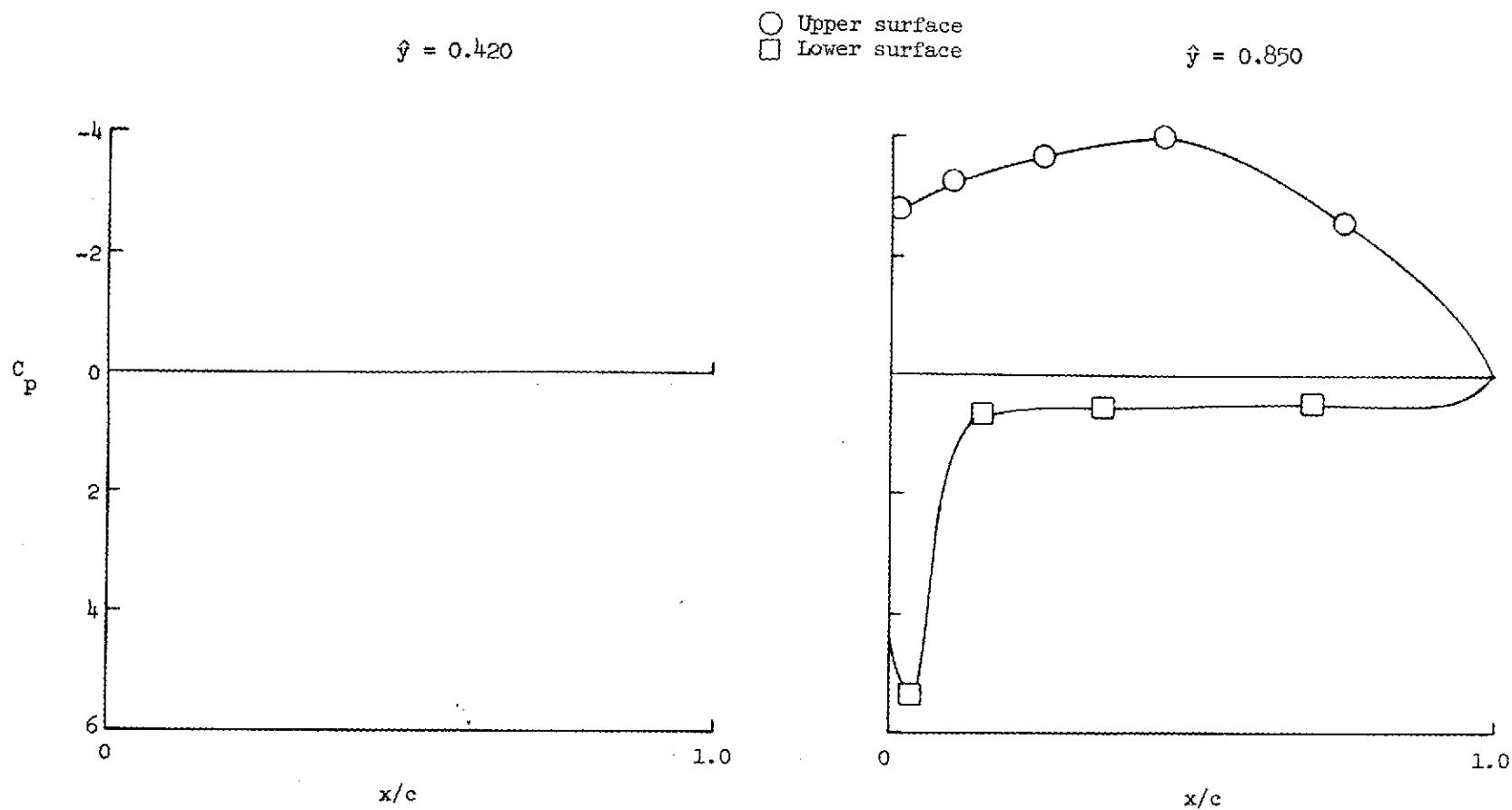
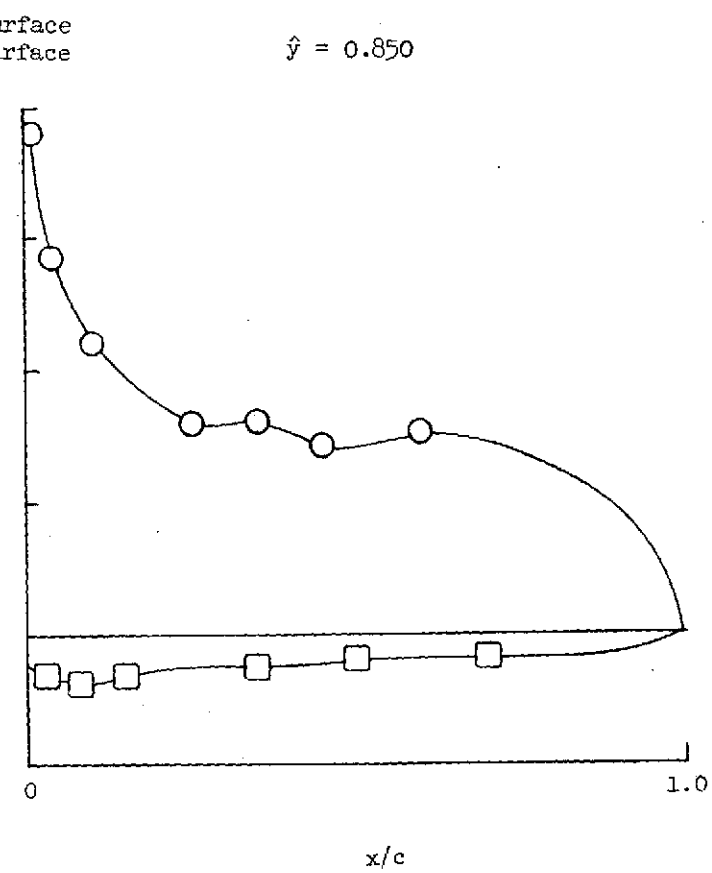
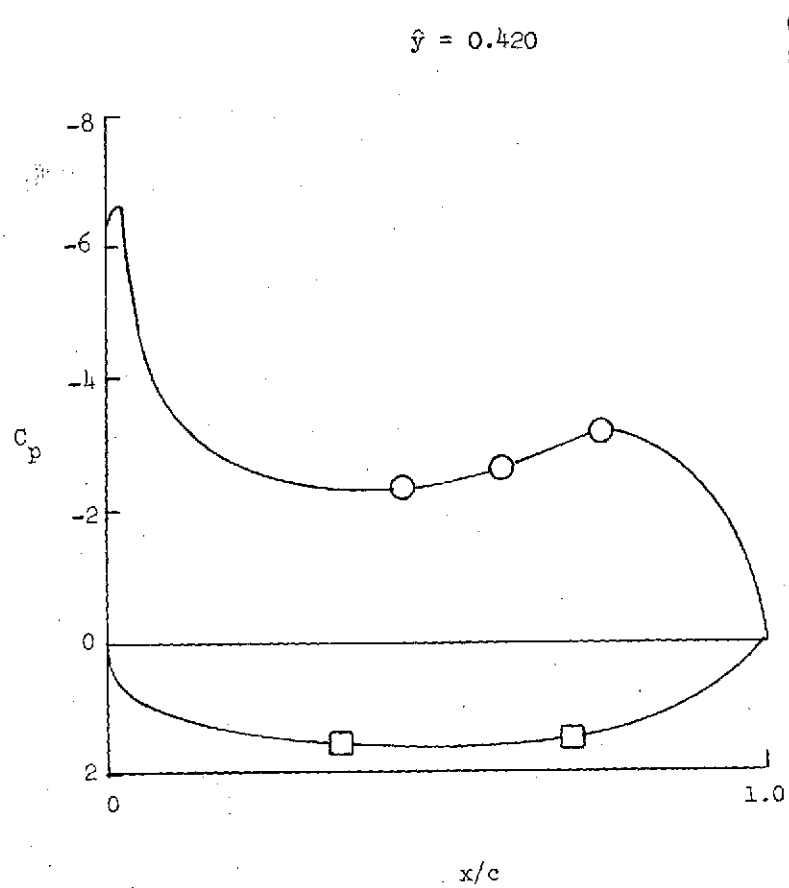


Figure 5. - Spanwise locations of rows of pressure orifices.



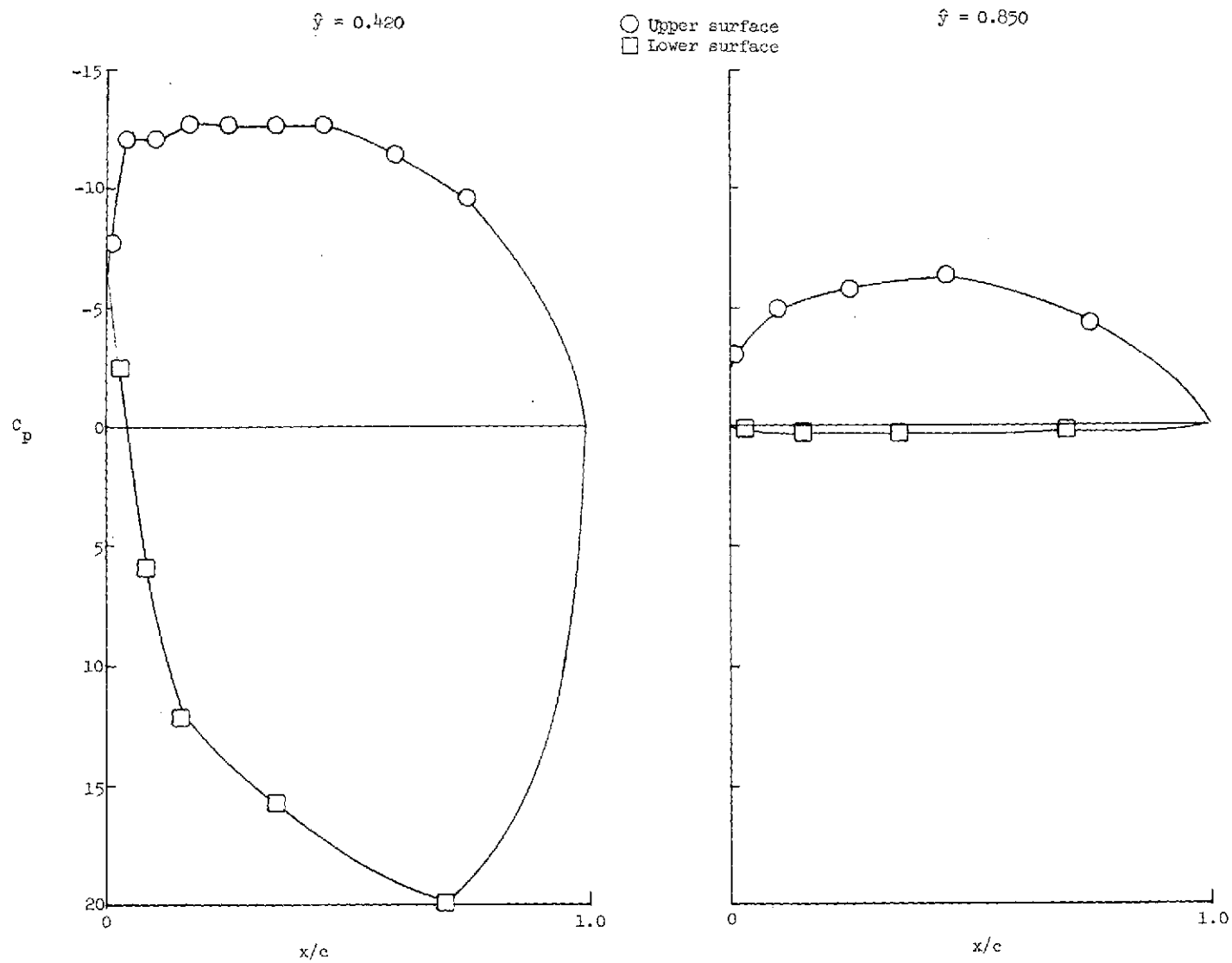
(a) Leading-edge slat.

Figure 6.- Chordwise pressure distributions on slat, wing, and flaps at spanwise stations 0.420 and 0.850.
 $C_{\mu} = 4.0$; $\delta = 15^\circ/35^\circ/55^\circ$; $\alpha = 7^\circ$.



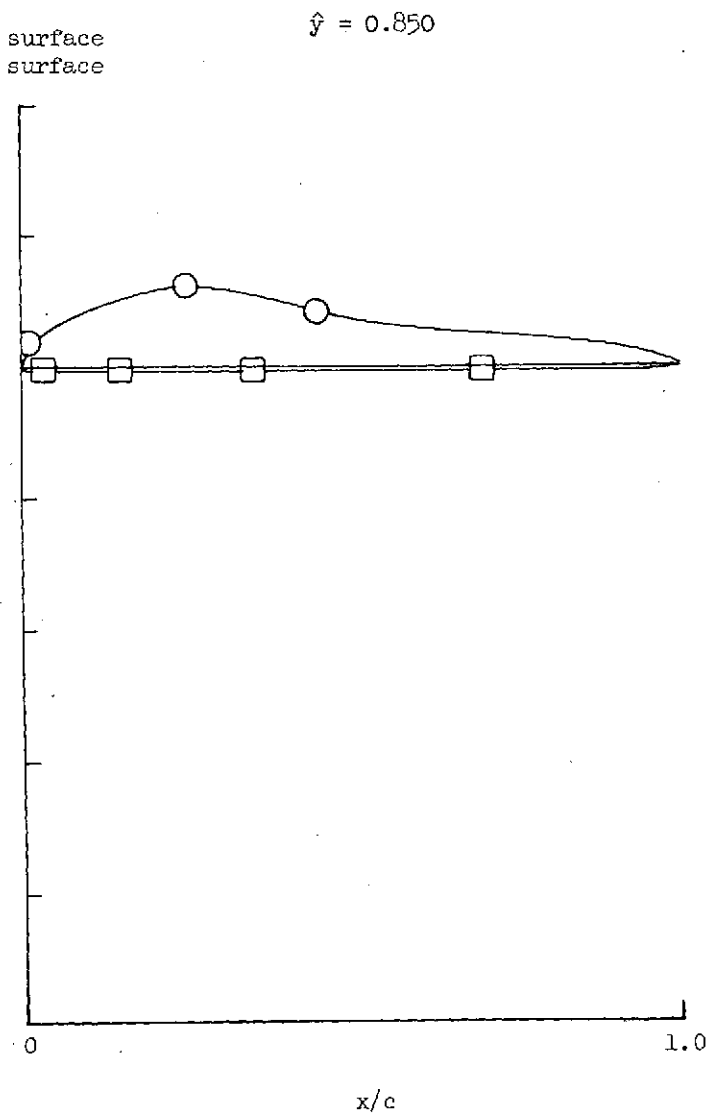
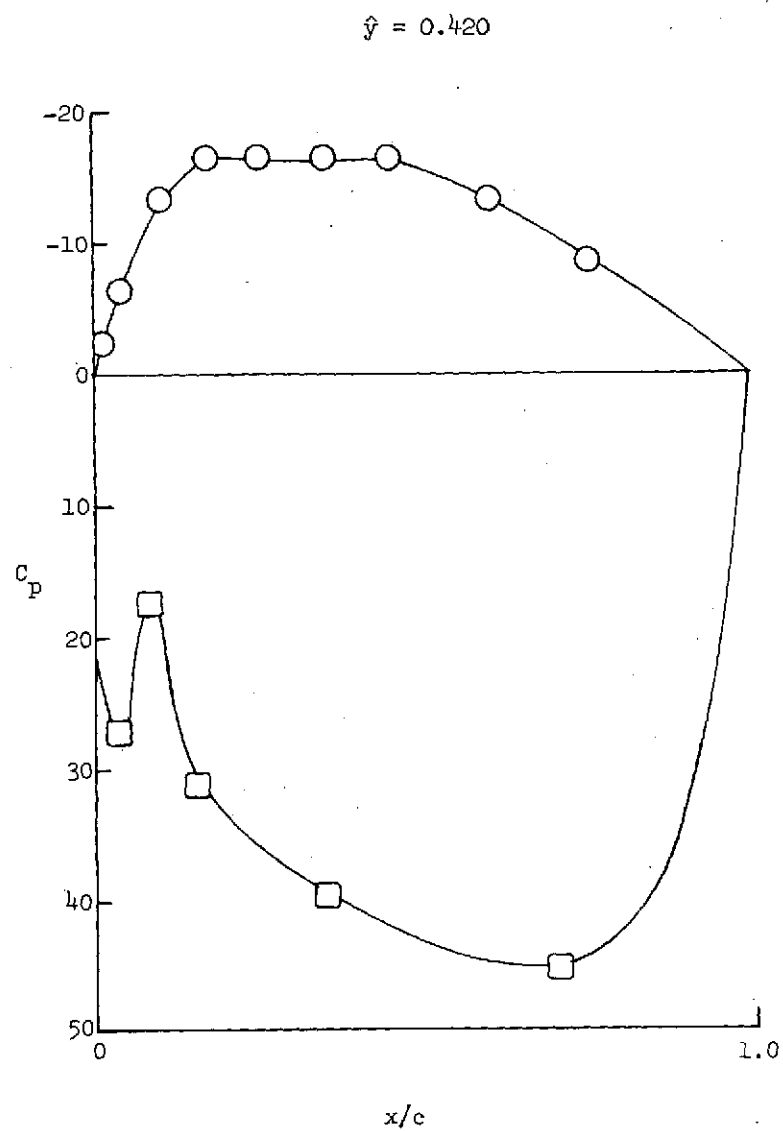
(b) Wing.

Figure 6.- Continued.



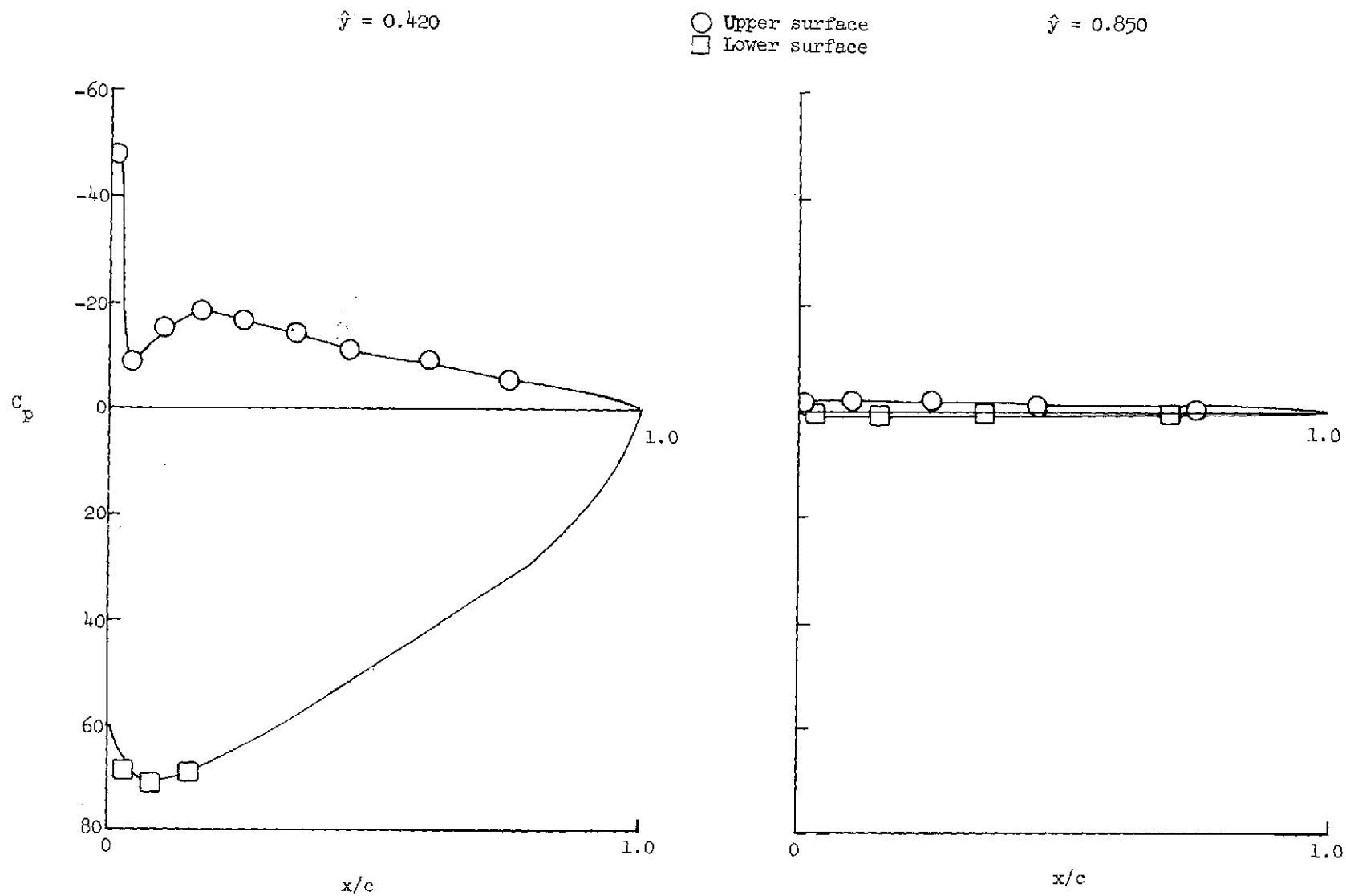
(c) Flap 1.

Figure 6.- Continued.



(d) Flap 2.

Figure 6. - Continued.



(e) Flap 3.

Figure 6.- Concluded.

ORIGINAL PAGE IS
OF POOR QUALITY

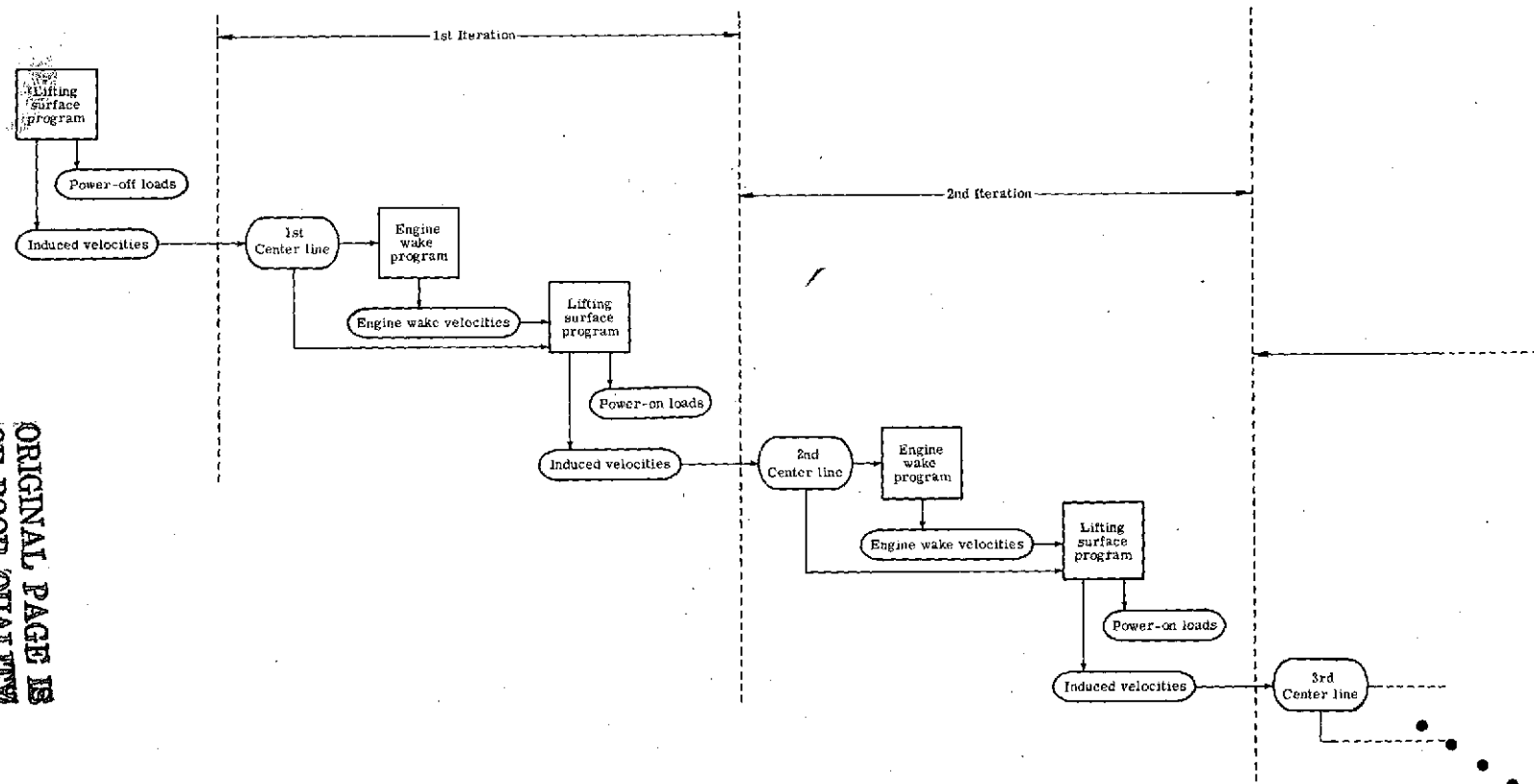


Figure 7.- Flow chart of the analytical program of reference 19.

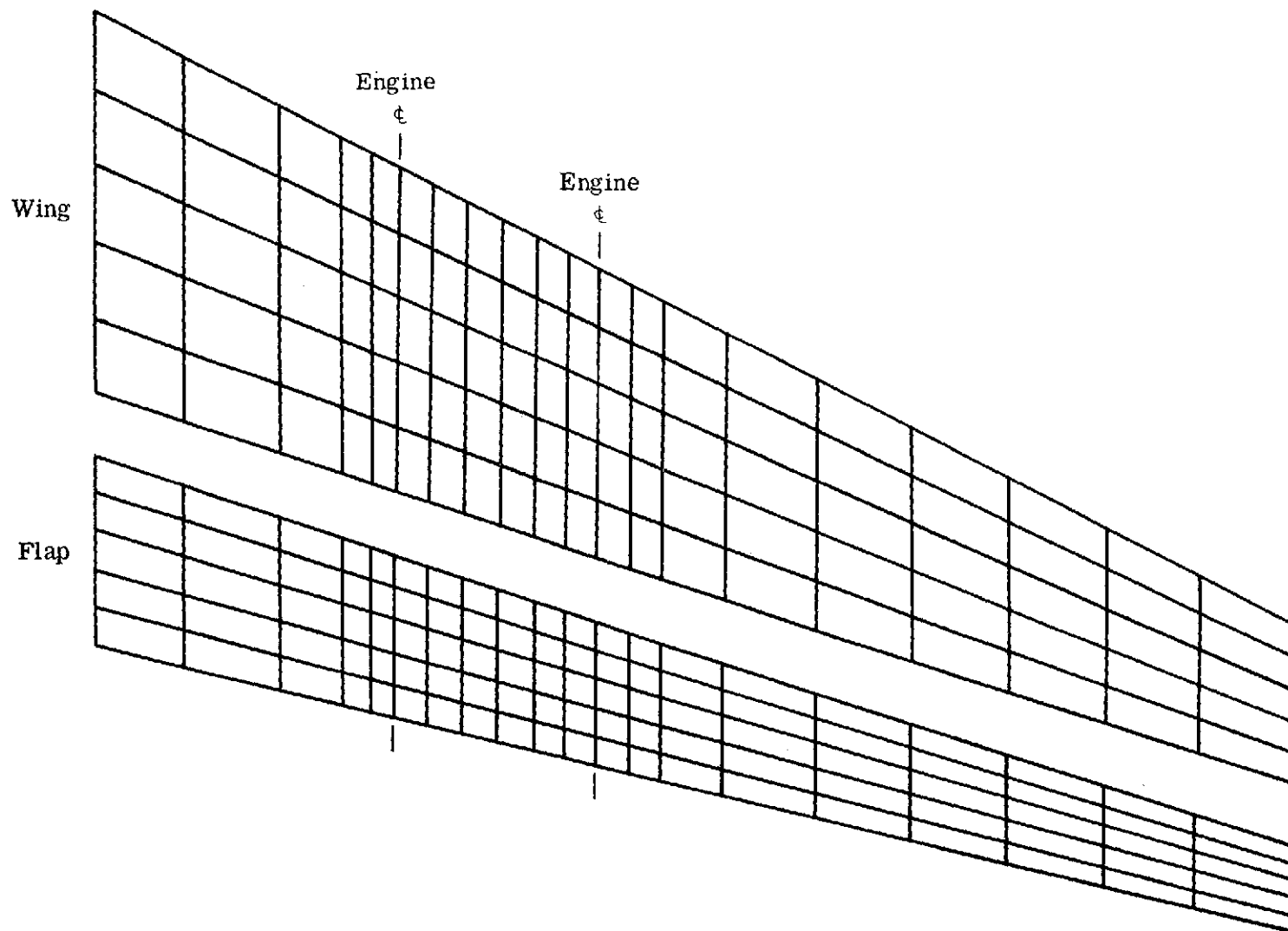
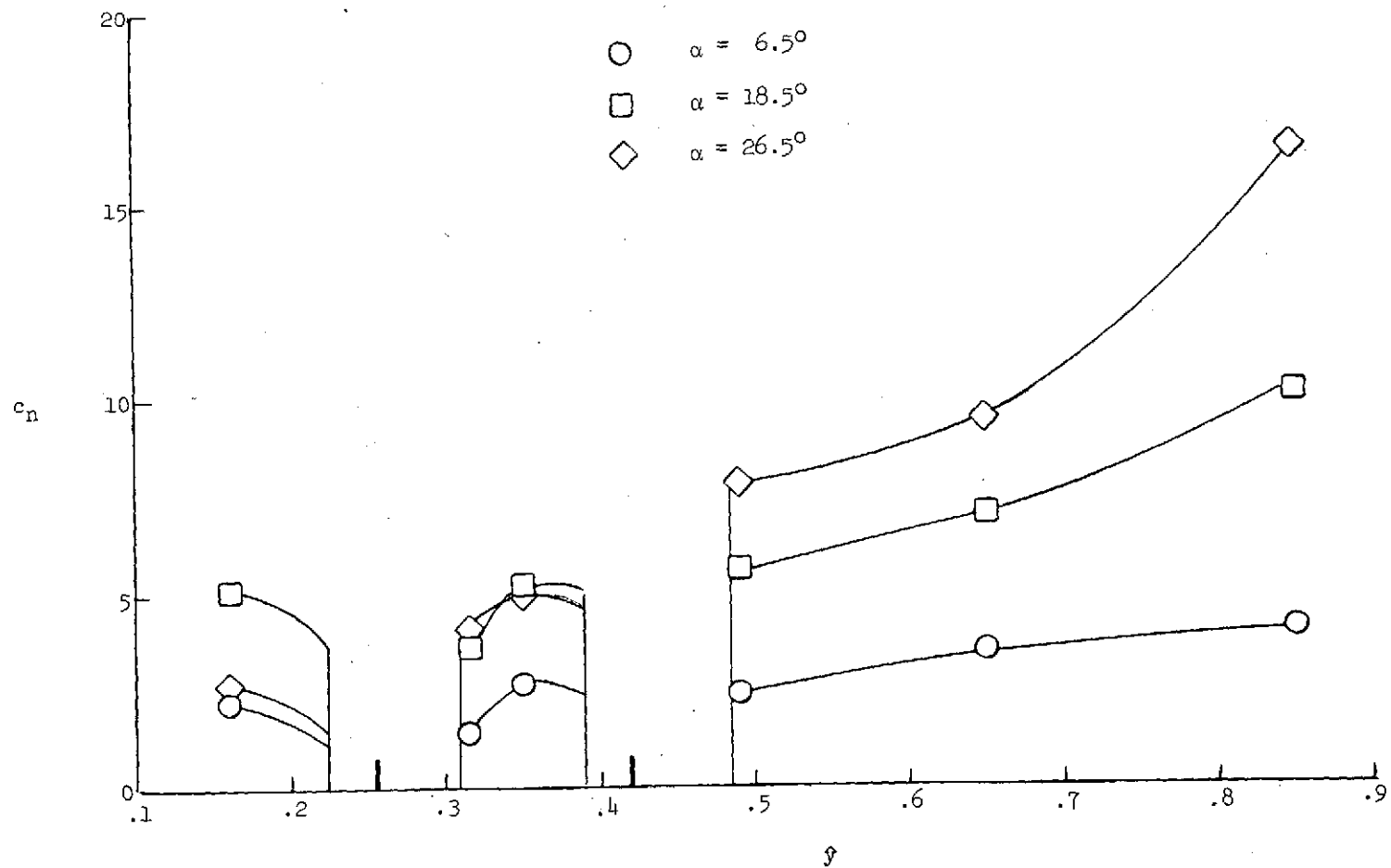


Figure 8.- Paneling arrangement on wing and flap.



(a) Leading-edge slat.

Figure 9.- Spanwise normal-force distributions on slat, wing, and flaps for three angles of attack.
 $C_\mu = 4.0$; $\delta = 15^\circ/35^\circ/55^\circ$.

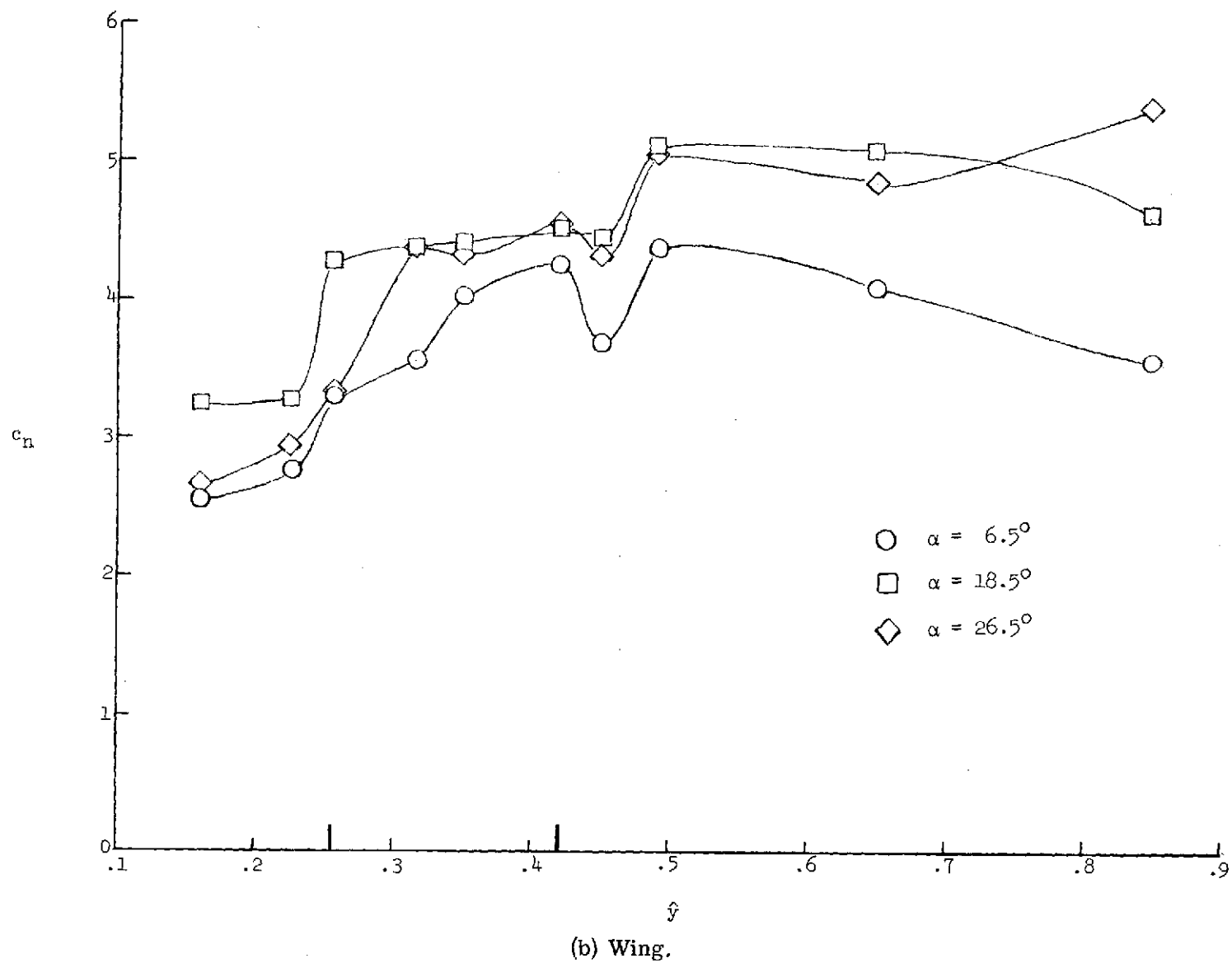
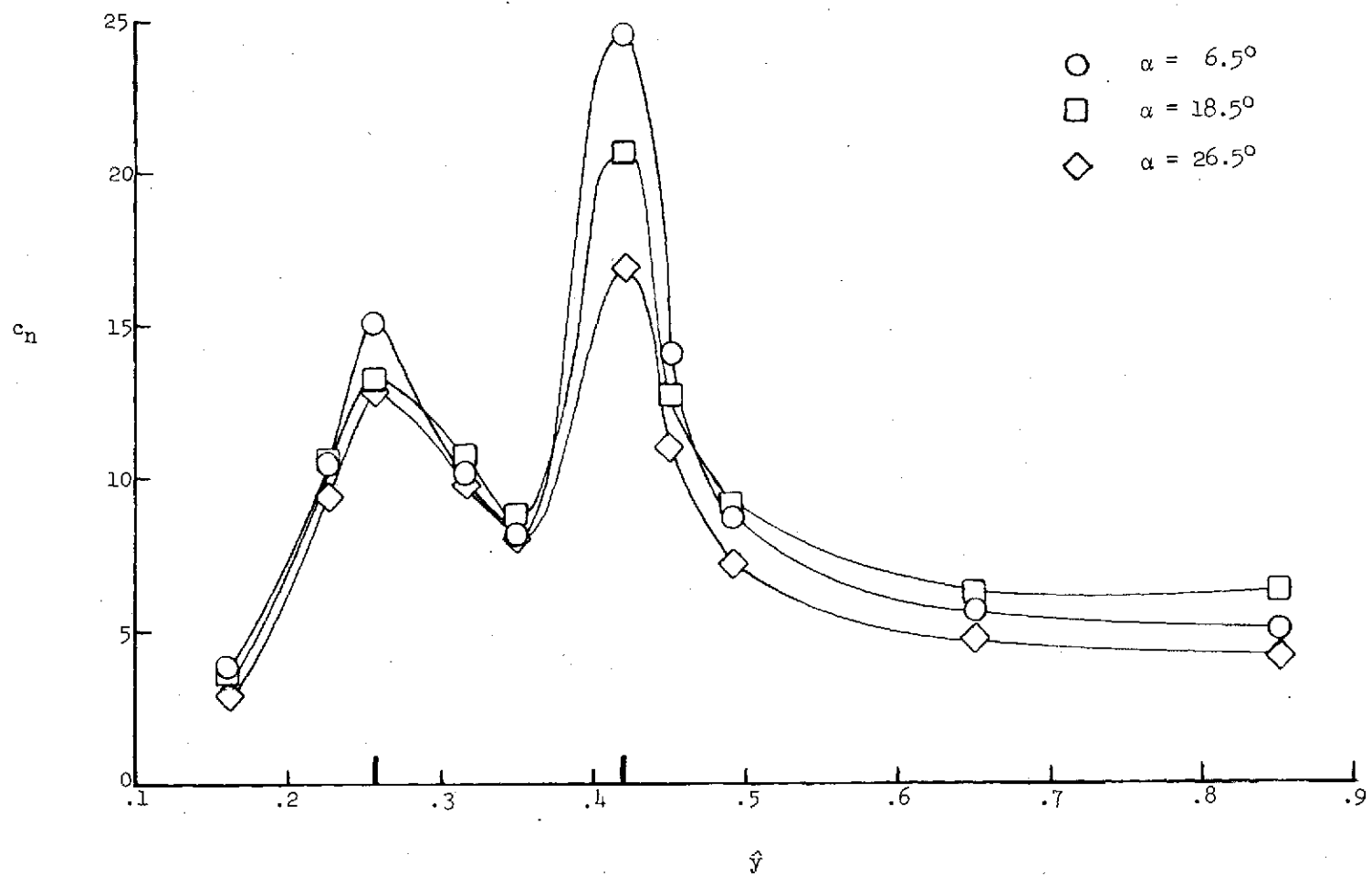
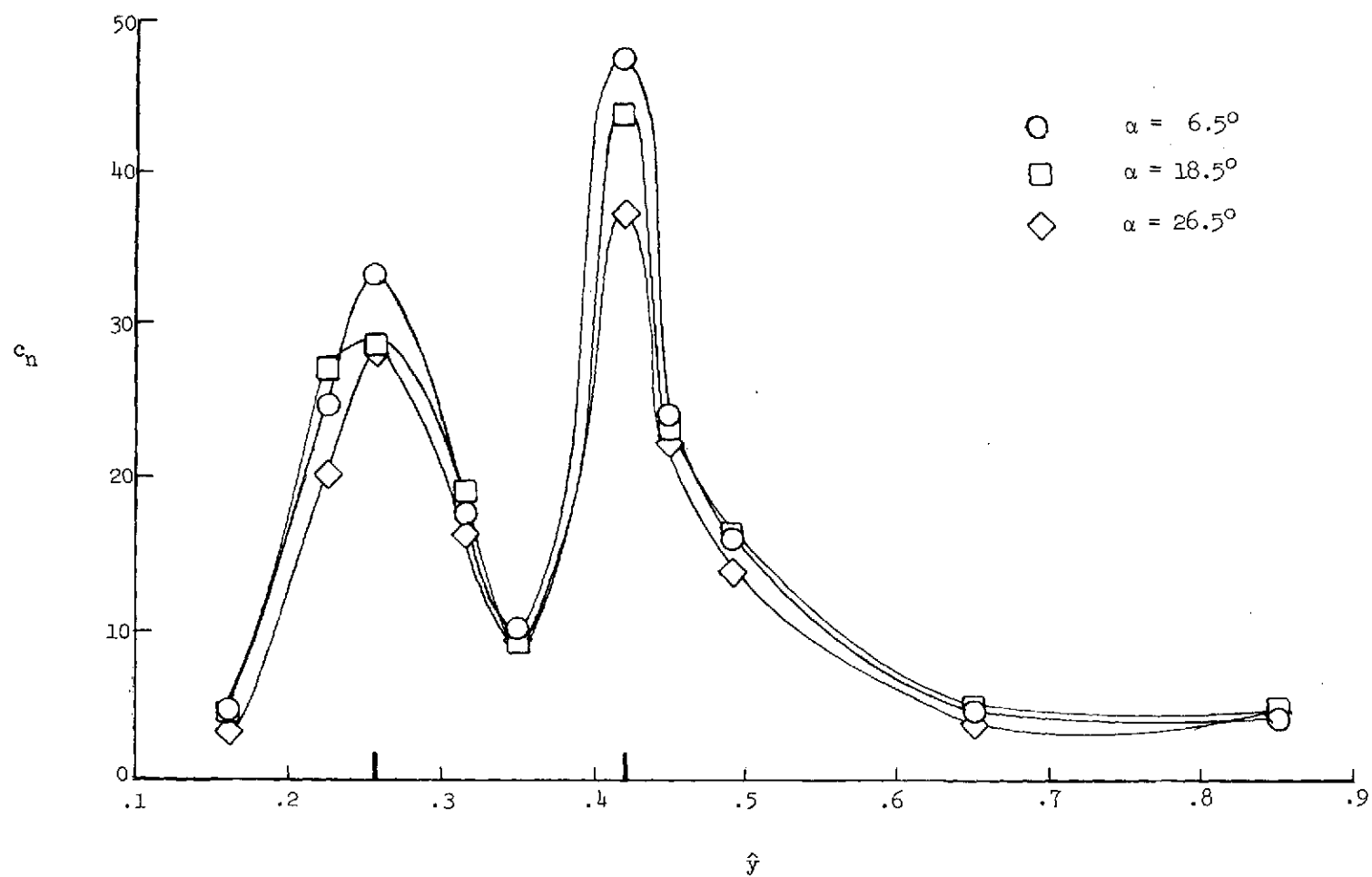


Figure 9.- Continued.



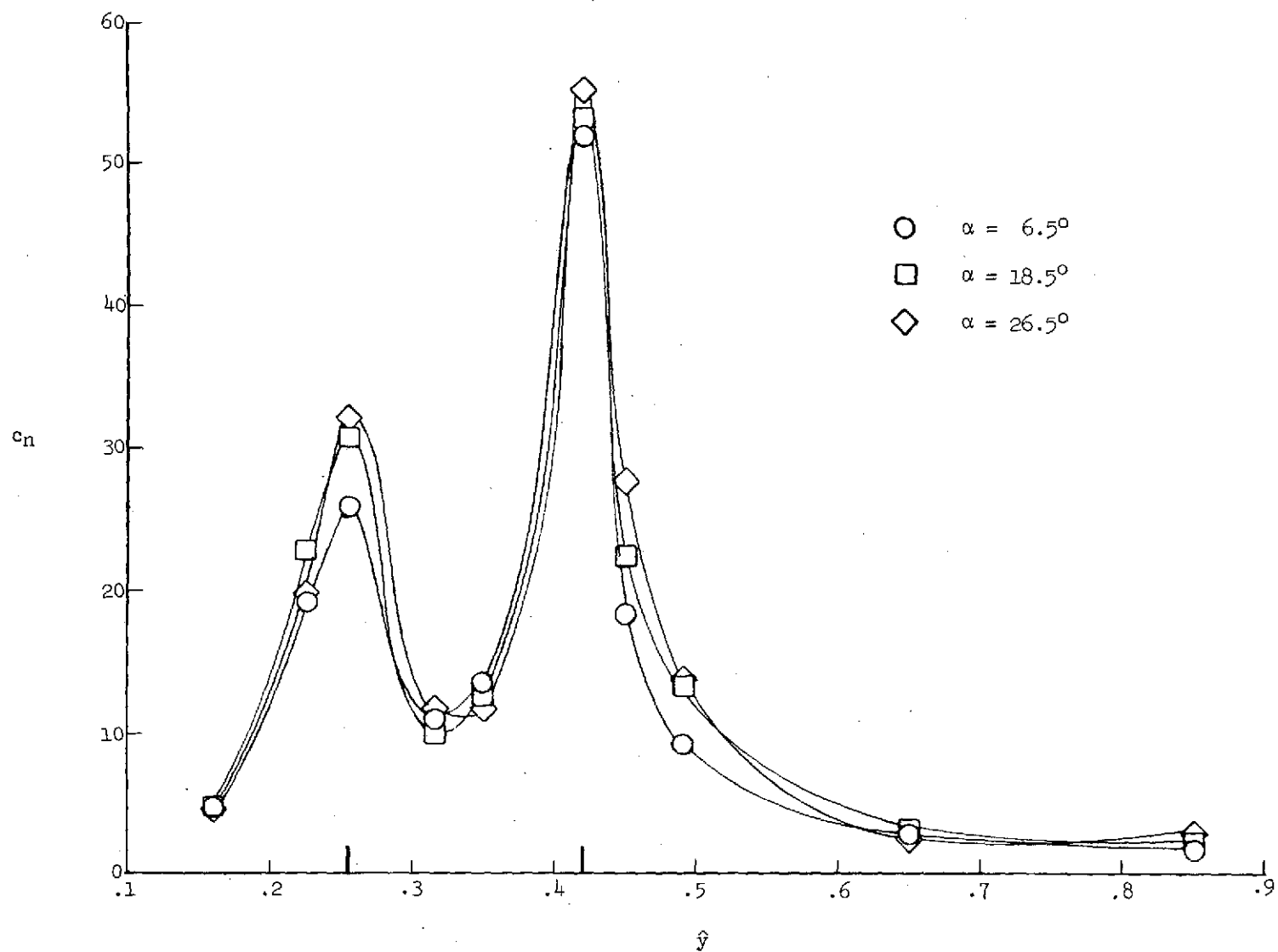
(c) Flap 1.

Figure 9. - Continued.



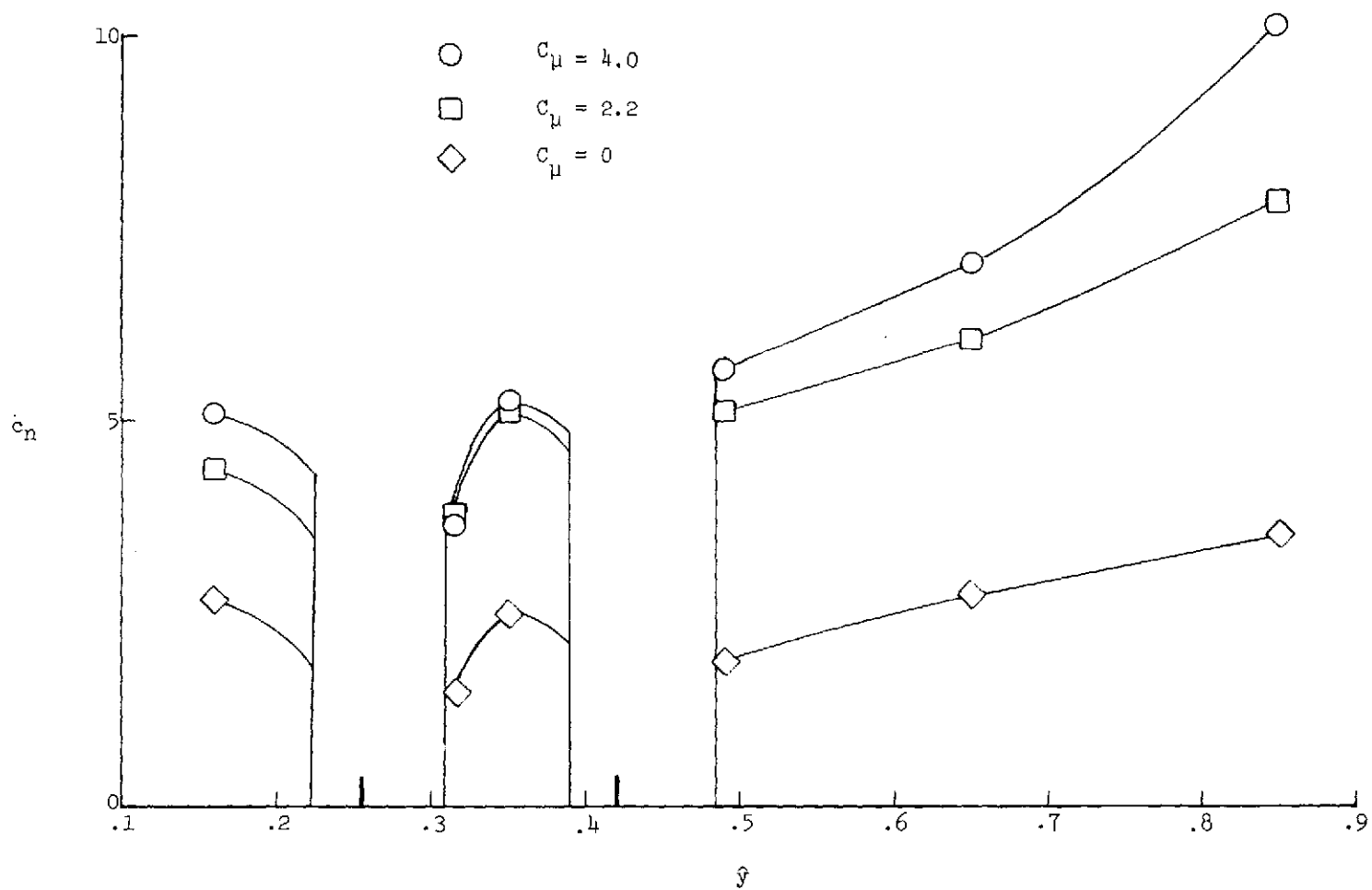
(d) Flap 2.

Figure 9.- Continued.



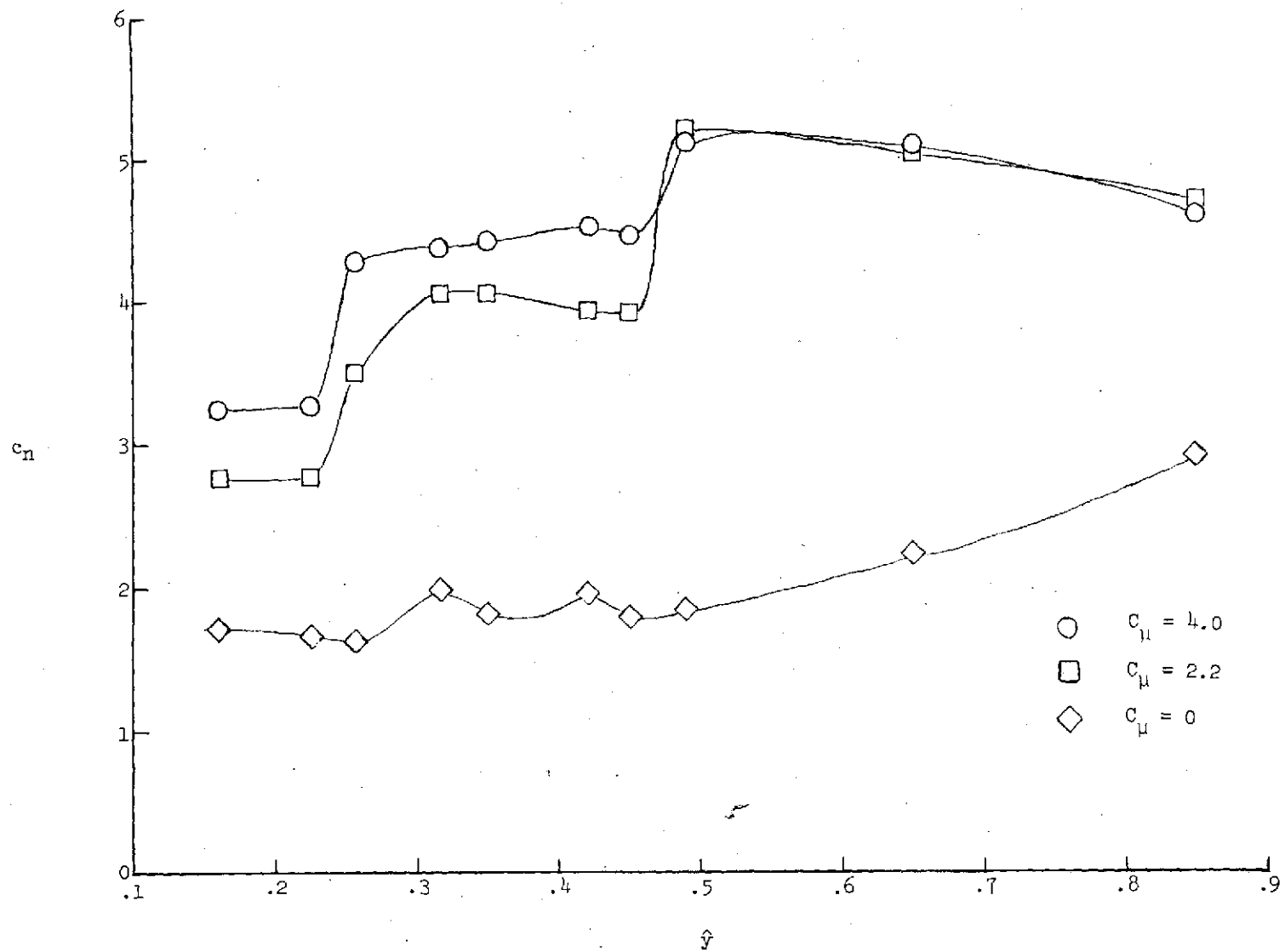
(e) Flap 3.

Figure 9.- Concluded.



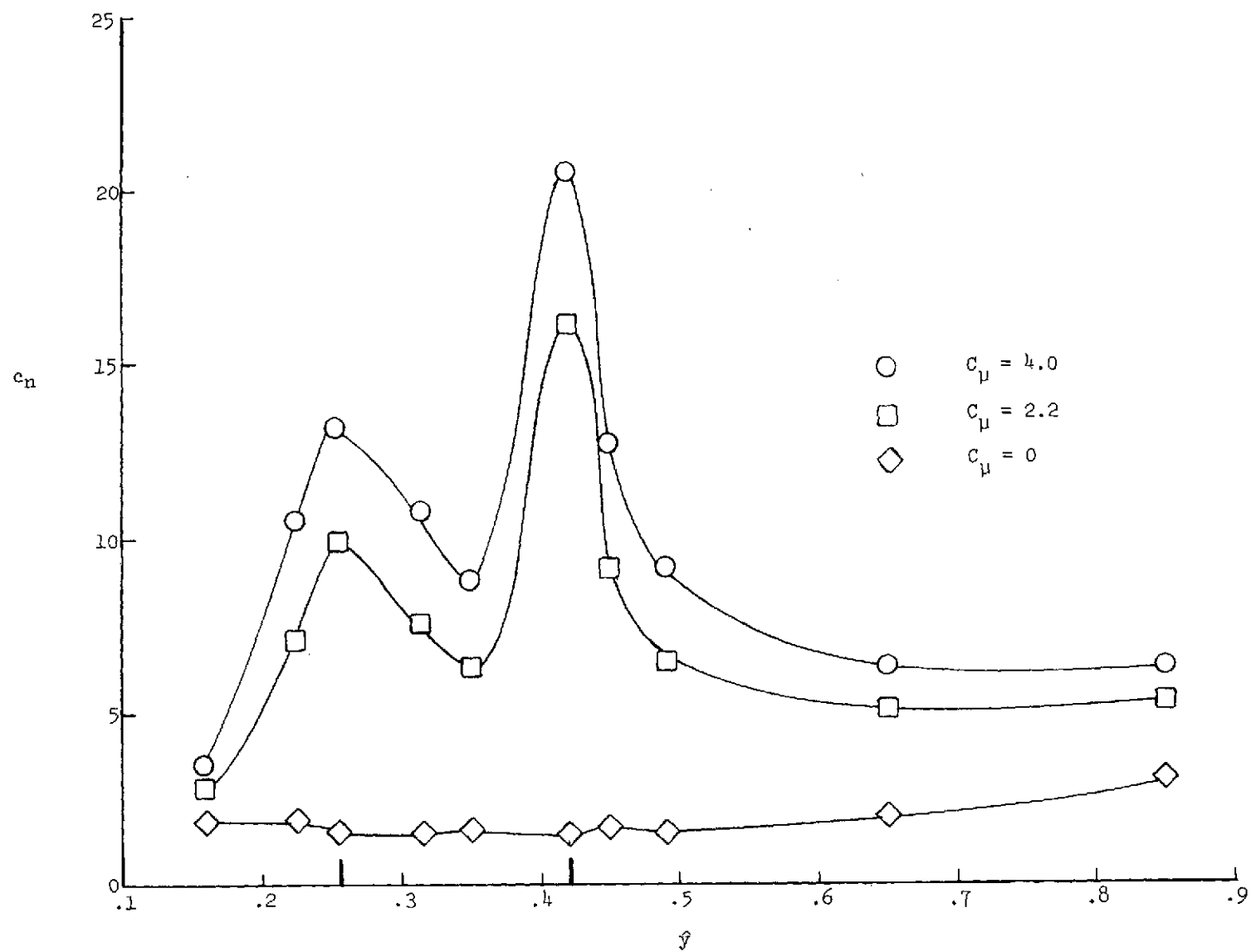
(a) Leading-edge slat.

Figure 10.- Spanwise normal-force distributions on slat, wing, and flaps for three thrust settings.
 $\delta = 15^\circ/35^\circ/55^\circ$; $\alpha_u = 16^\circ$.



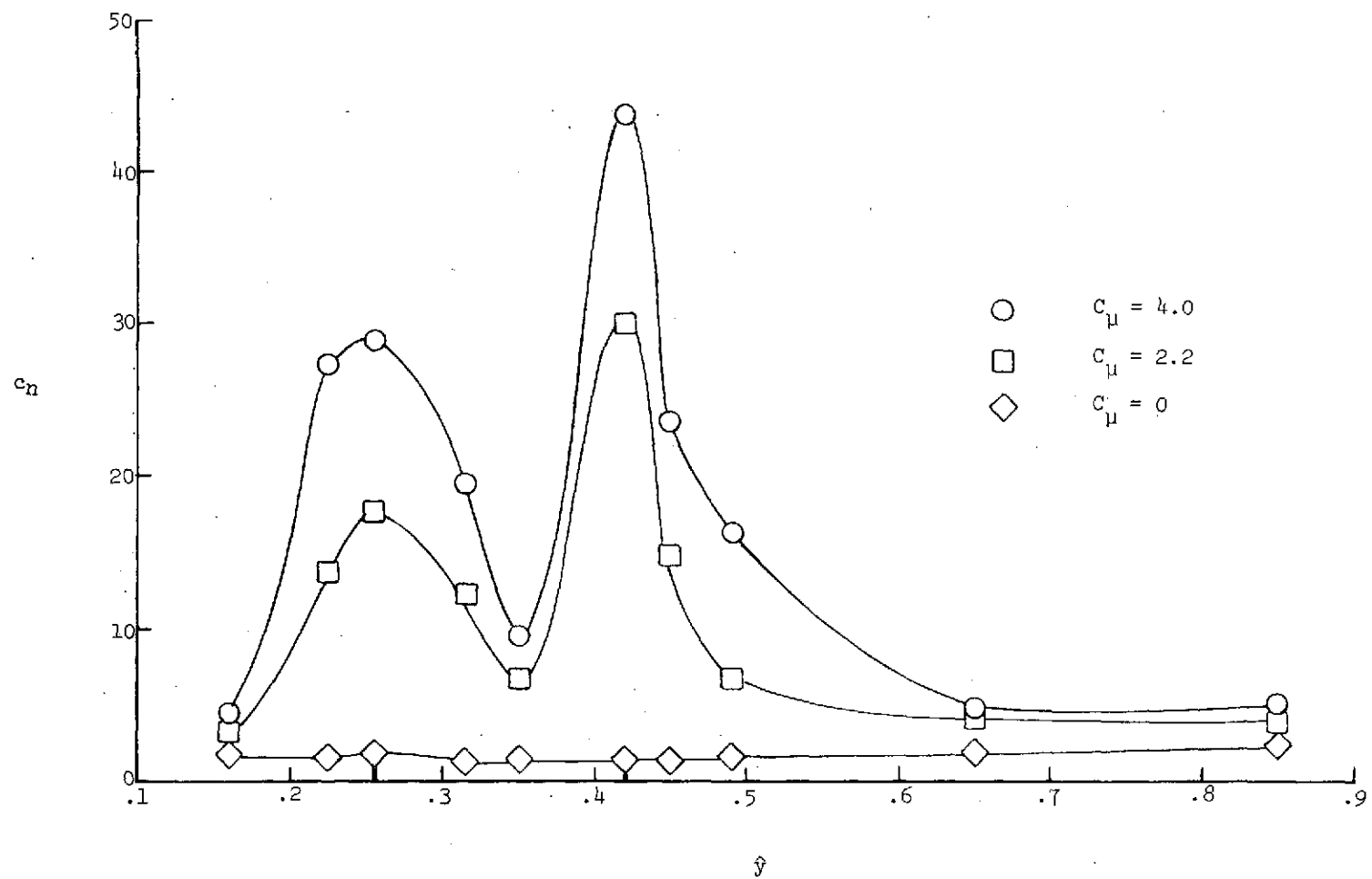
(b) Wing.

Figure 10.- Continued.



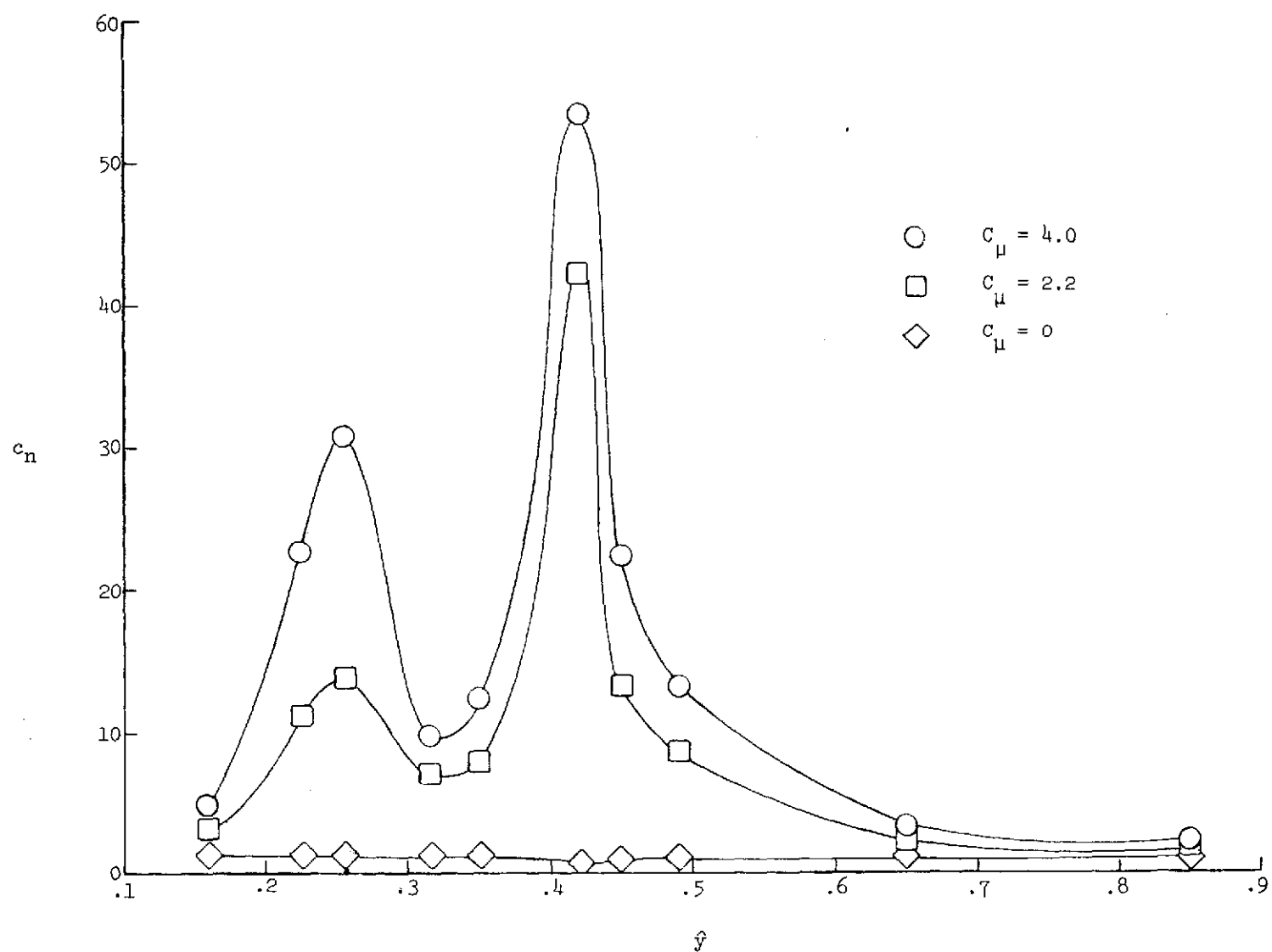
(c) Flap 1.

Figure 10.- Continued.



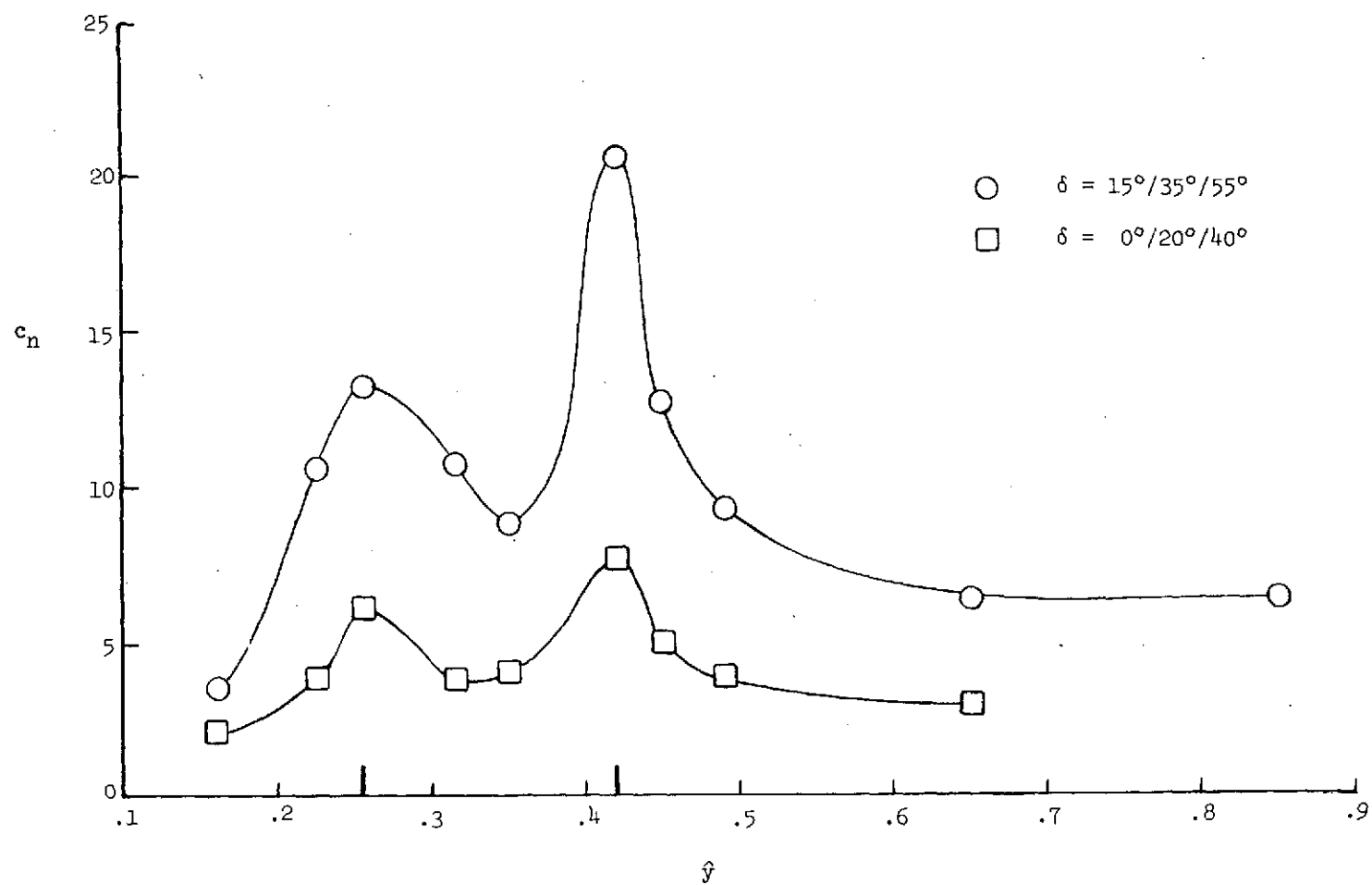
(d) Flap 2.

Figure 10.- Continued.



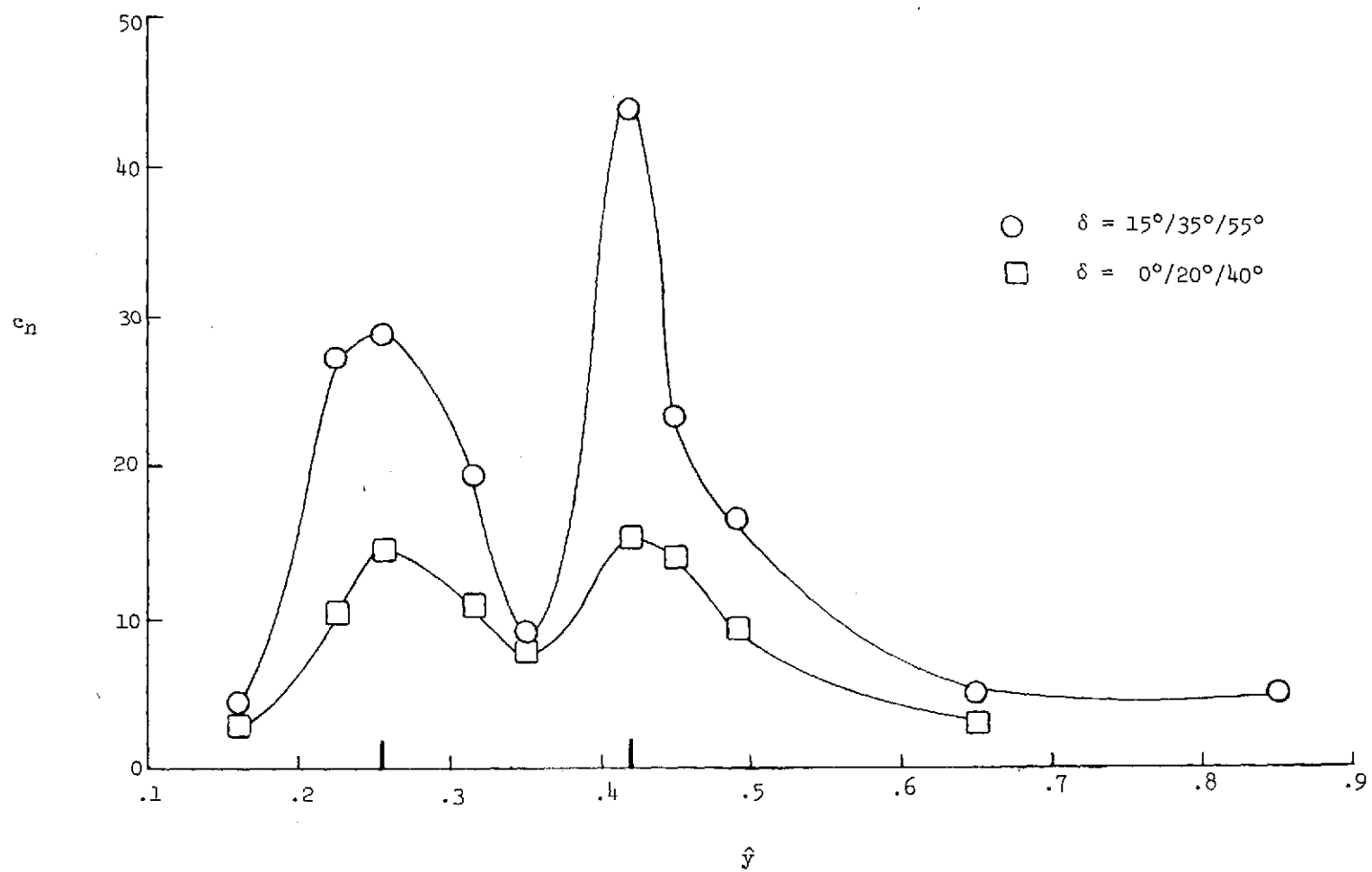
(e) Flap 3.

Figure 10.- Concluded.



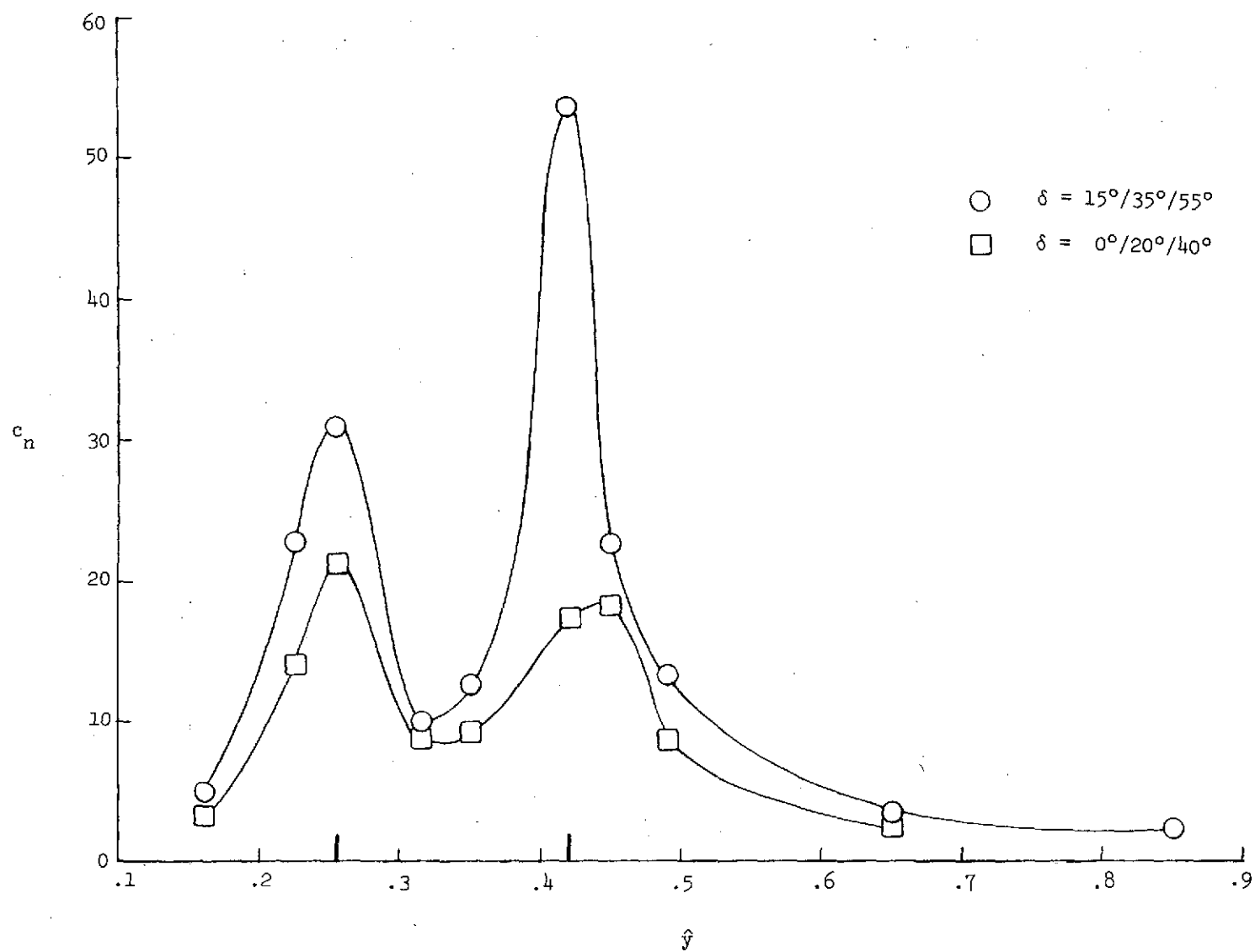
(a) Flap 1.

Figure 11.- Spanwise normal-force distributions on flaps for two flap deflection configurations. $C_\mu = 4.0$; $\alpha_u = 16^\circ$.



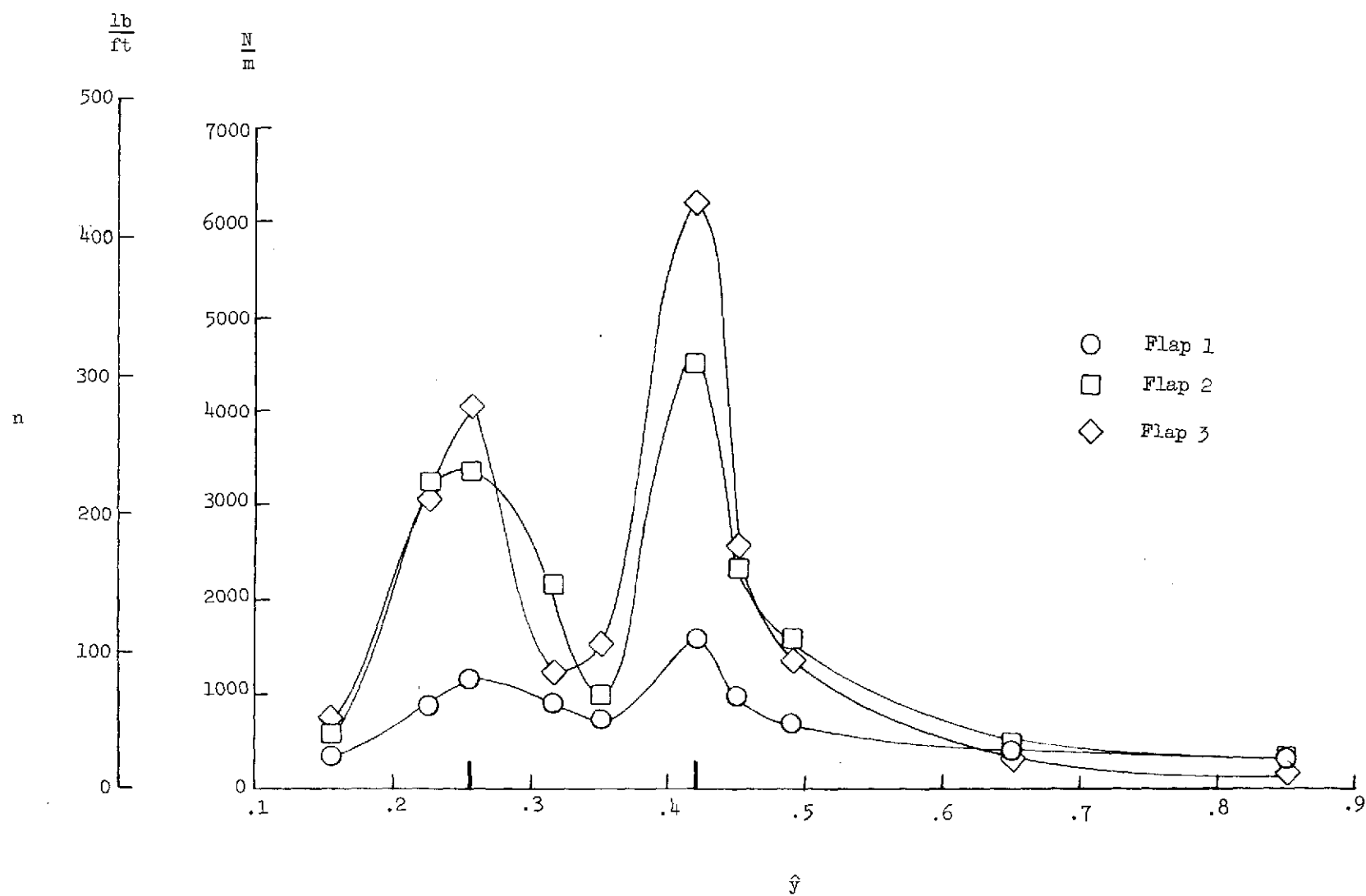
(b) Flap 2.

Figure 11.- Continued.



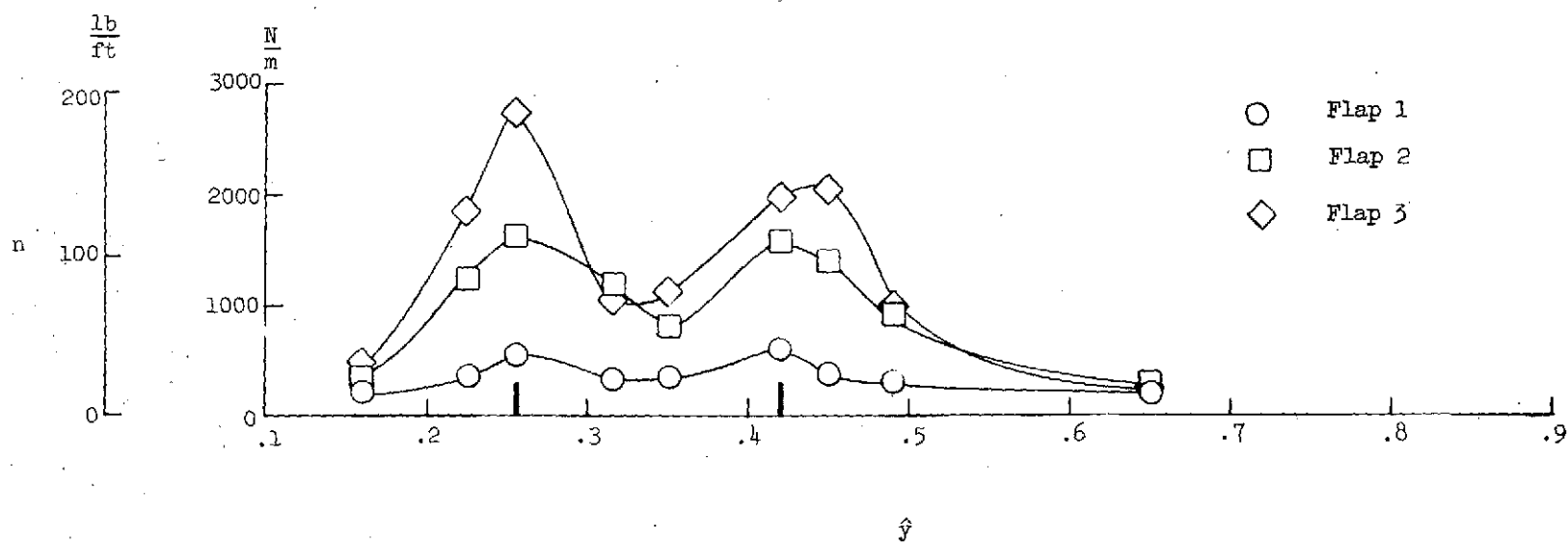
(c) Flap 3.

Figure 11.- Concluded.



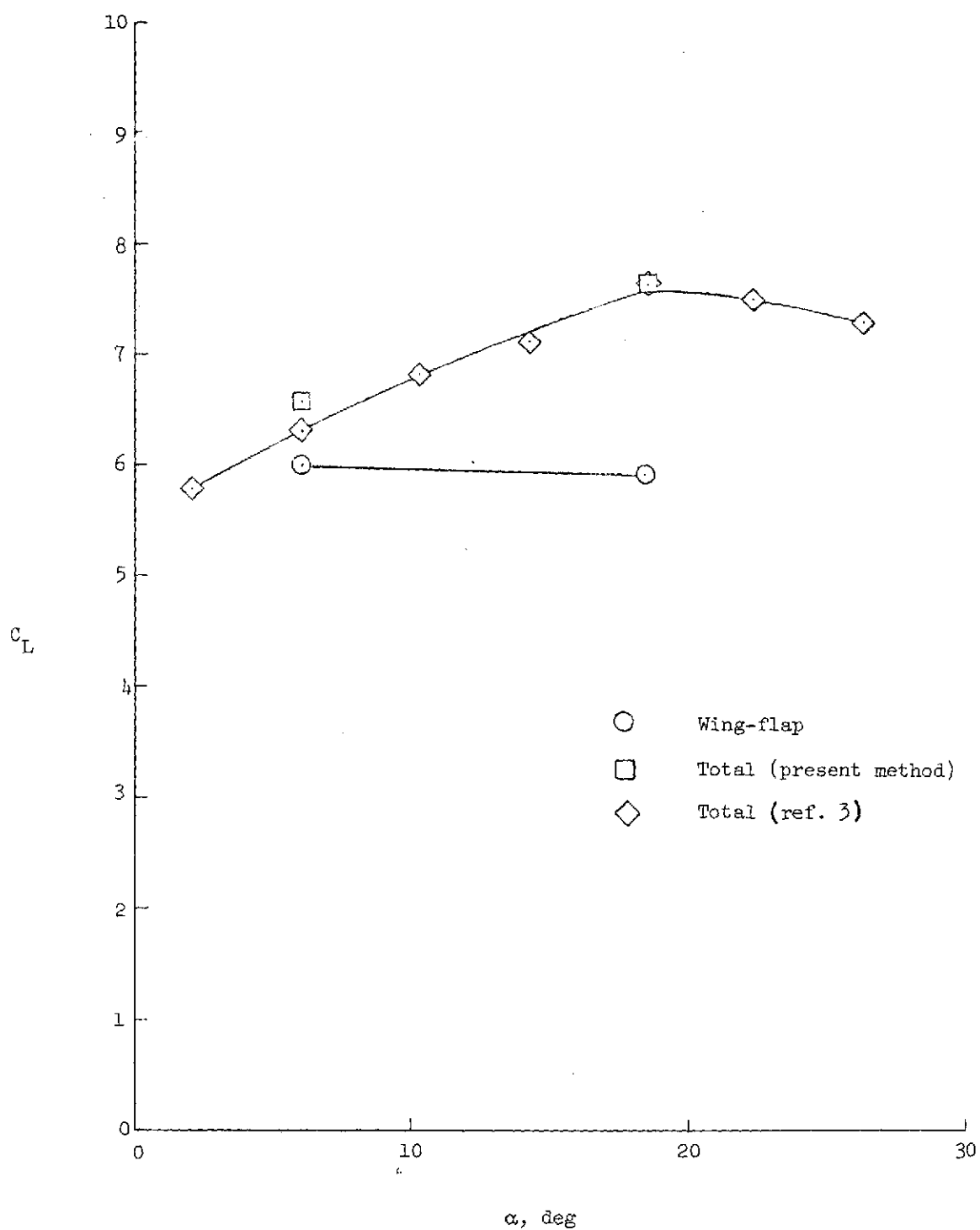
(a) $\delta = 15^\circ/35^\circ/55^\circ$; $\alpha = 19.0^\circ$.

Figure 12.- Comparison of individual flap normal-force distributions for two flap deflection configurations. $C_{\mu} = 4.0$.



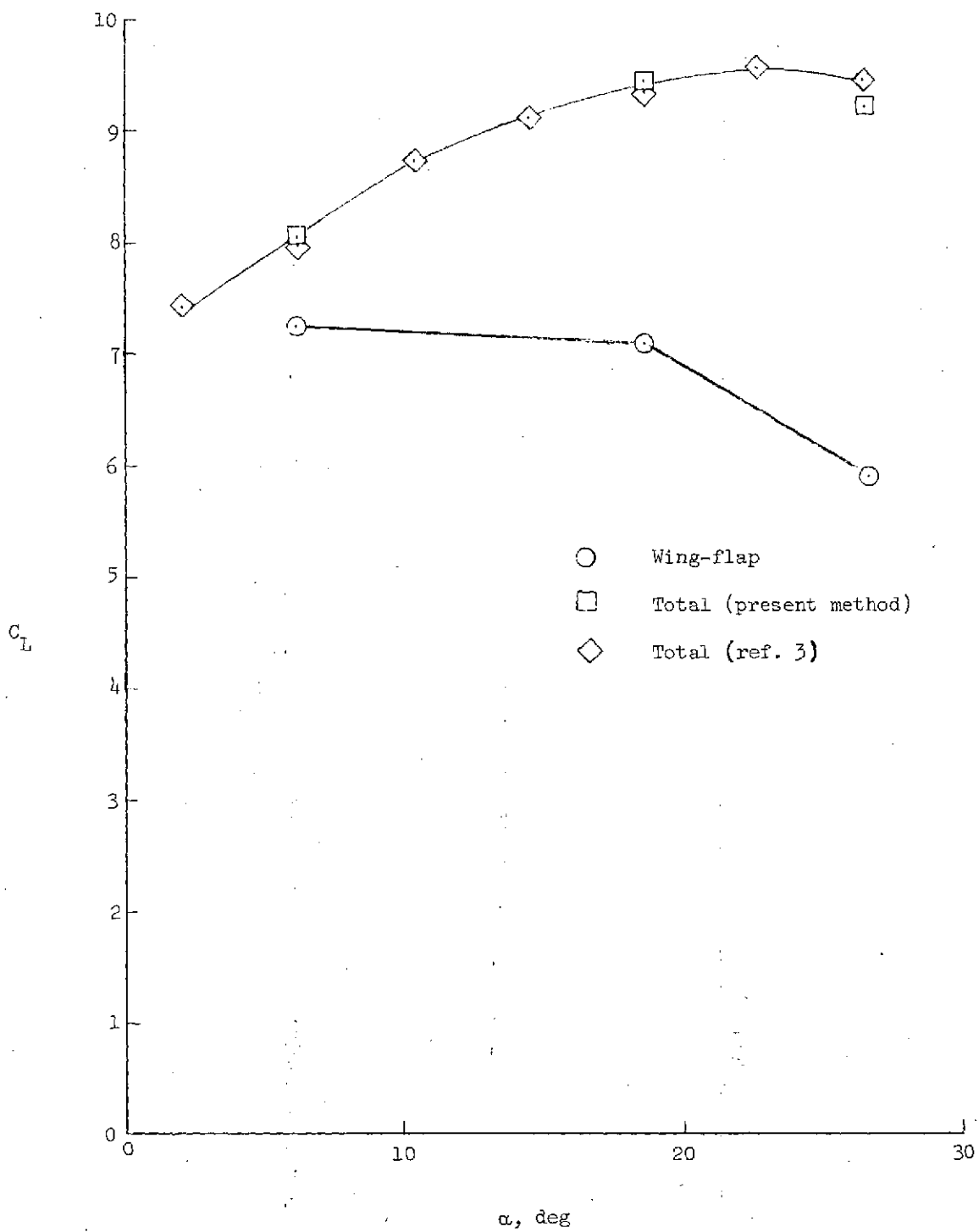
(b) $\delta = 0^\circ/20^\circ/40^\circ$; $\alpha = 18^\circ$.

Figure 12.- Concluded.



(a) $C_{\mu} = 2.2$.

Figure 13.- Lift curves as determined from pressure orifices compared with lift curves from reference 3.



(b) $C_{\mu} = 4.0$.

Figure 13.- Concluded.

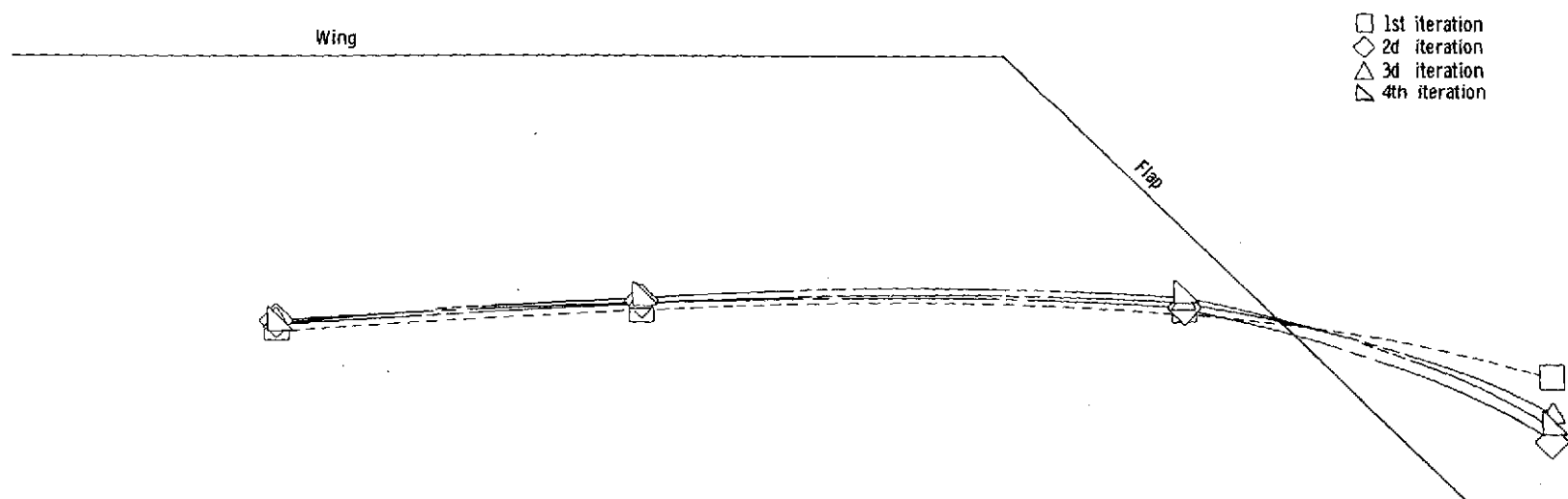
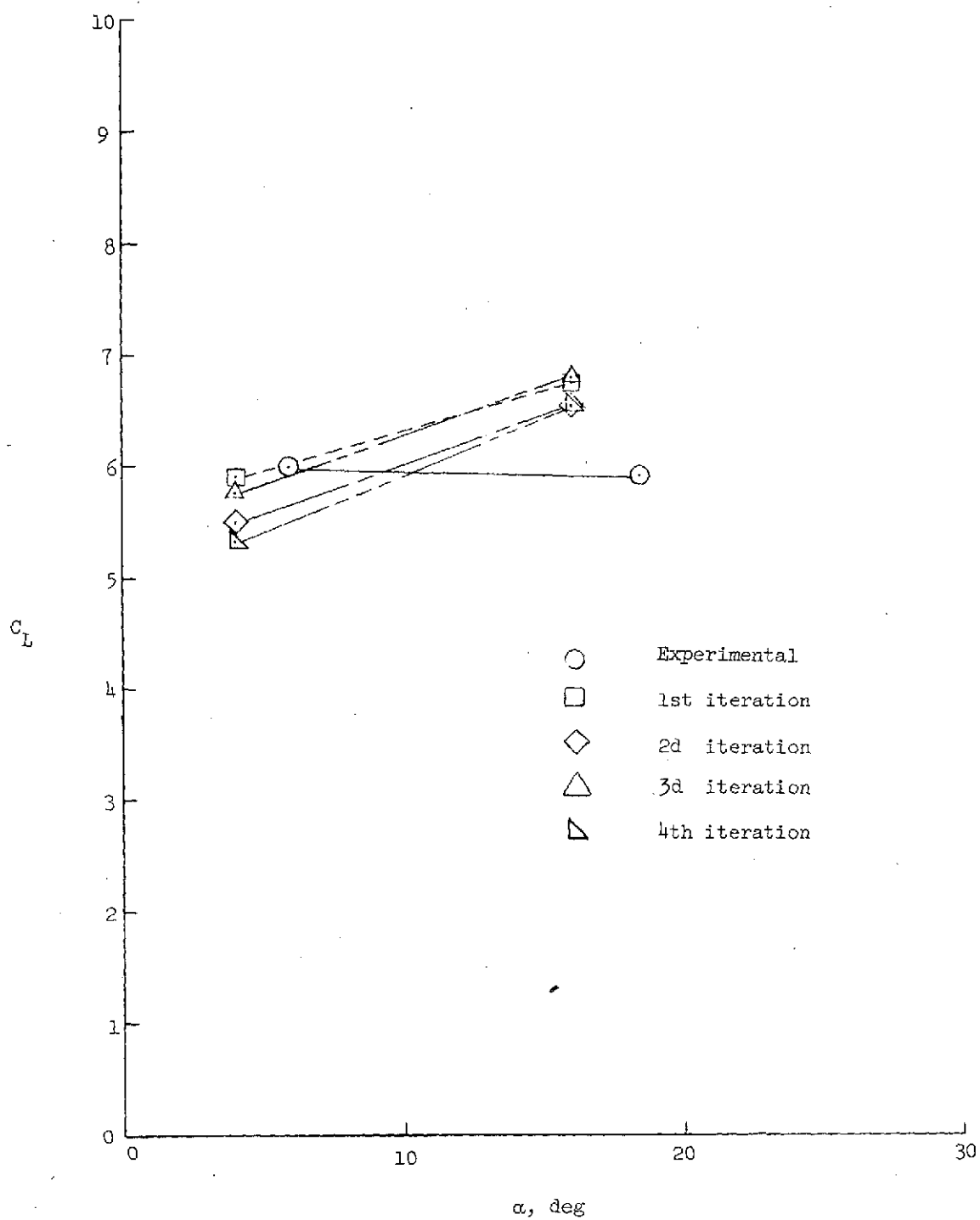
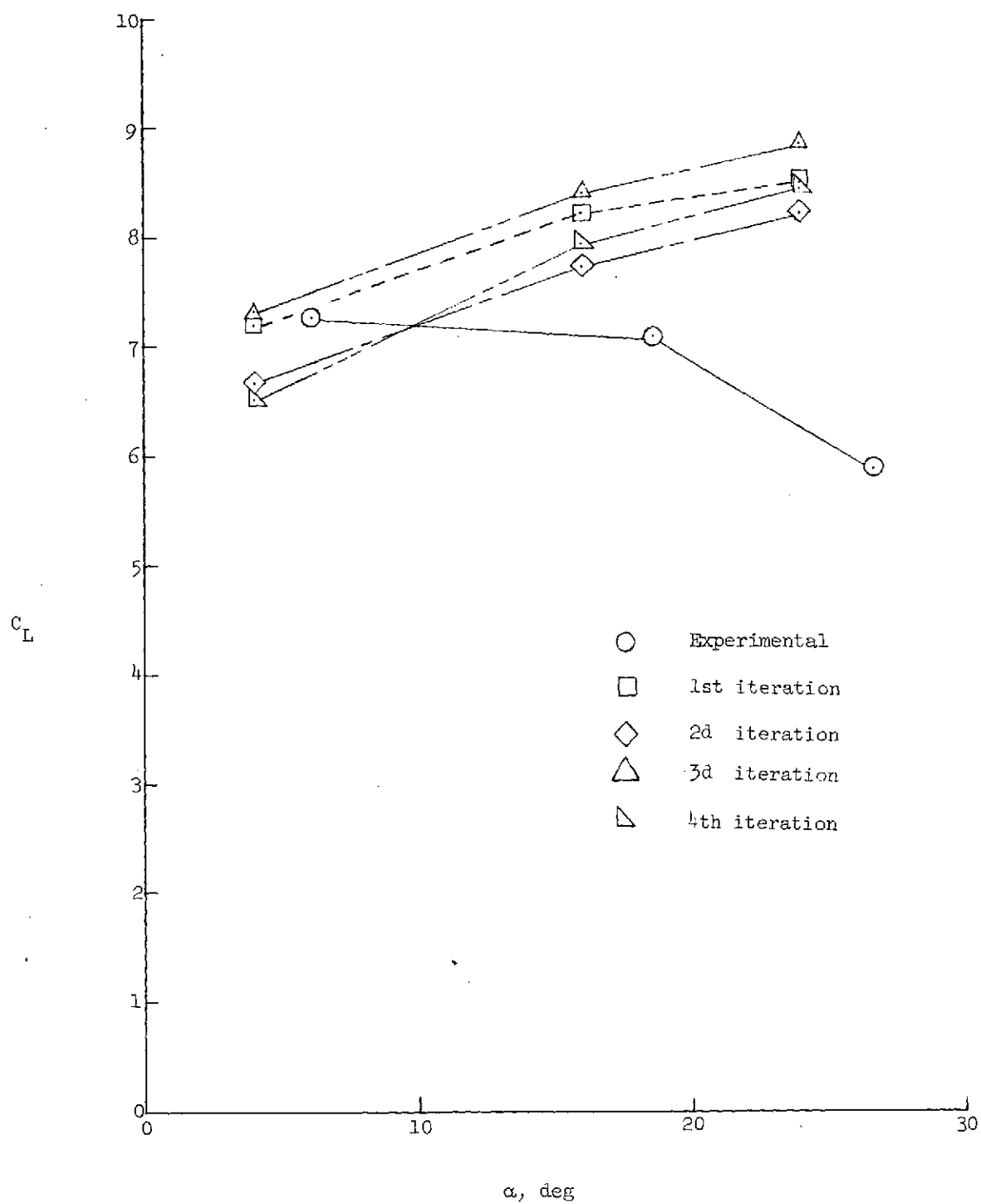


Figure 14.- Typical engine wake center-line variations for four iterations of the basic procedure.
Outboard engine; $C_{\mu} = 4.0$; $\alpha = 4^{\circ}$.



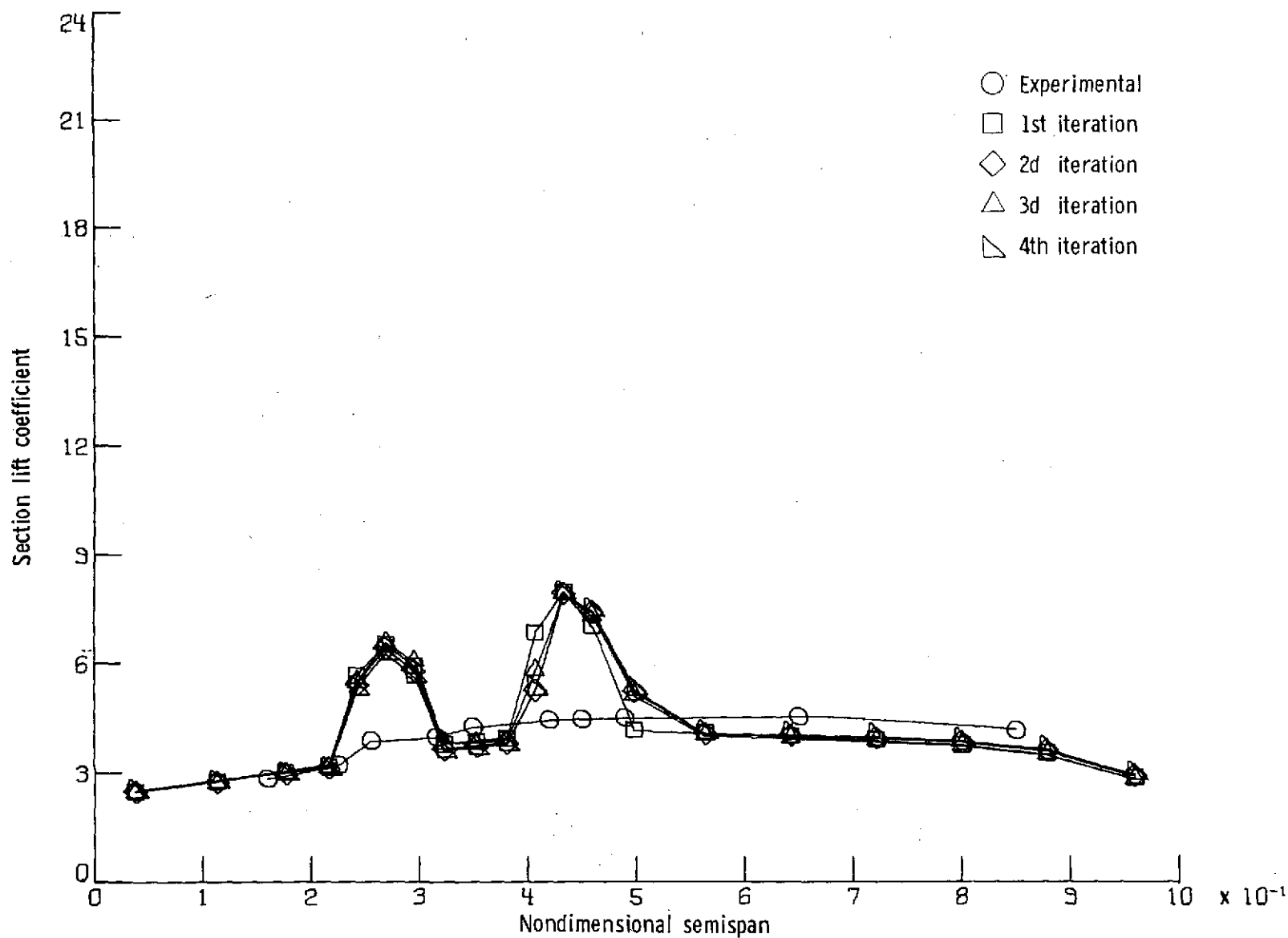
(a) $C_{\mu} = 2.2$.

Figure 15.- Comparison of experimental and theoretical lift curves. Basic procedure.



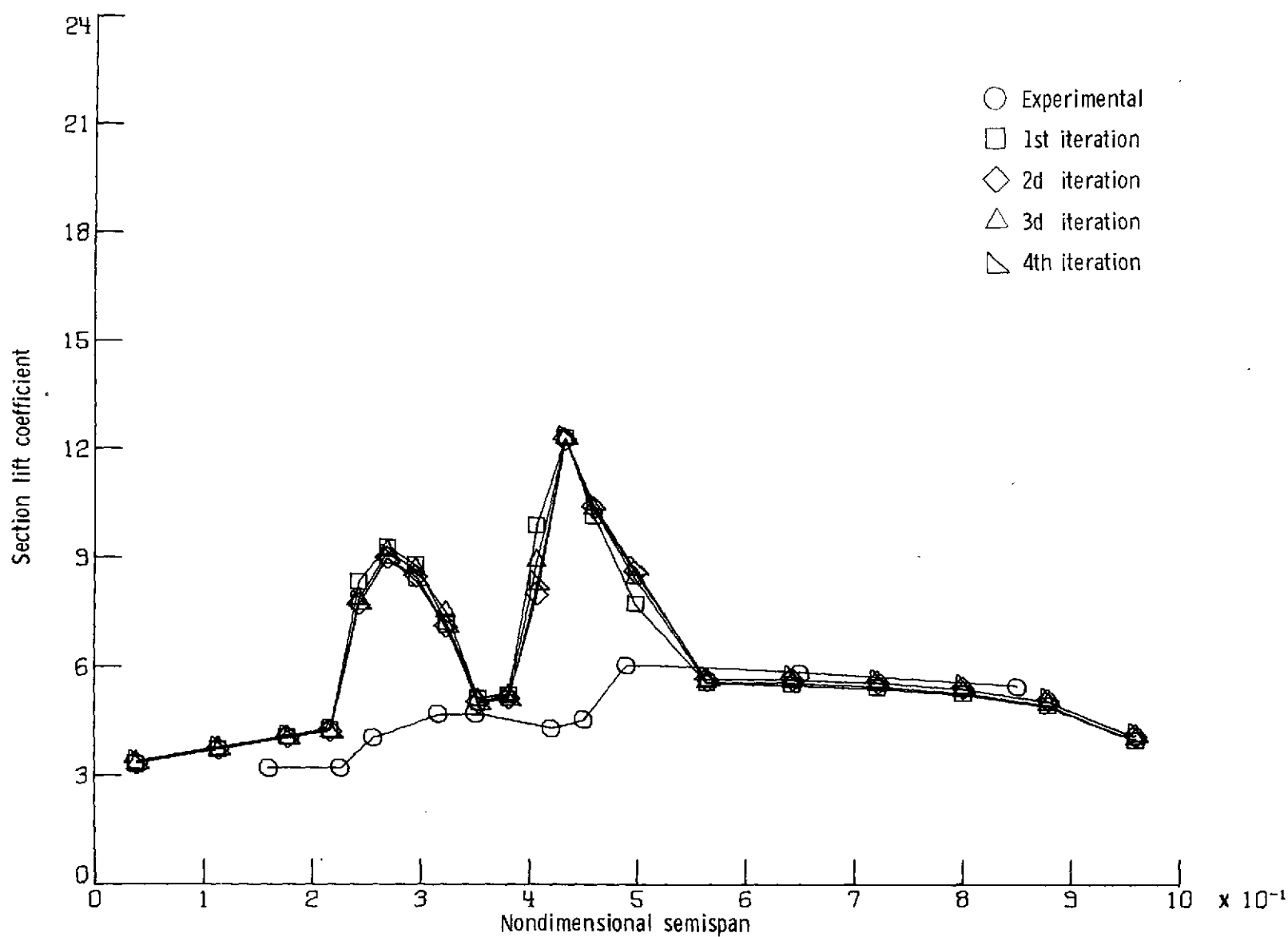
(b) $C_{\mu} = 4.0$.

Figure 15.- Concluded.



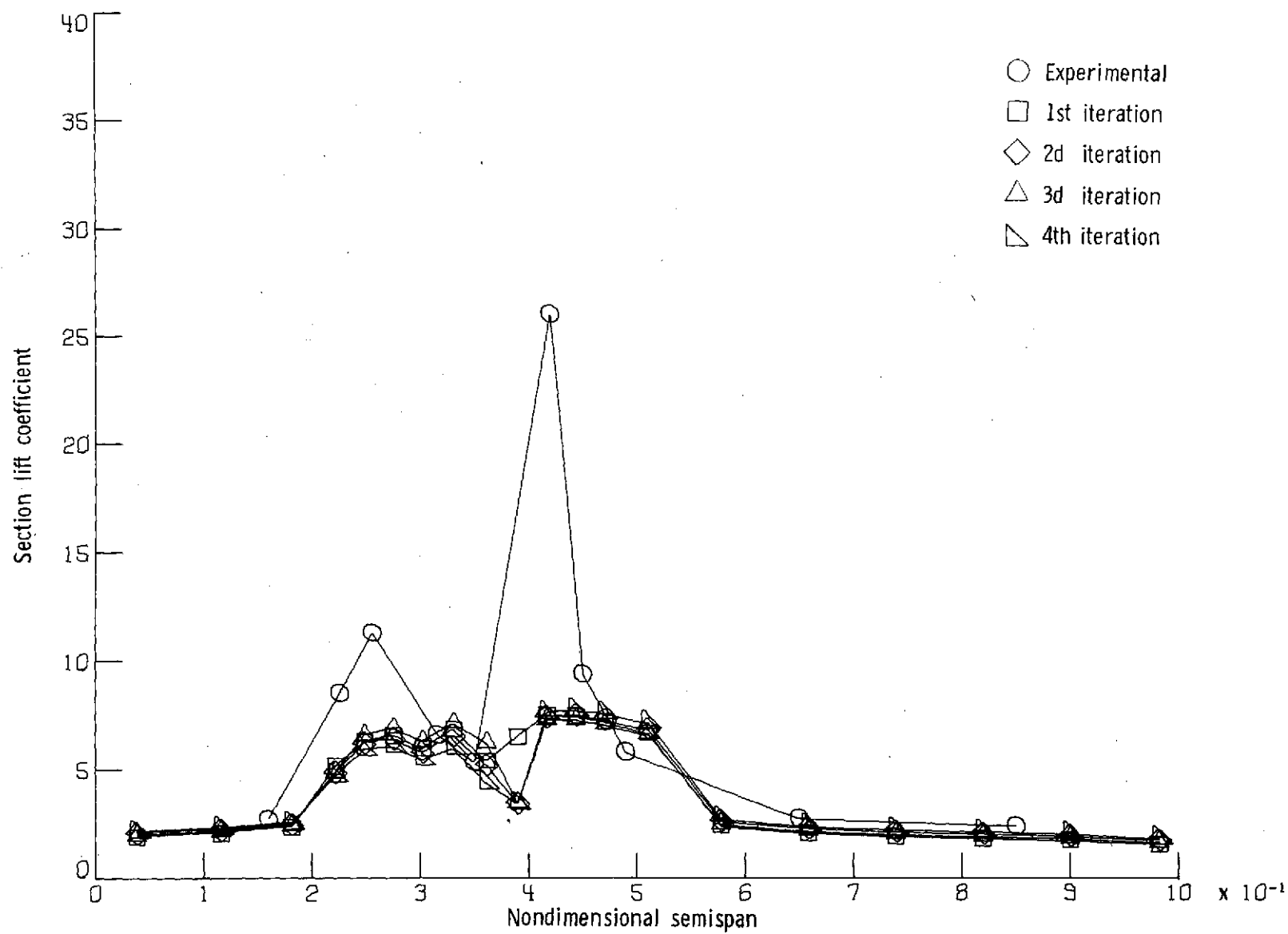
(a) Wing. $C_{\mu} = 2.2$; $\alpha = 4^{\circ}$.

69 Figure 16.- Comparison of distributions of experimental and theoretical section lift coefficients. Basic procedure.



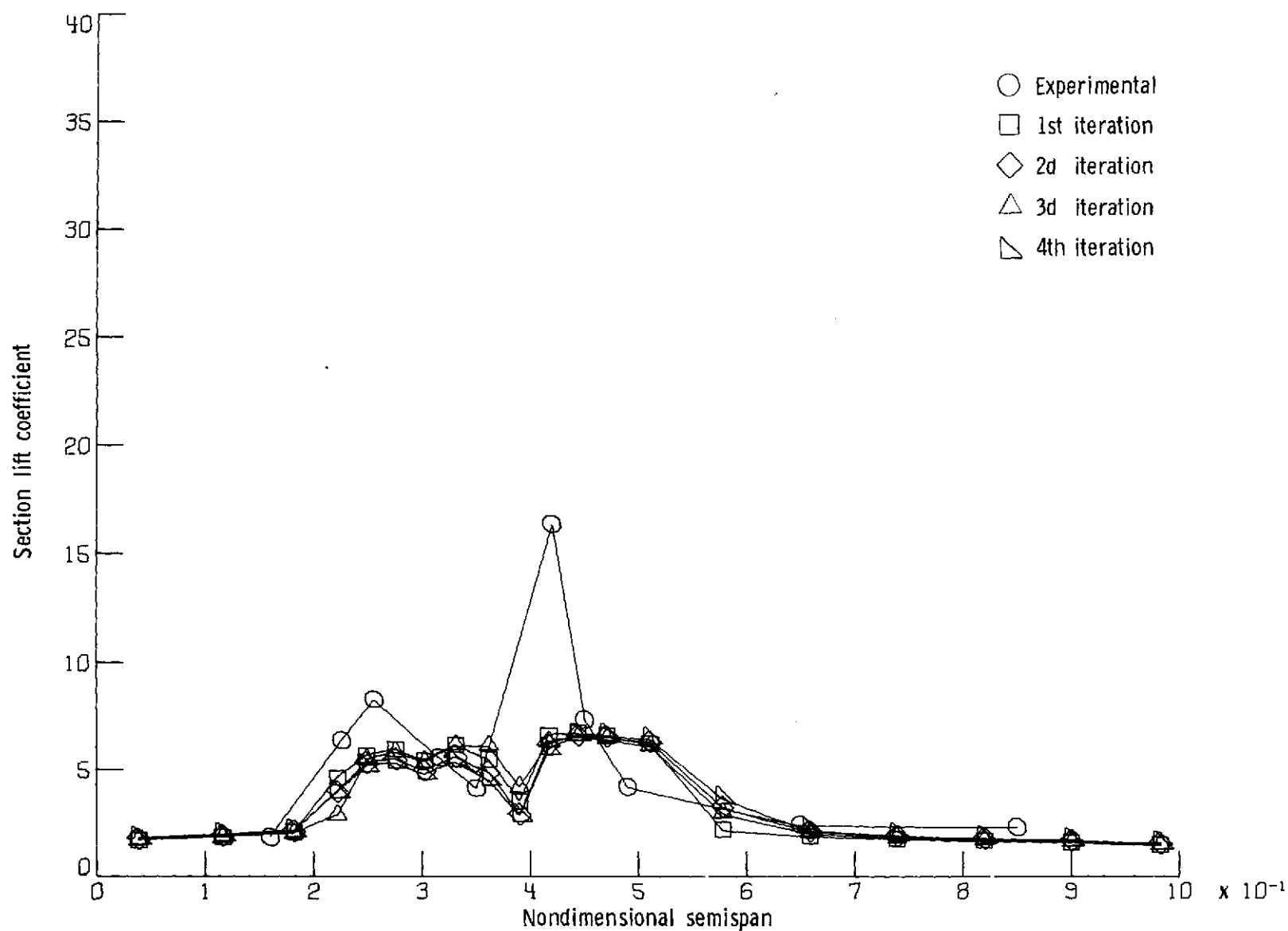
(b) Wing. $C_{\mu} = 2.2$; $\alpha = 16^{\circ}$.

Figure 16.- Continued.



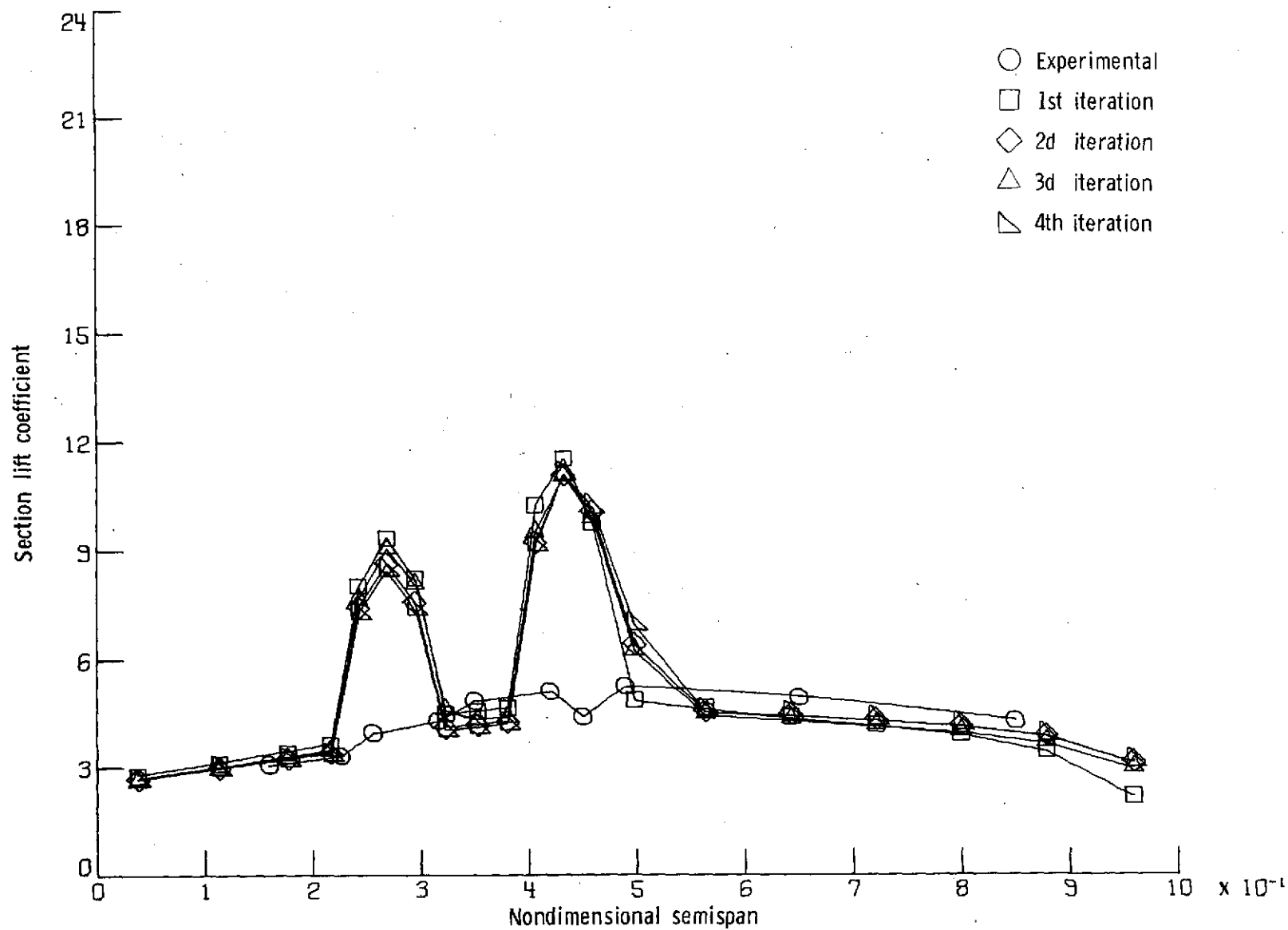
(c) Flap. $C_{\mu} = 2.2$; $\alpha = 4^{\circ}$.

Figure 16.- Continued.



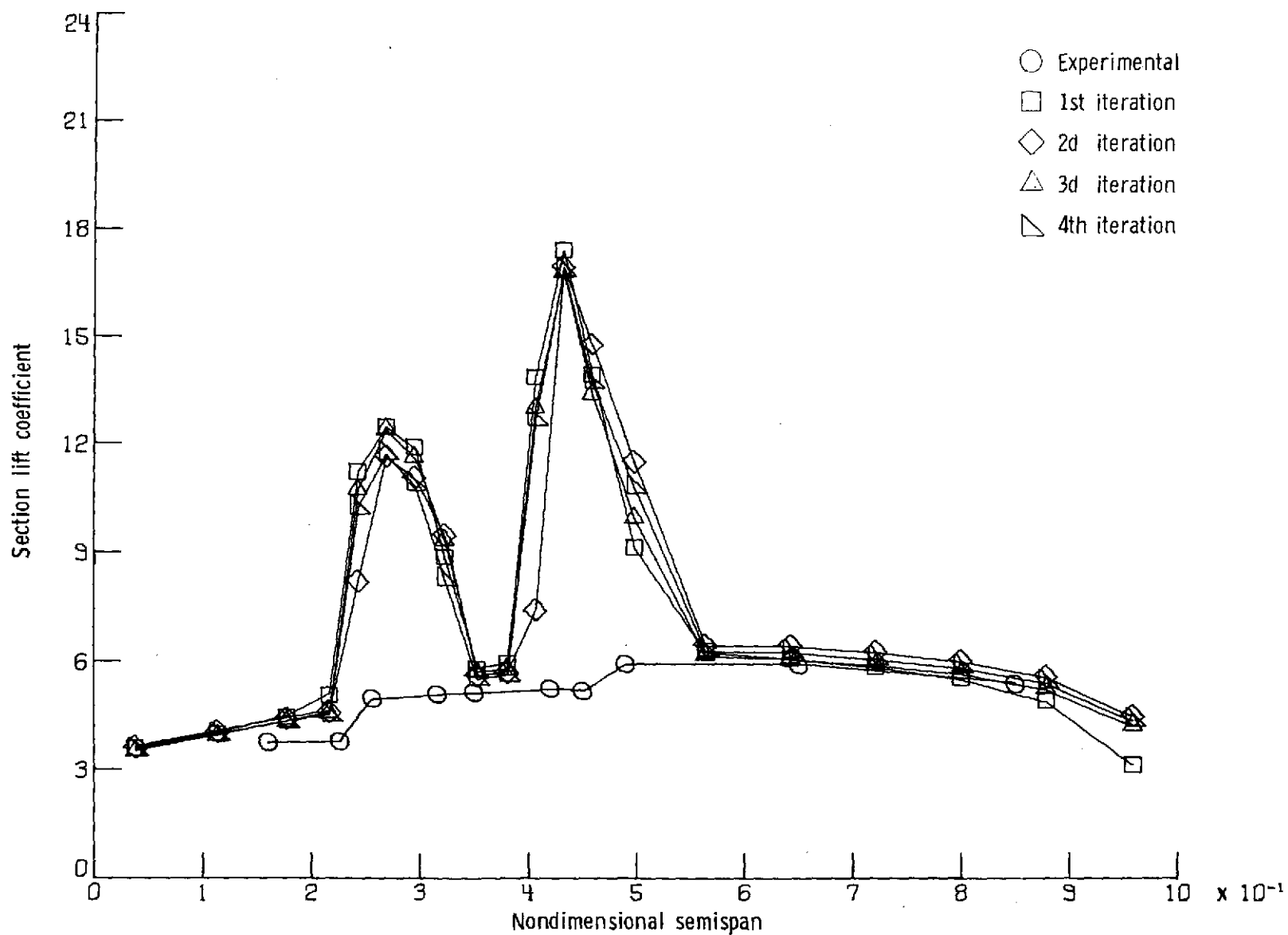
(d) Flap. $C_{\mu} = 2.2$; $\alpha = 16^{\circ}$.

Figure 16. - Continued.



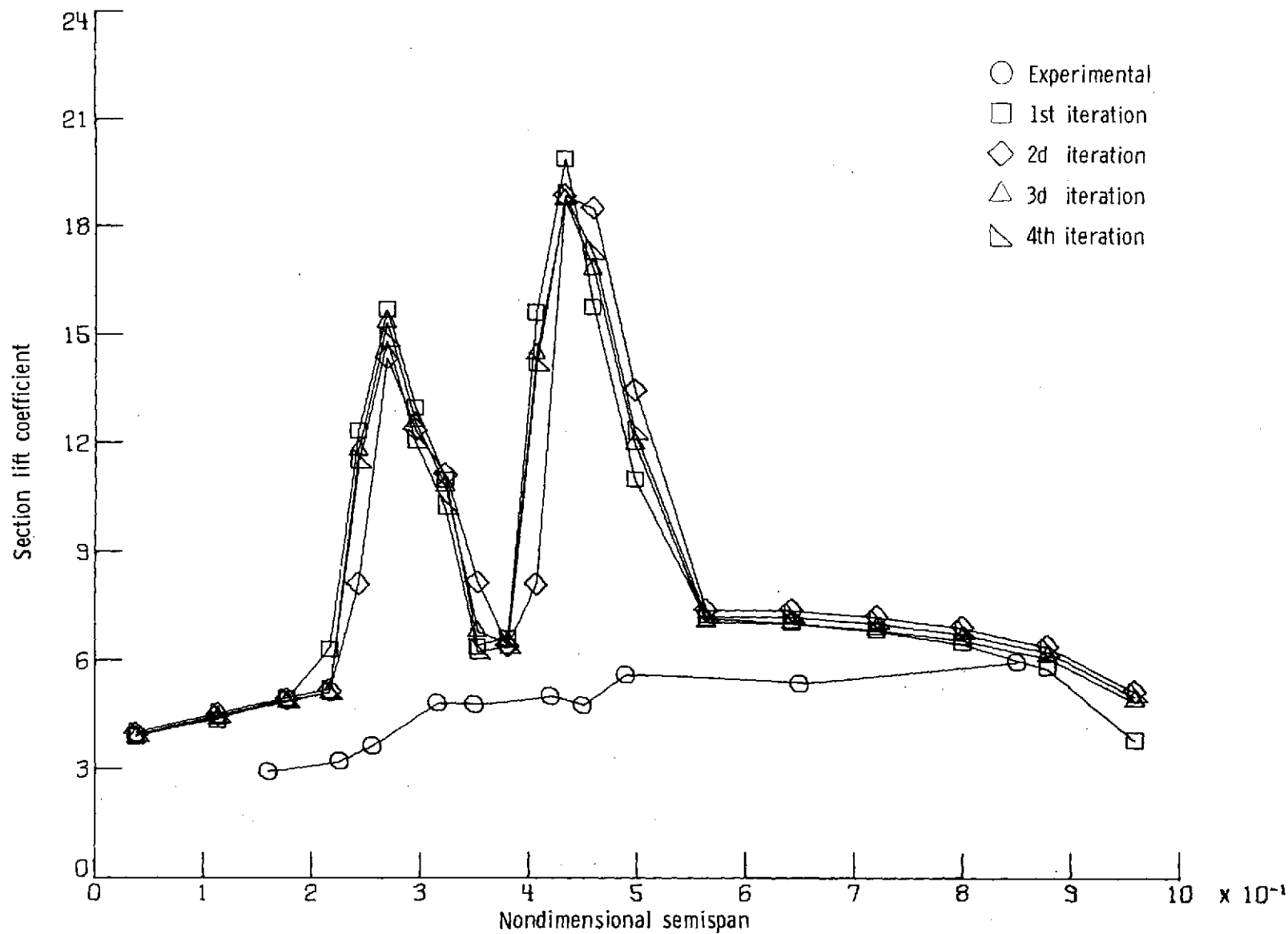
(e) Wing. $C_{\mu} = 4.0$; $\alpha = 4^{\circ}$.

Figure 16.- Continued.



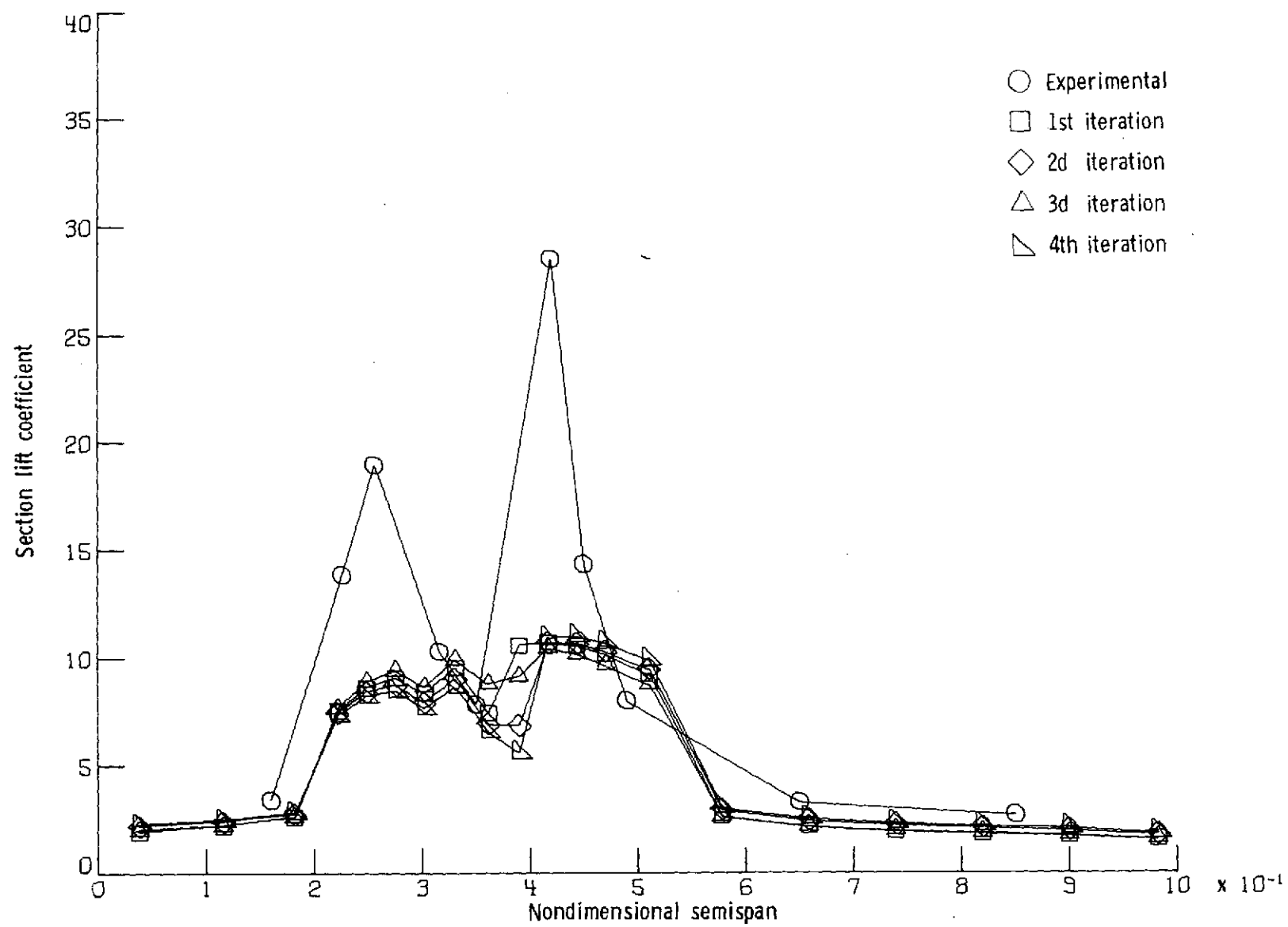
(f) Wing. $C_{\mu} = 4.0$; $\alpha = 16^{\circ}$.

Figure 16.- Continued.



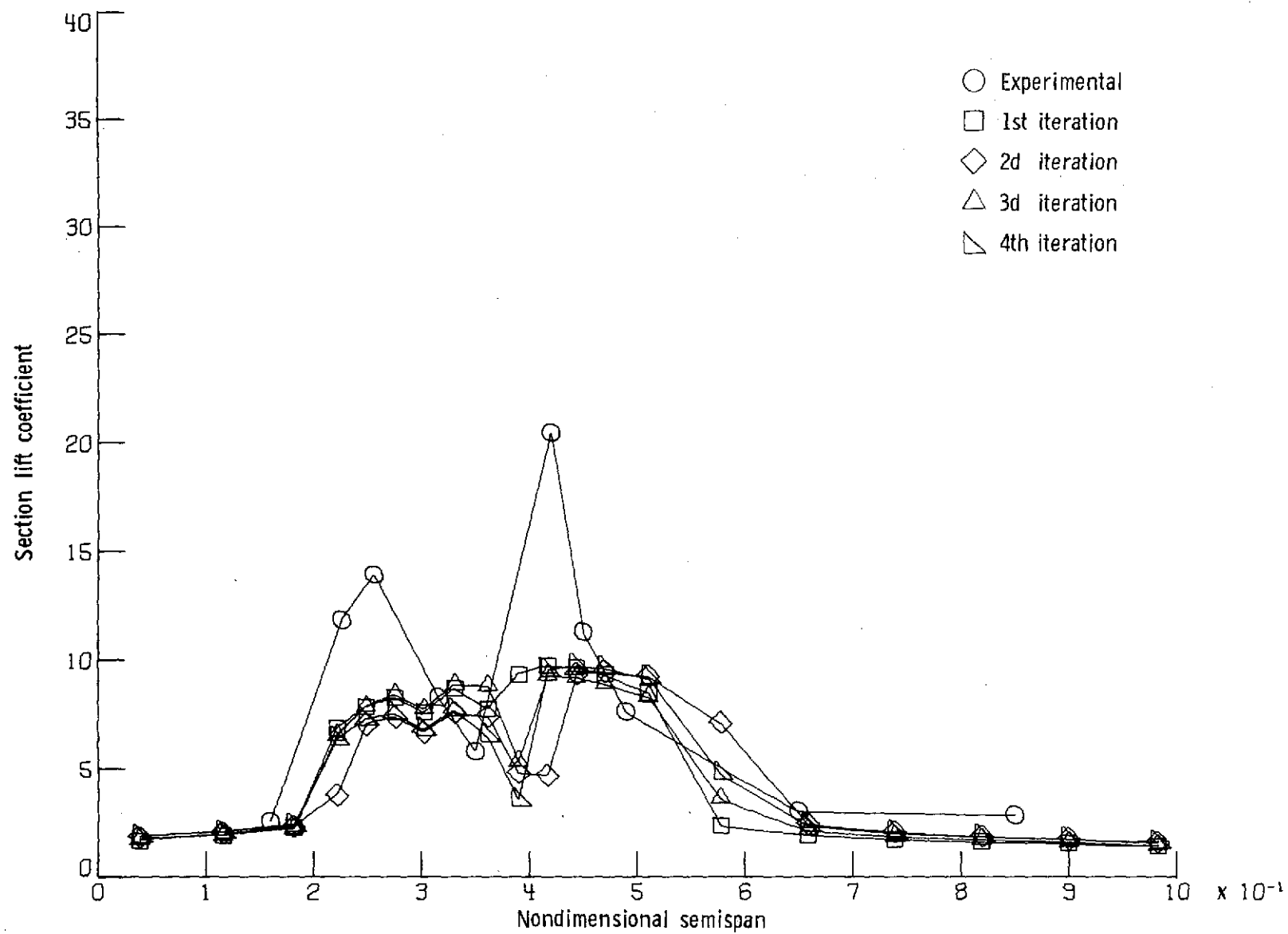
(g) Wing. $C_{\mu} = 4.0$; $\alpha = 24^{\circ}$.

Figure 16.- Continued.



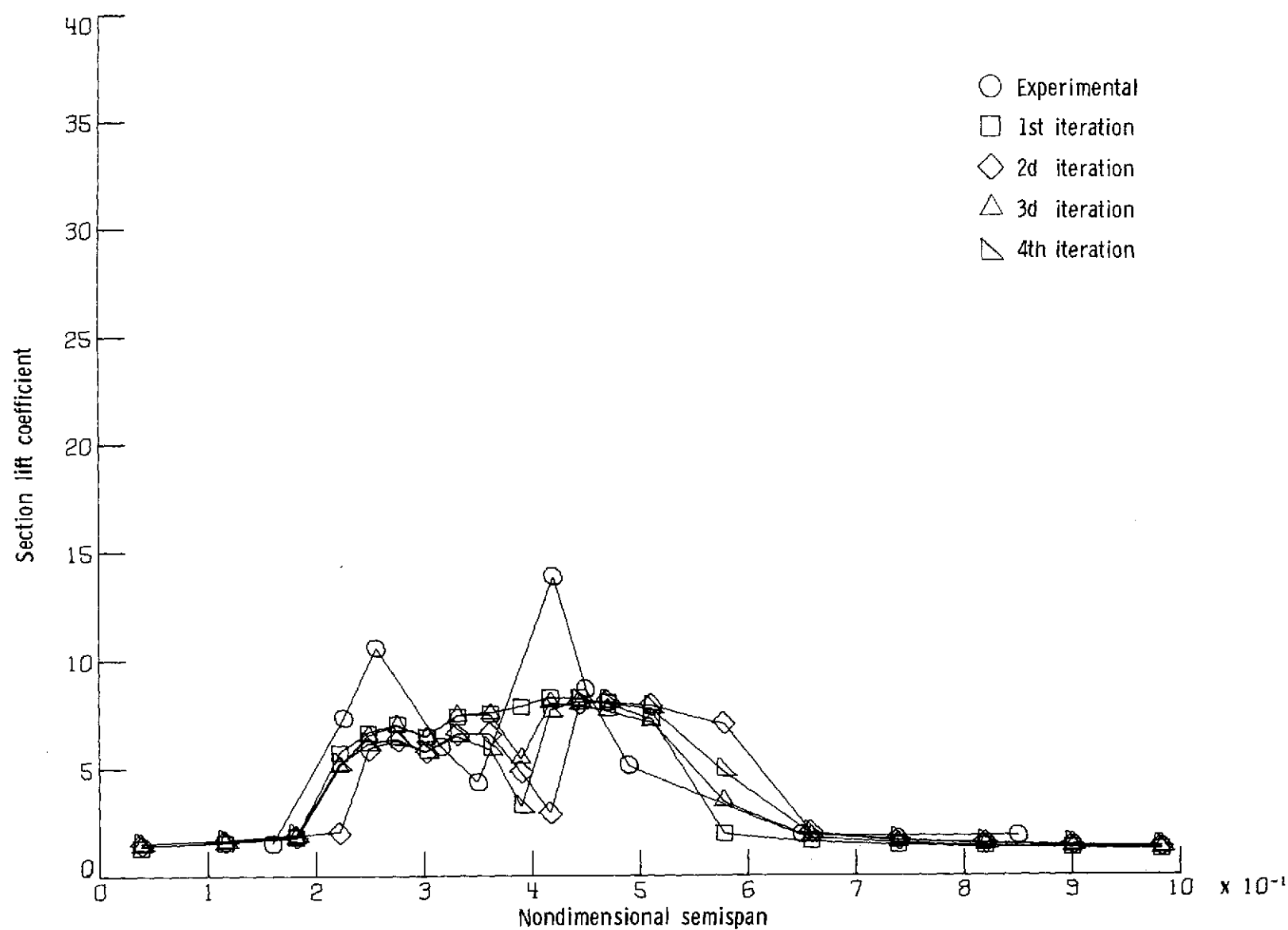
(h) Flap. $C_{\mu} = 4.0$; $\alpha = 4^{\circ}$.

Figure 16.- Continued.



(i) Flap. $C_{\mu} = 4.0$; $\alpha = 16^{\circ}$.

Figure 16.- Continued.



(j) Flap. $C_{\mu} = 4.0$; $\alpha = 24^{\circ}$.

Figure 16.- Concluded.

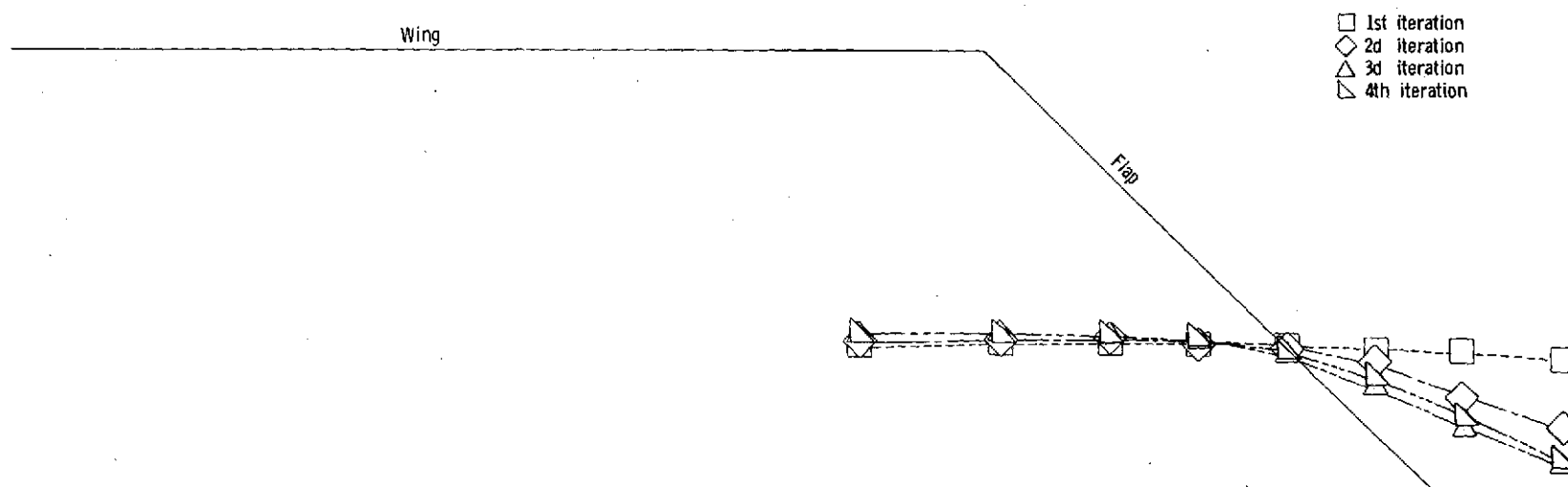


Figure 17.- Typical engine wake center-line variations for four iterations of alternate procedure 1.
Outboard engine; $C_{\mu} = 4.0$; $\alpha = 4^{\circ}$.

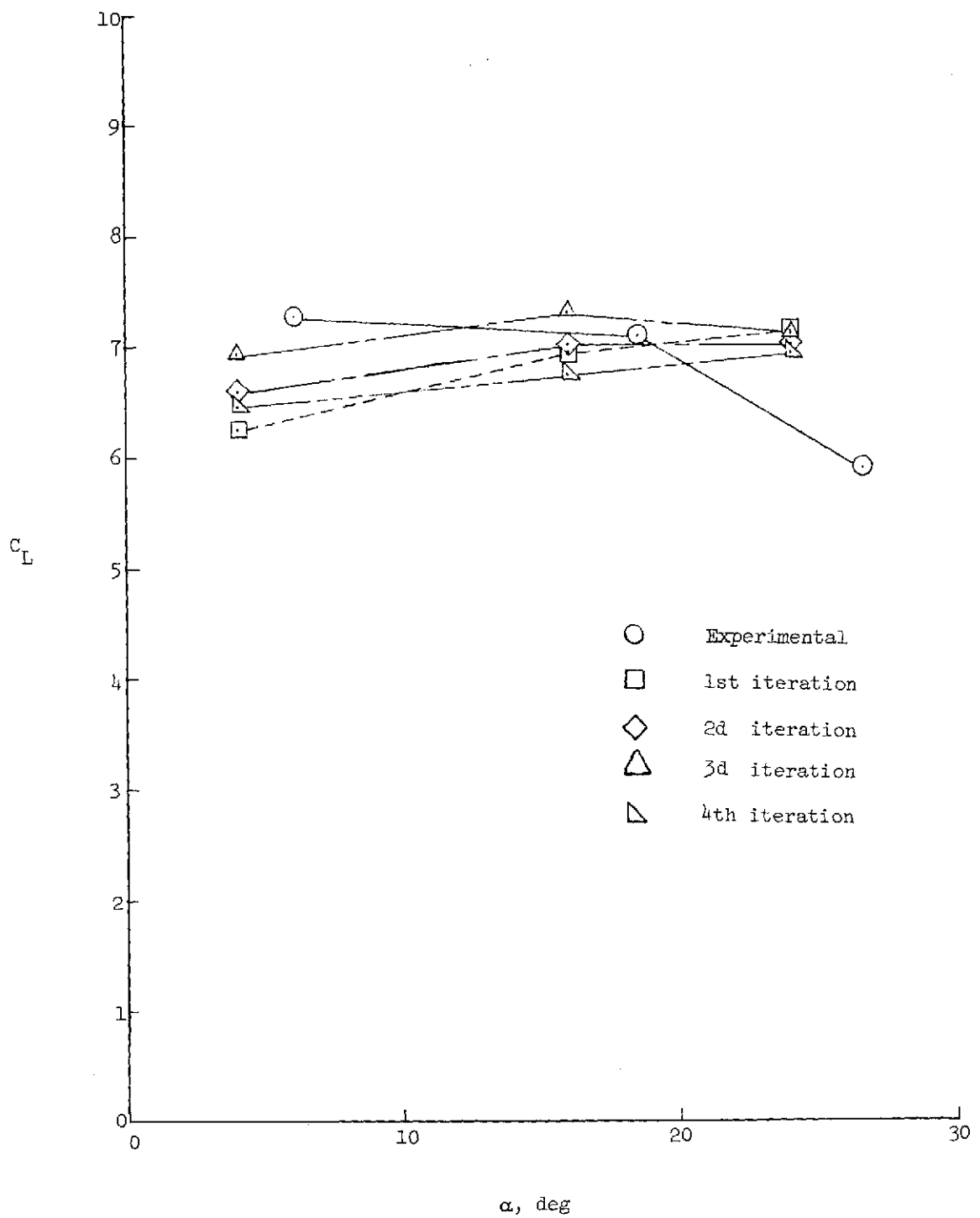
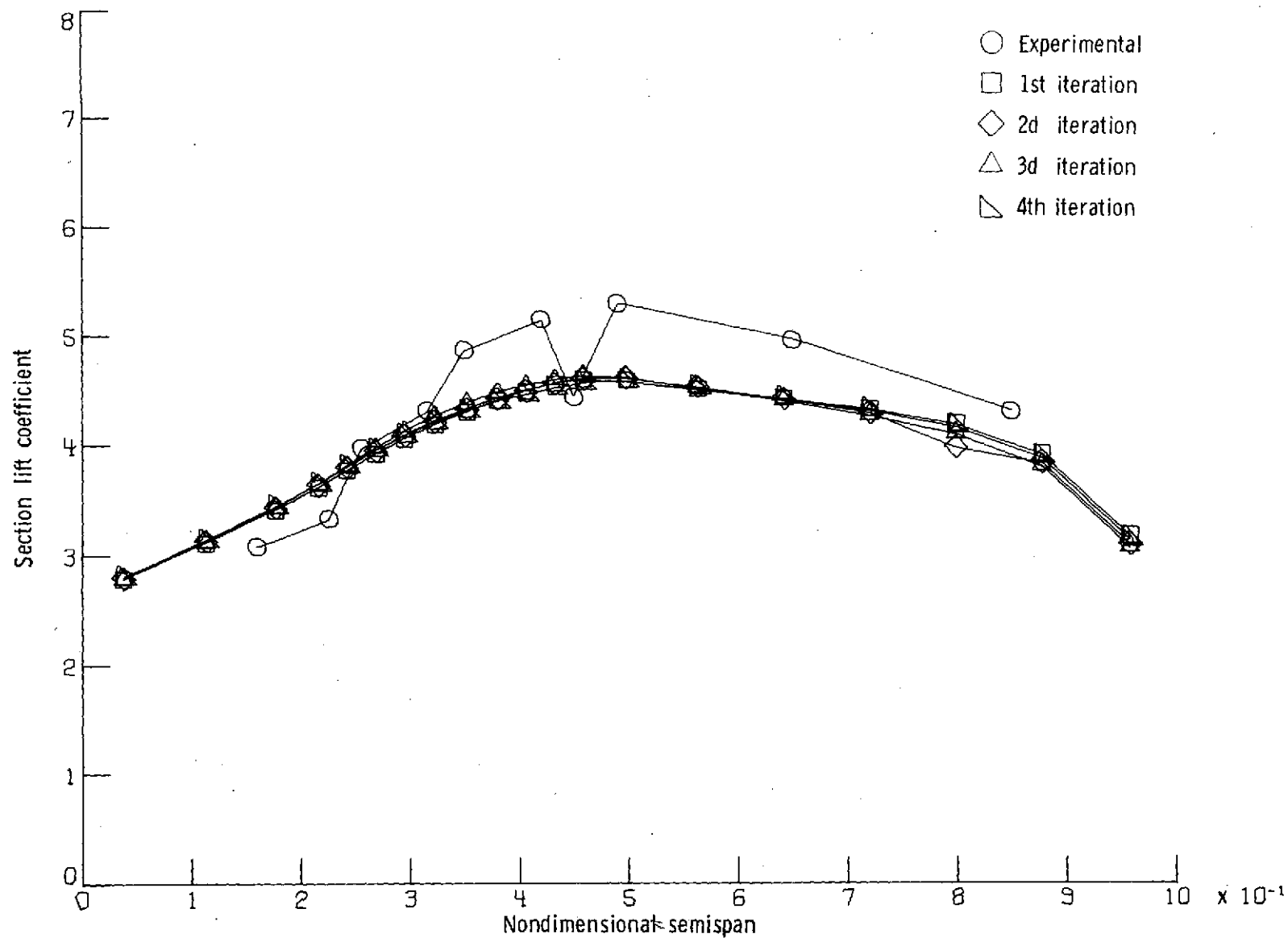
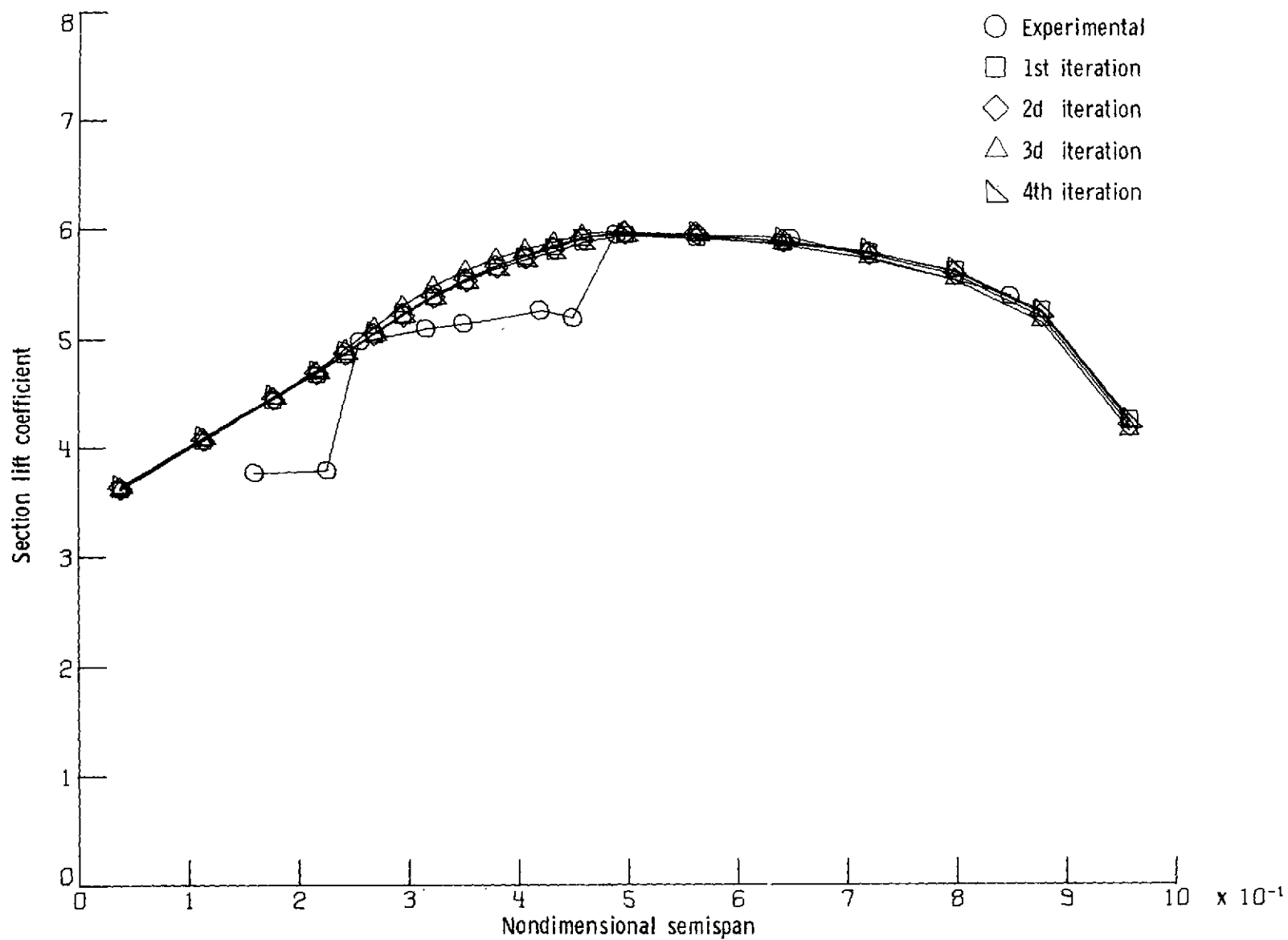


Figure 18.- Comparison of experimental and theoretical lift curves.
Alternate procedure 1; $C_{\mu} = 4.0$.



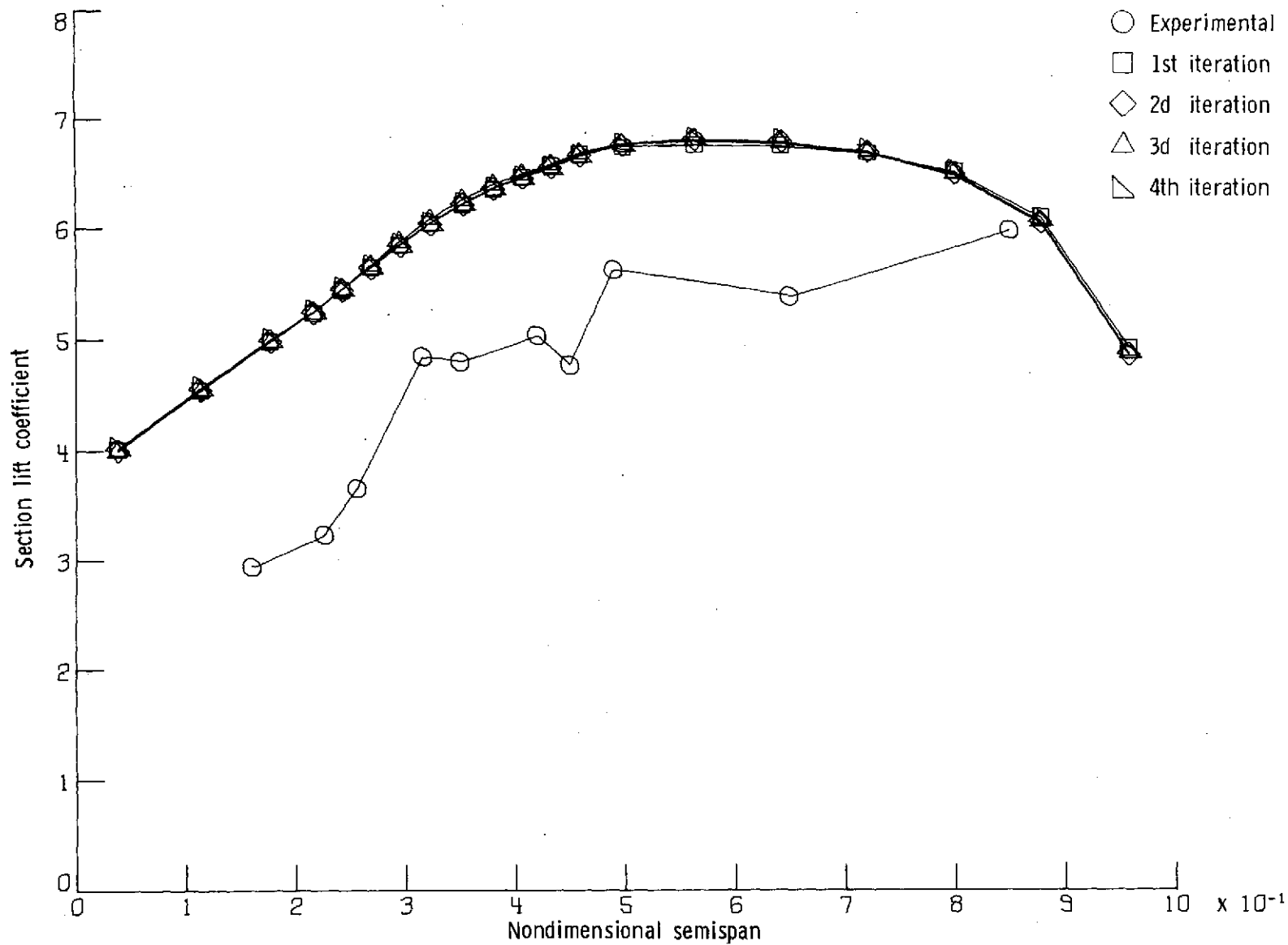
(a) Wing. $C_{\mu} = 4.0$; $\alpha = 4^{\circ}$.

64 Figure 19. - Comparison of distributions of experimental and theoretical section lift coefficients. Alternate procedure 1.



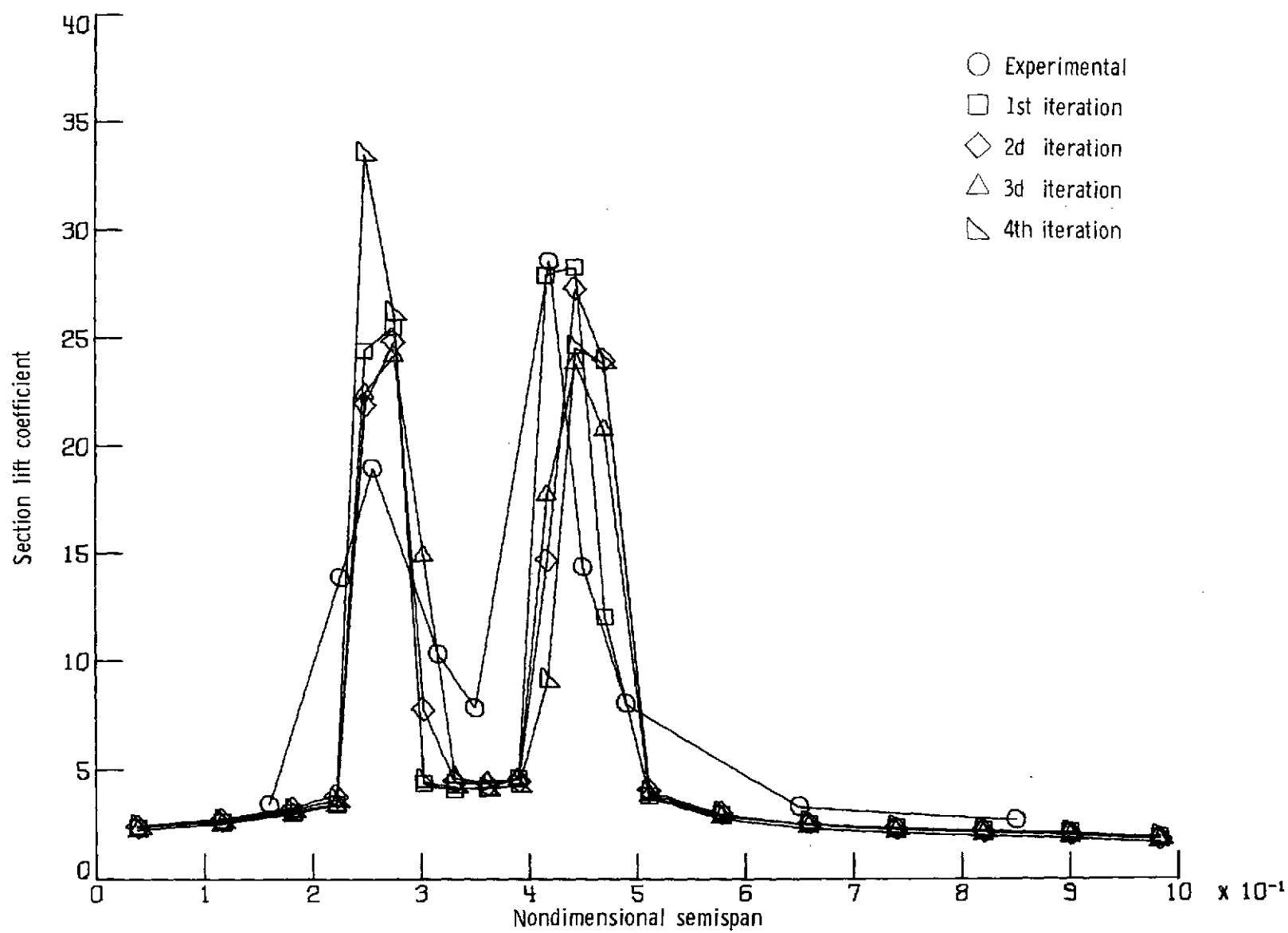
(b) Wing. $C_{\mu} = 4.0$; $\alpha = 16^{\circ}$.

Figure 19.- Continued.



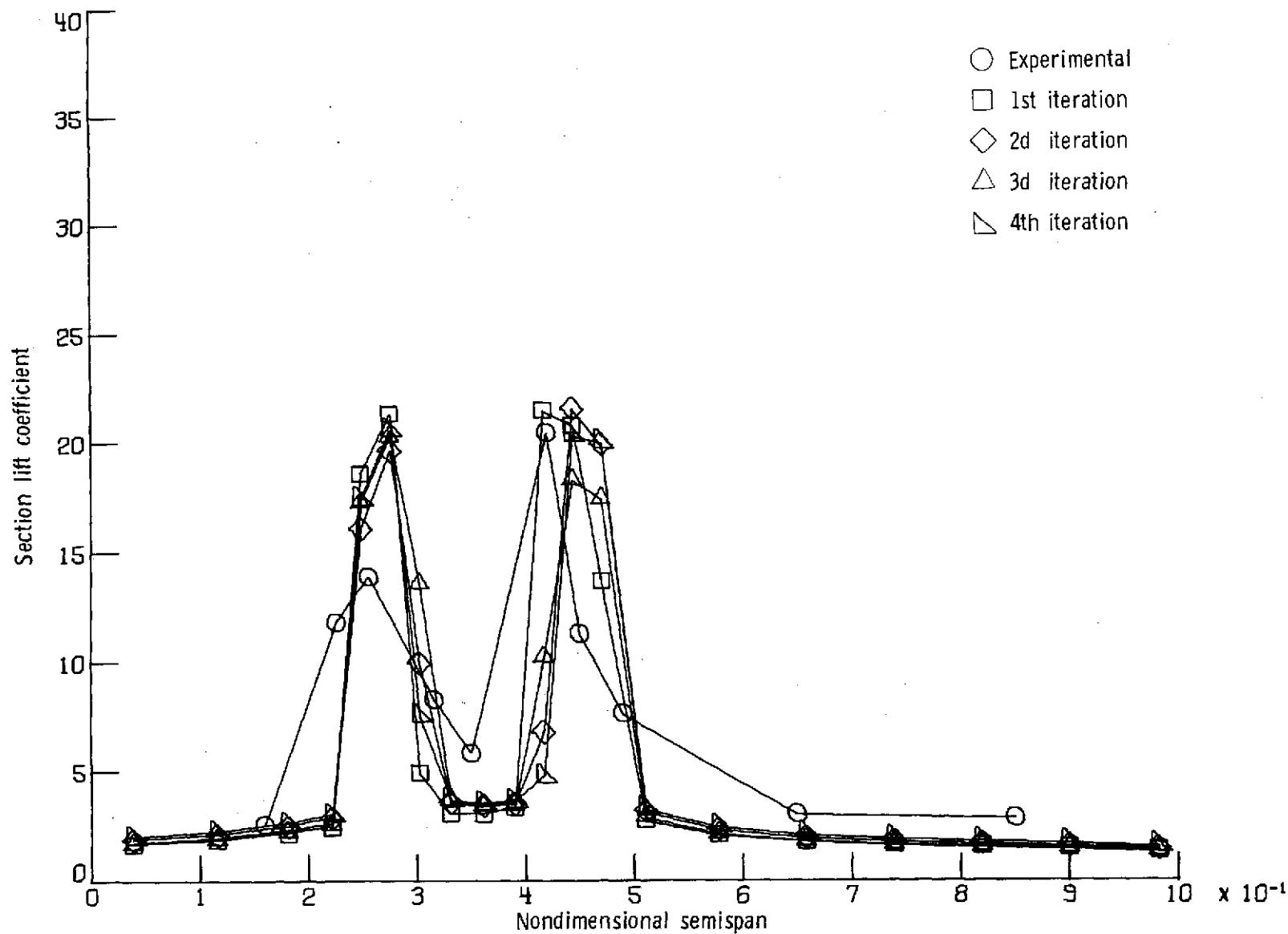
(c) Wing. $C_{\mu} = 4.0$; $\alpha = 24^{\circ}$.

Figure 19.- Continued.



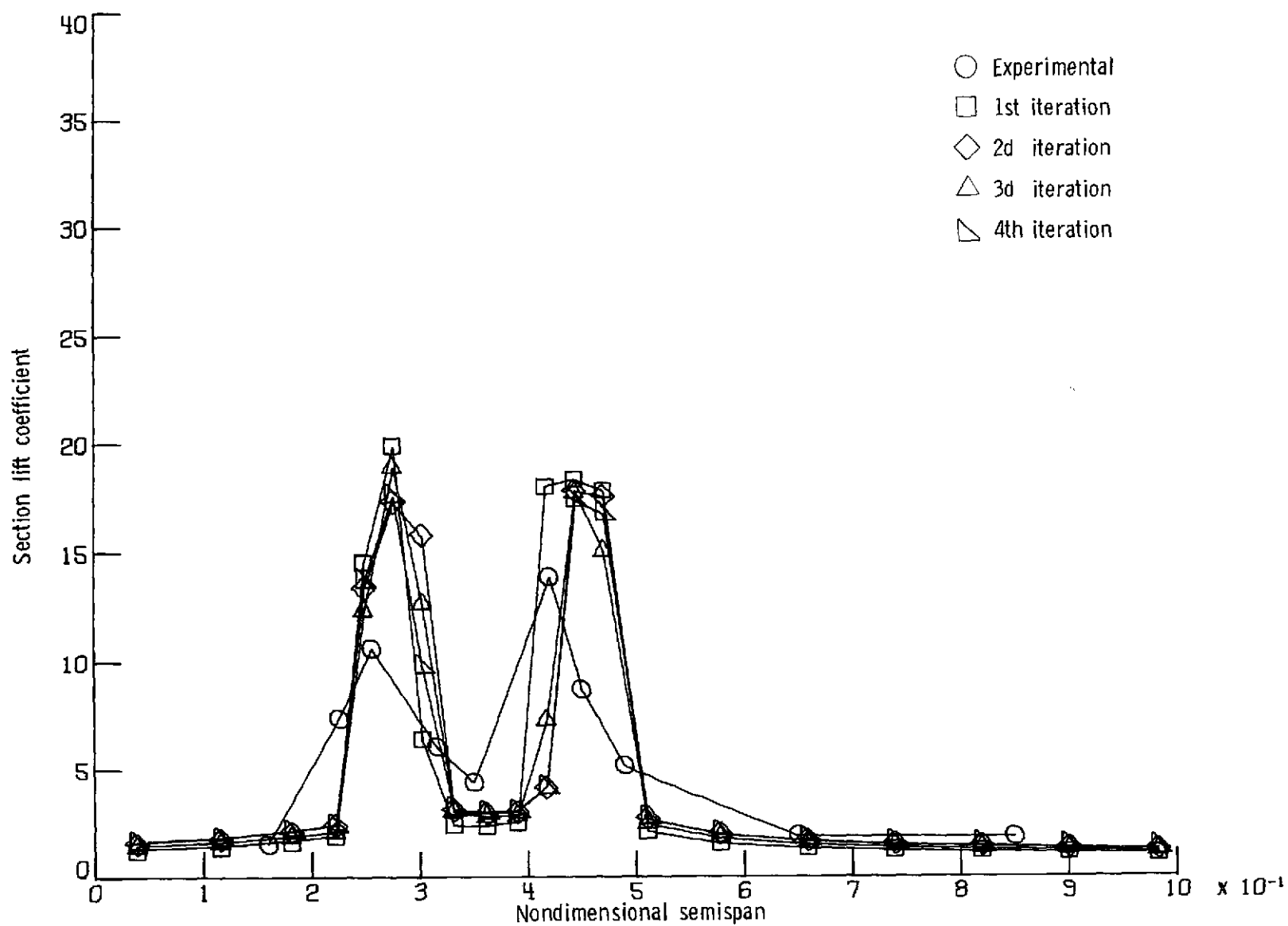
(d) Flap. $C_{\mu} = 4.0$; $\alpha = 4^{\circ}$.

Figure 19.- Continued.



(e) Flap. $C_{\mu} = 4.0$; $\alpha = 16^{\circ}$.

Figure 19.- Continued.



(f) Flap. $C_{\mu} = 4.0$; $\alpha = 24^{\circ}$.

Figure 19.- Concluded.

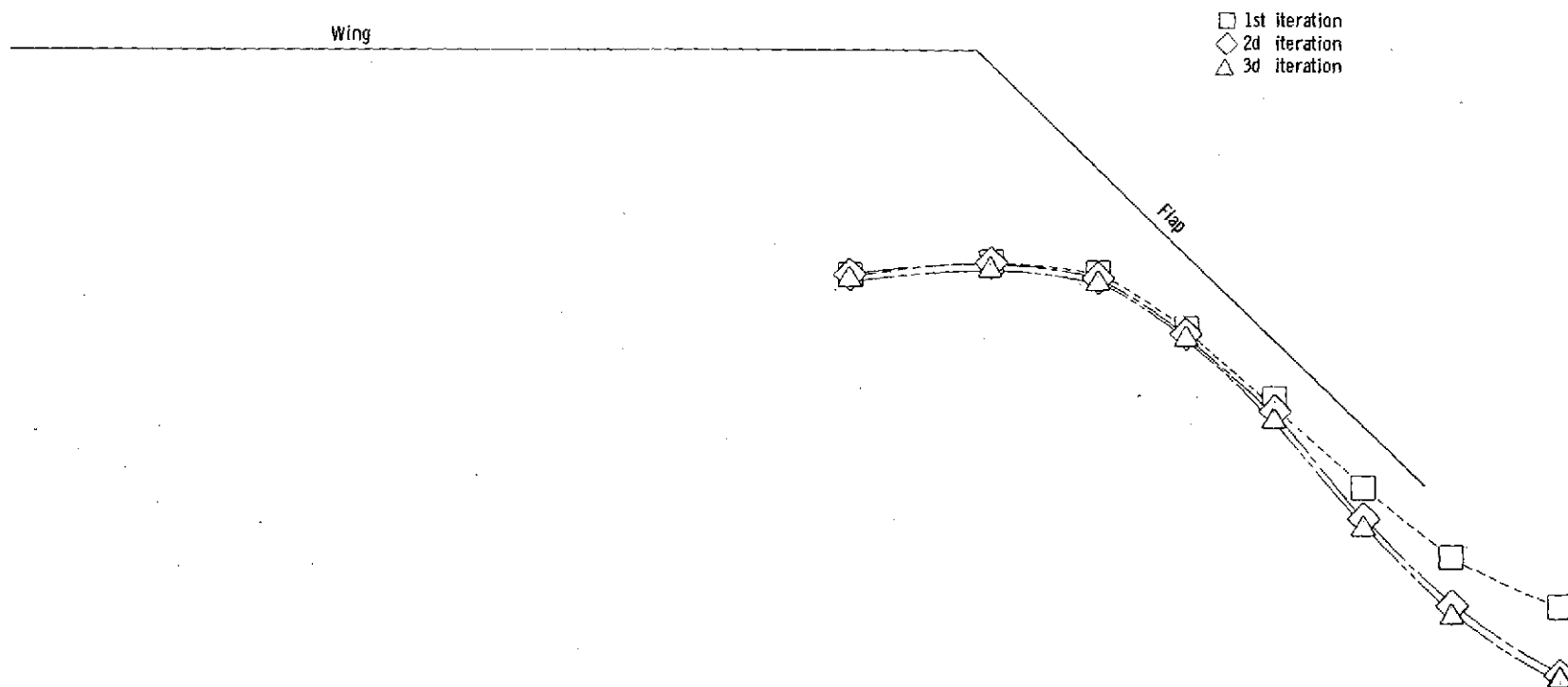


Figure 20. - Typical engine wake center-line variations for three iterations of alternate procedure 2.
Outboard engine; $C_{\mu} = 4.0$; $\alpha = 4^{\circ}$.

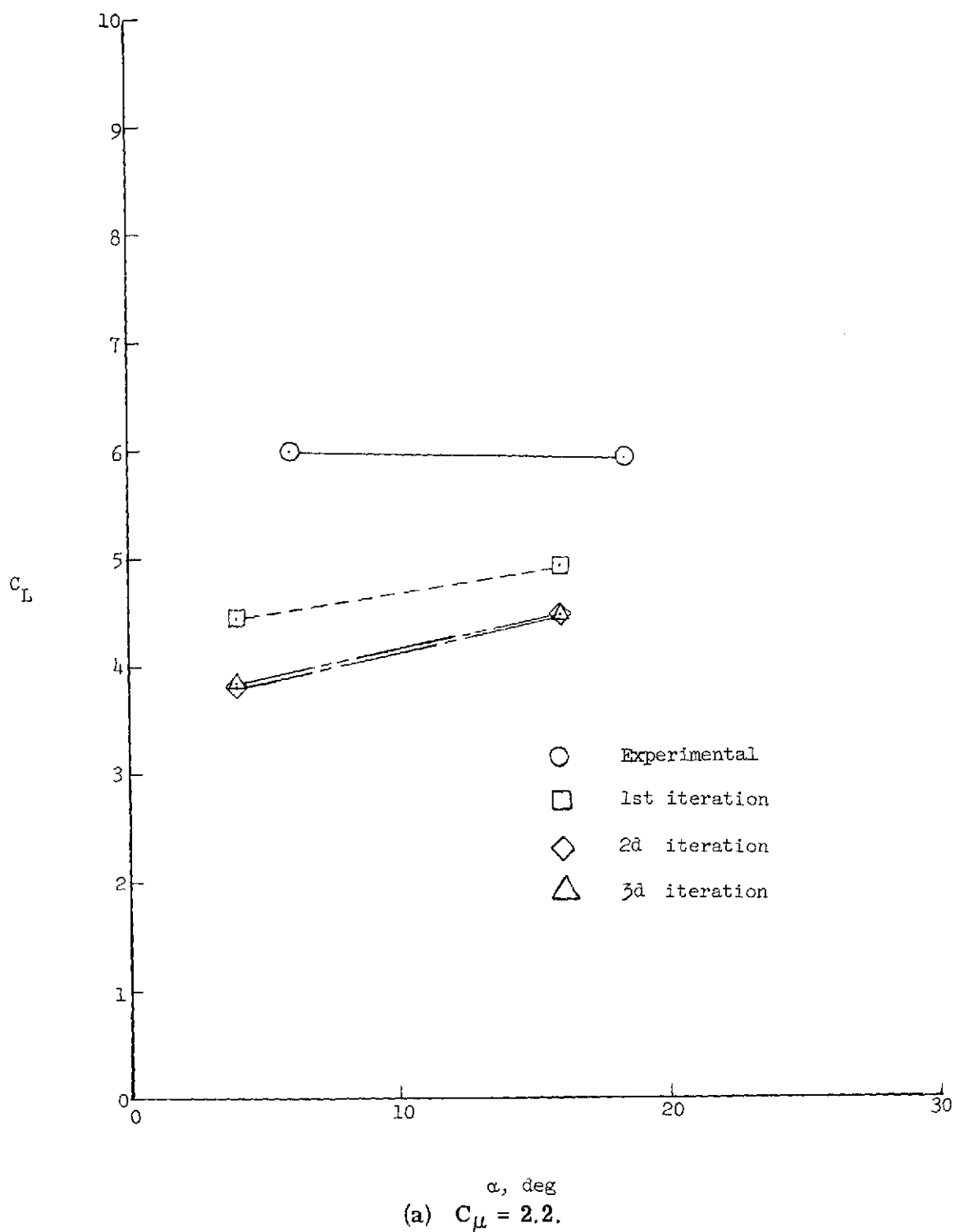
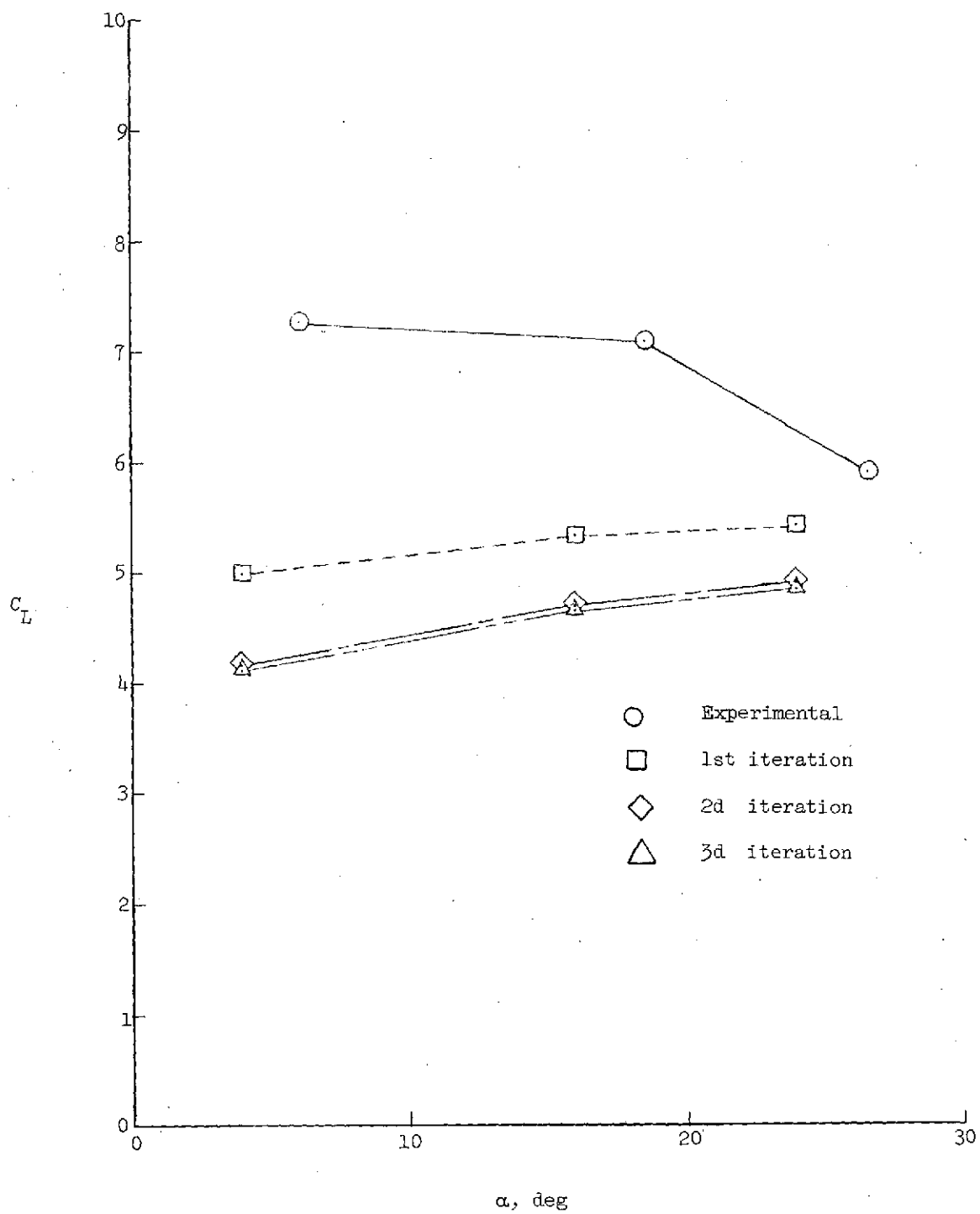
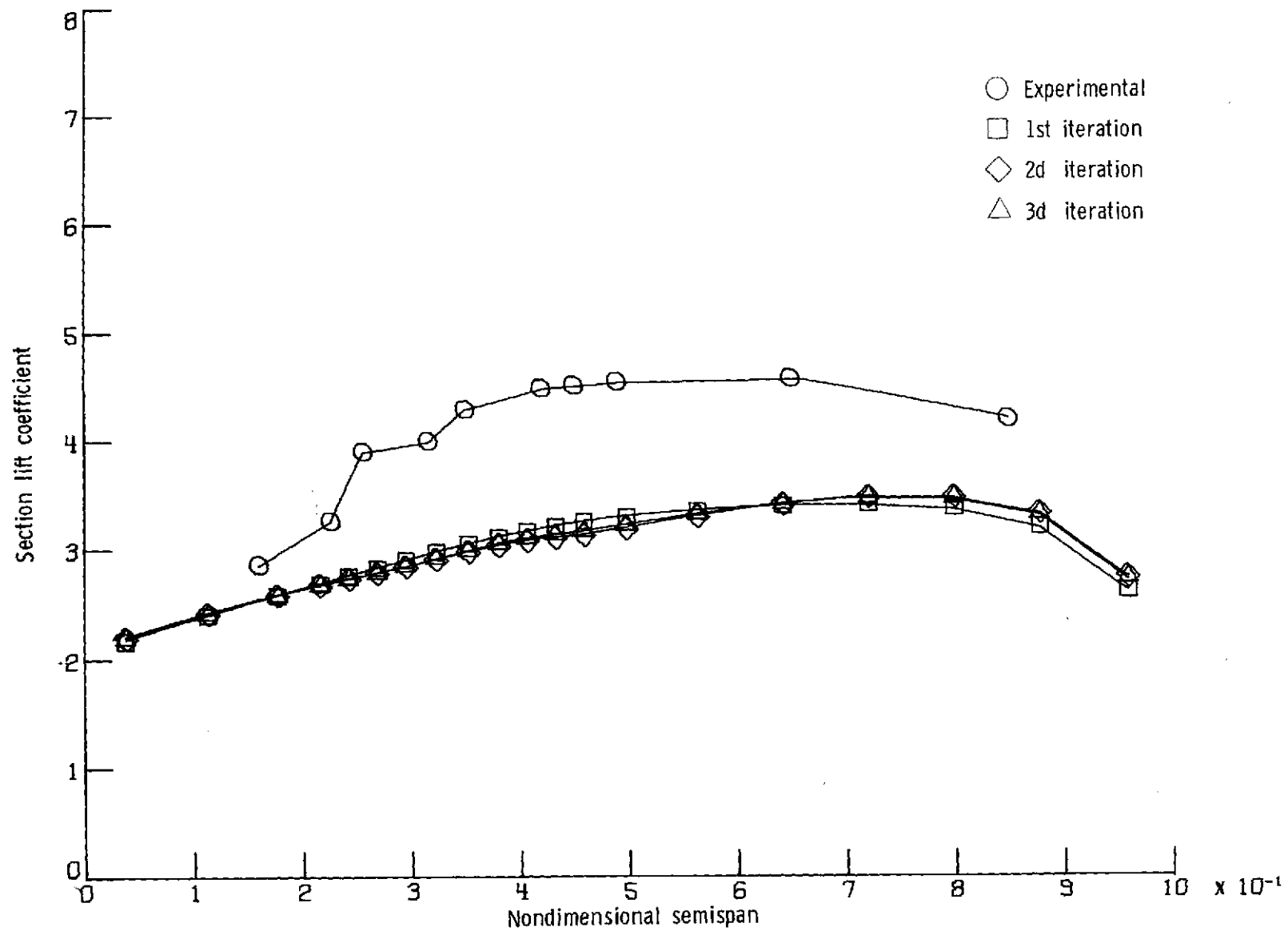


Figure 21. - Comparison of experimental and theoretical lift curves.
Alternate procedure 2.

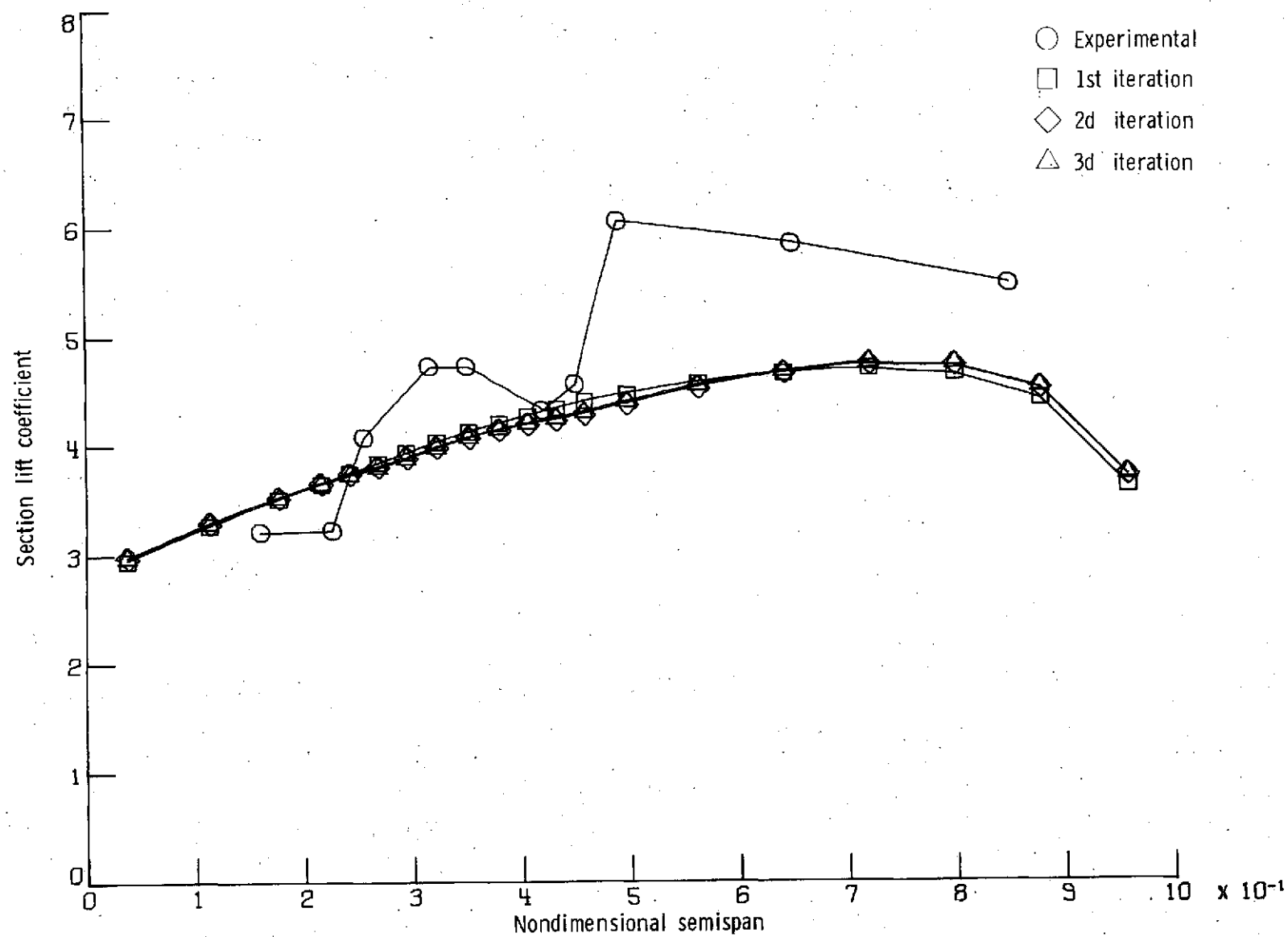


(b) $C_{\mu} = 4.0$.
Figure 21. - Concluded.



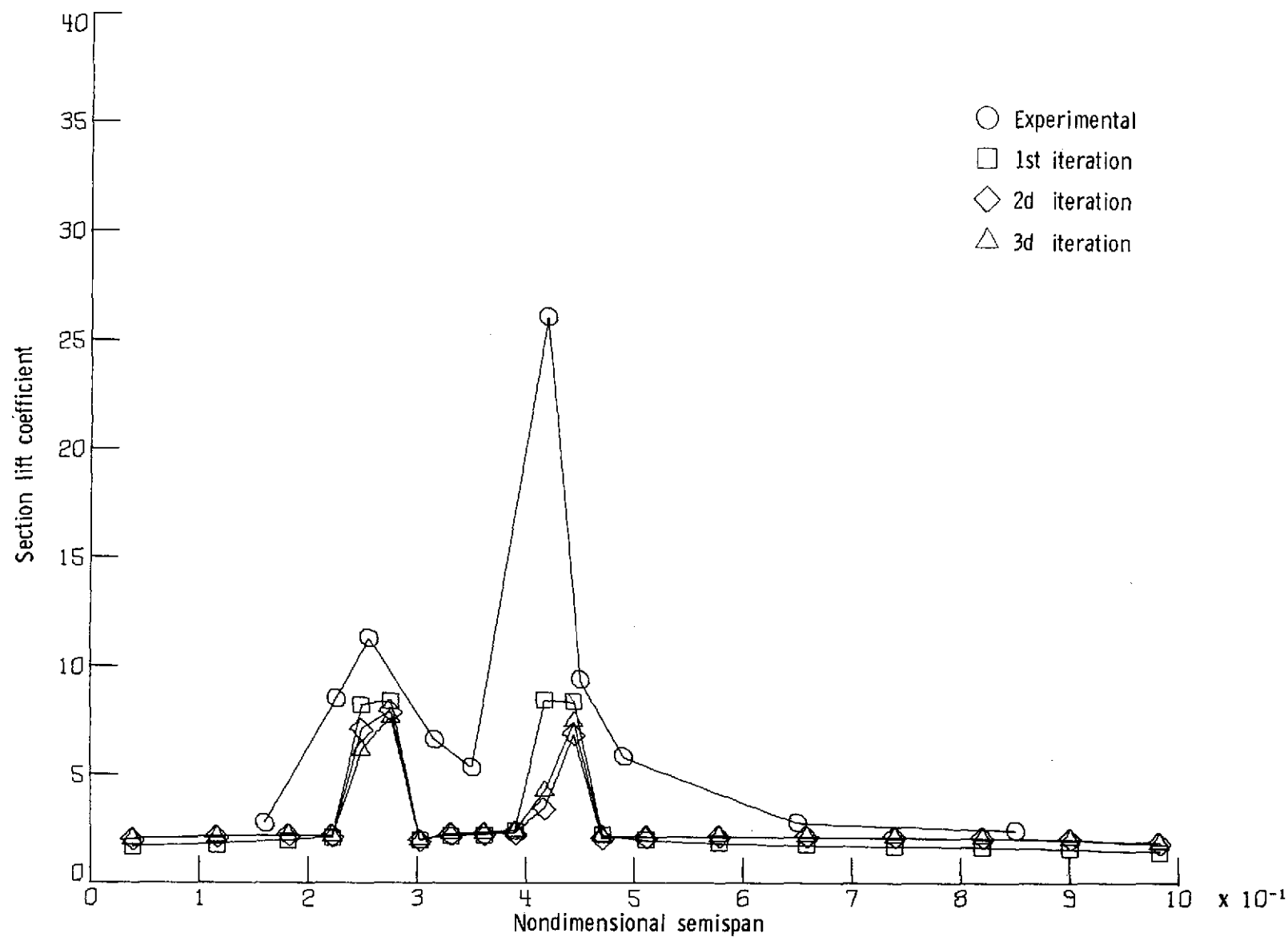
(a) Wing. $C_{\mu} = 2.2$; $\alpha = 4^{\circ}$.

Figure 22.- Comparison of distributions of experimental and theoretical section lift coefficients.
Alternate procedure 2.



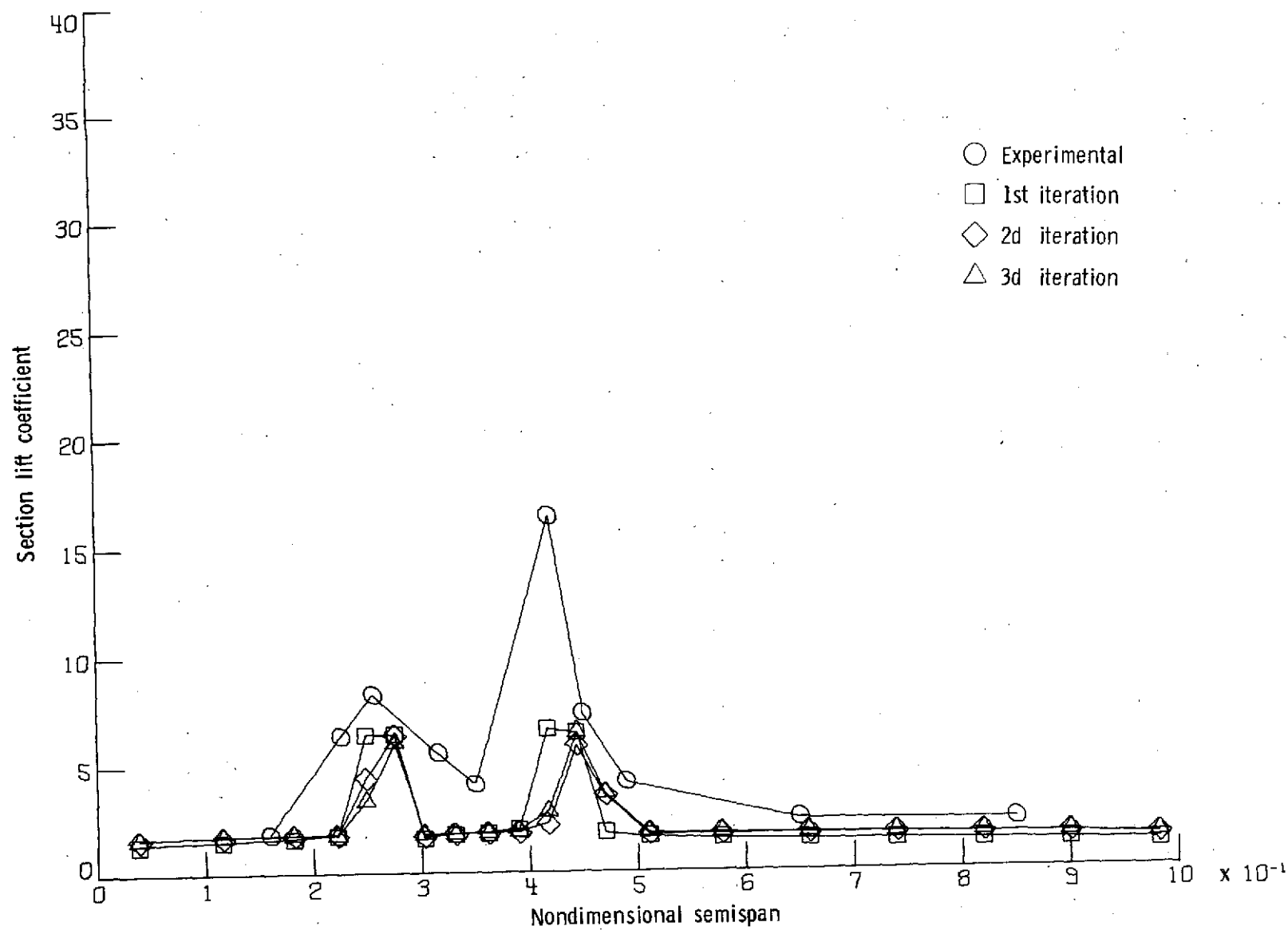
(b) Wing. $C_{\mu} = 2.2$; $\alpha = 16^{\circ}$.

Figure 22. - Continued.



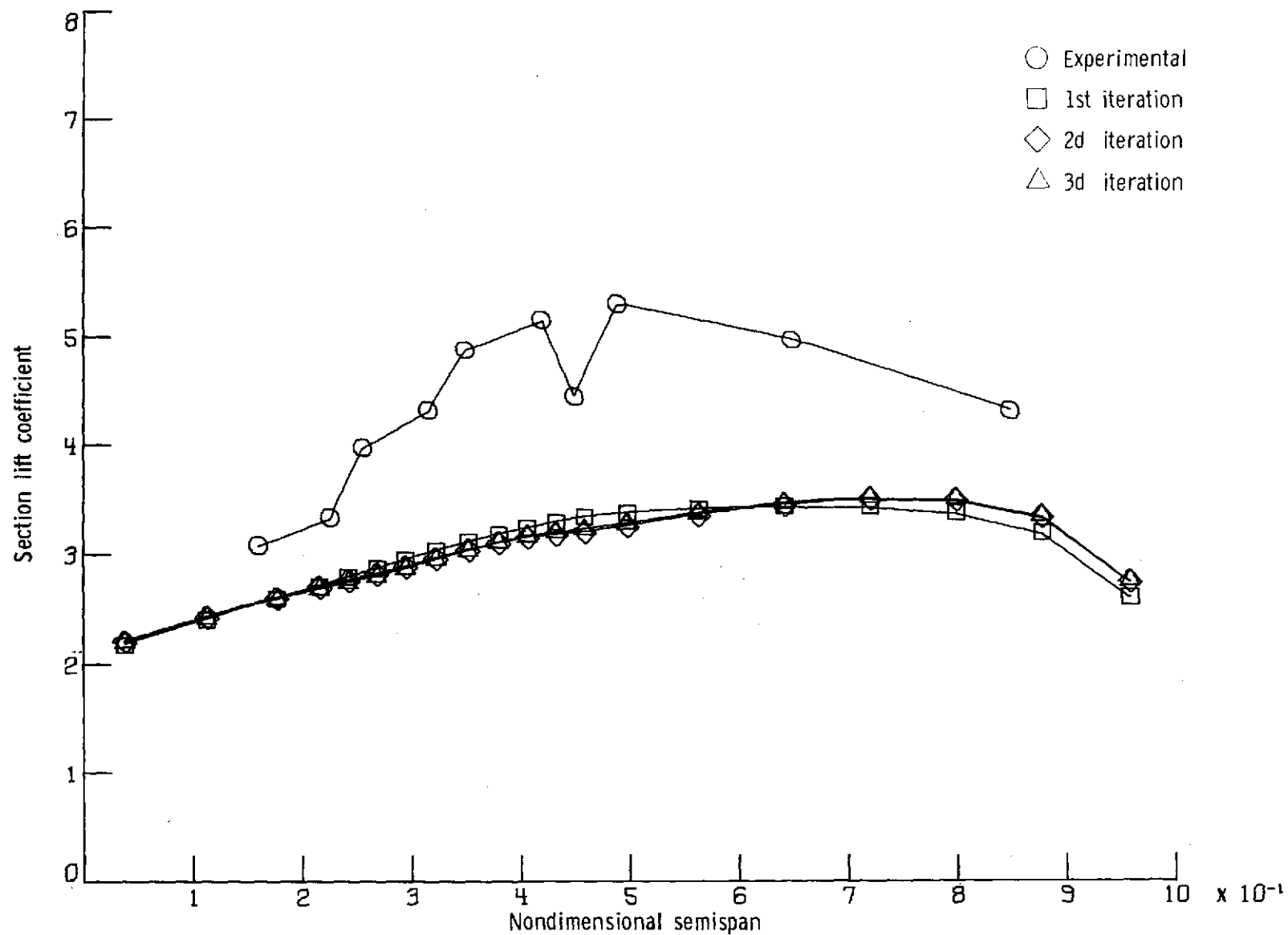
(c) Flap. $C_{\mu} = 2.2$; $\alpha = 4^{\circ}$.

Figure 22. - Continued.



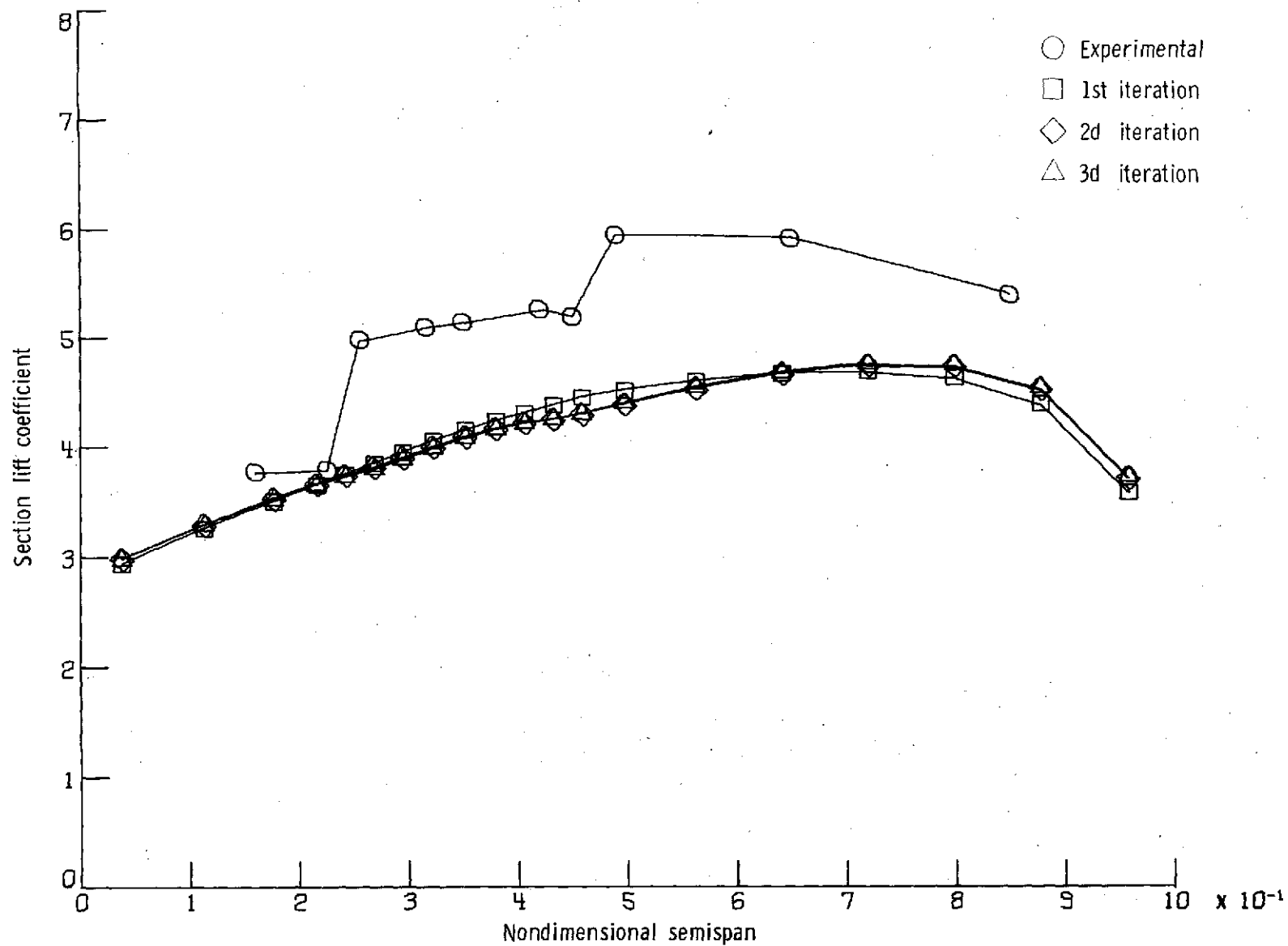
(d) Flap. $C_{\mu} = 2.2$; $\alpha = 16^{\circ}$.

Figure 22.- Continued.



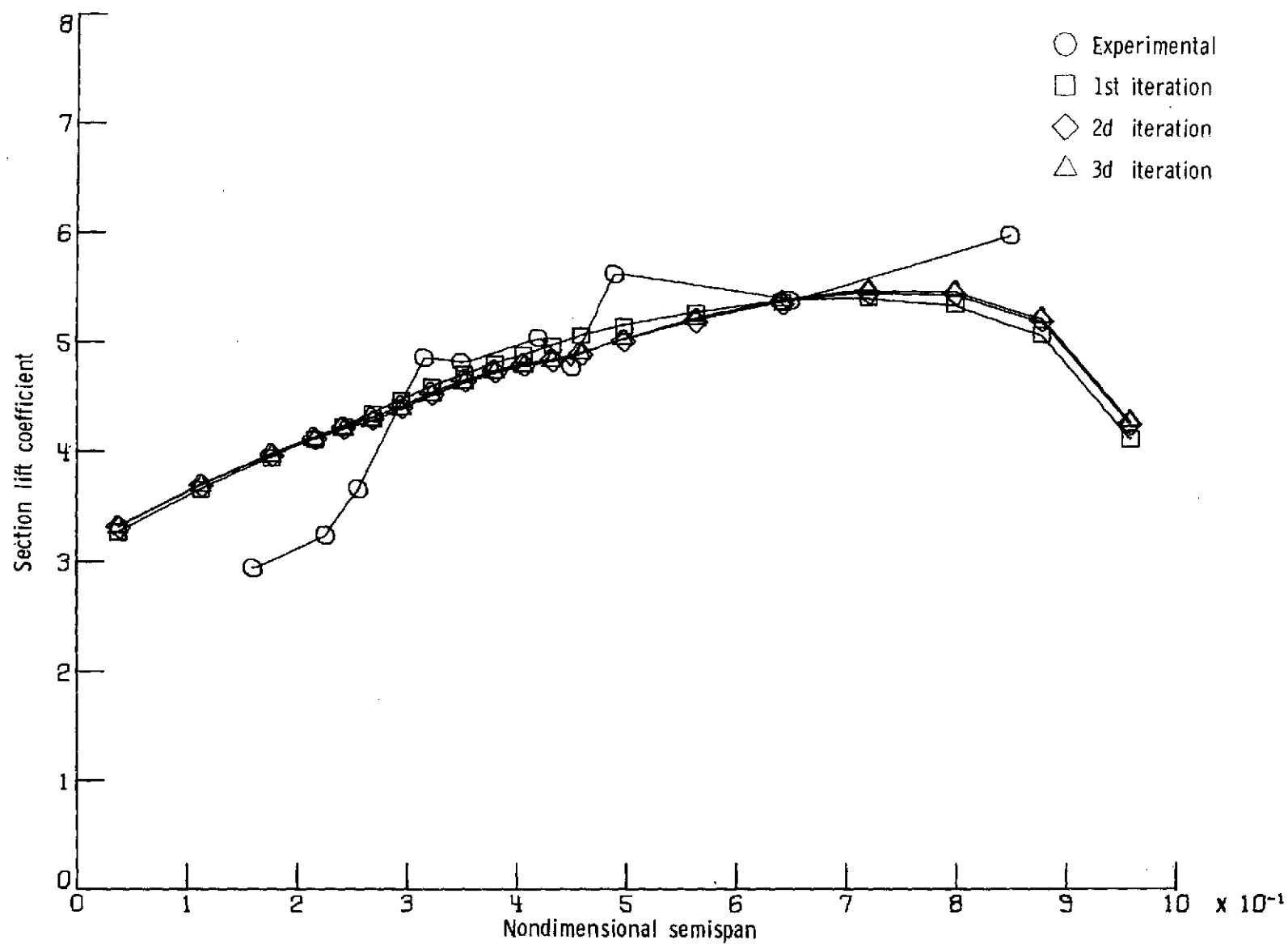
(e) Wing. $C_{\mu} = 4.0$; $\alpha = 40^\circ$.

Figure 22.- Continued.



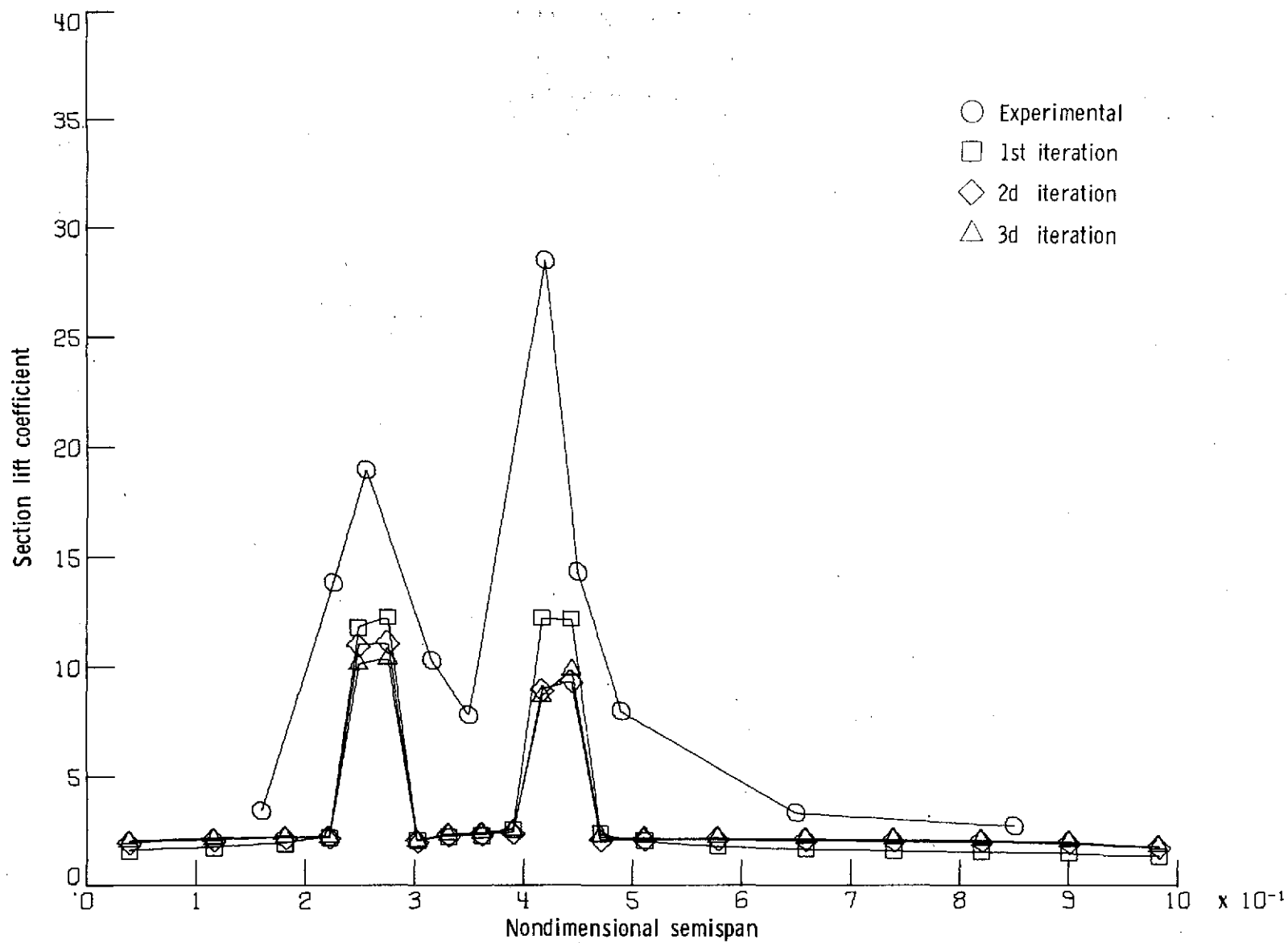
(f) Wing. $C_{\mu} = 4.0$; $\alpha = 16^{\circ}$.

Figure 22. - Continued.



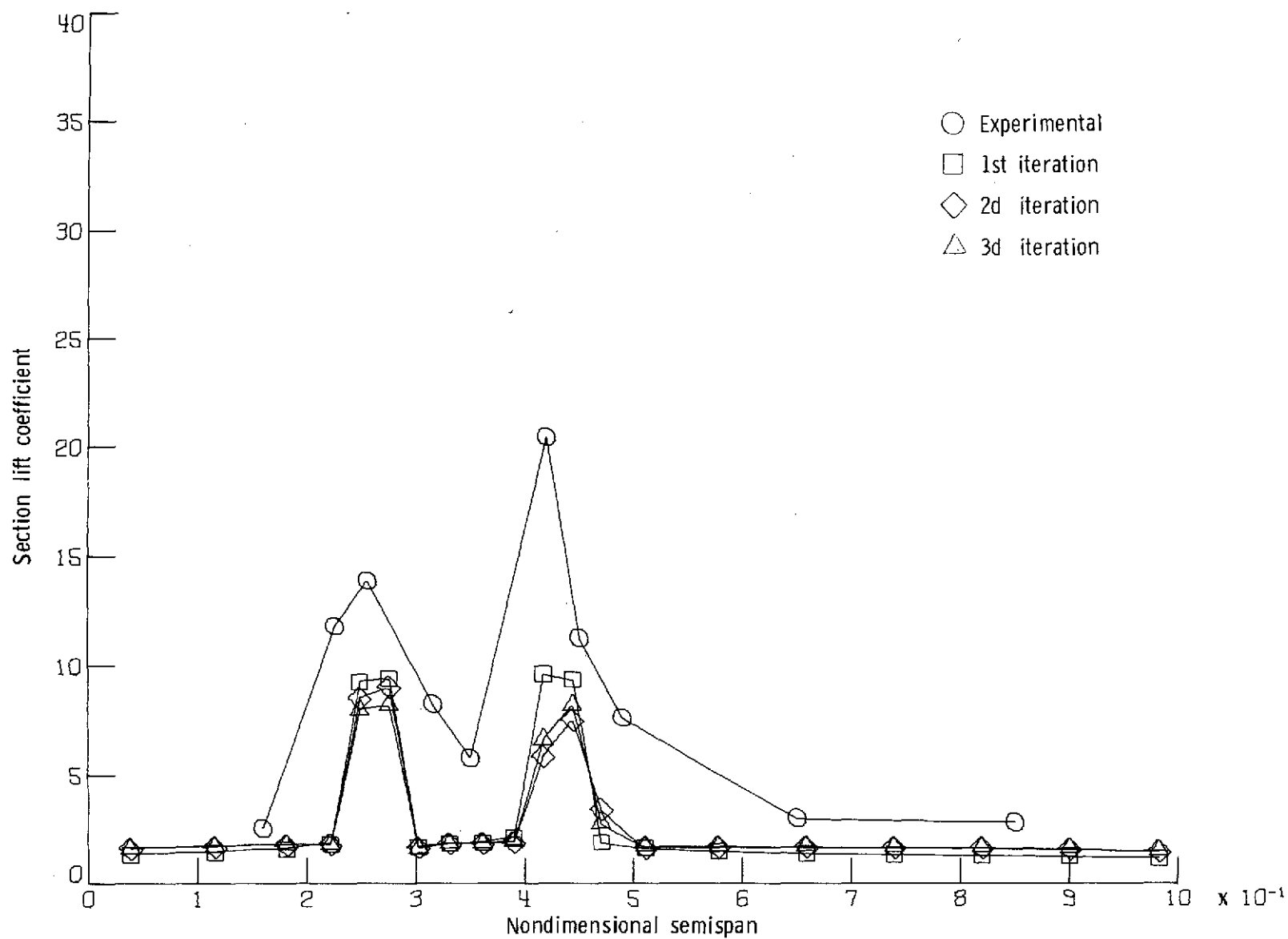
(g) Wing. $C_{\mu} = 4.0$; $\alpha = 24^{\circ}$.

Figure 22. - Continued.



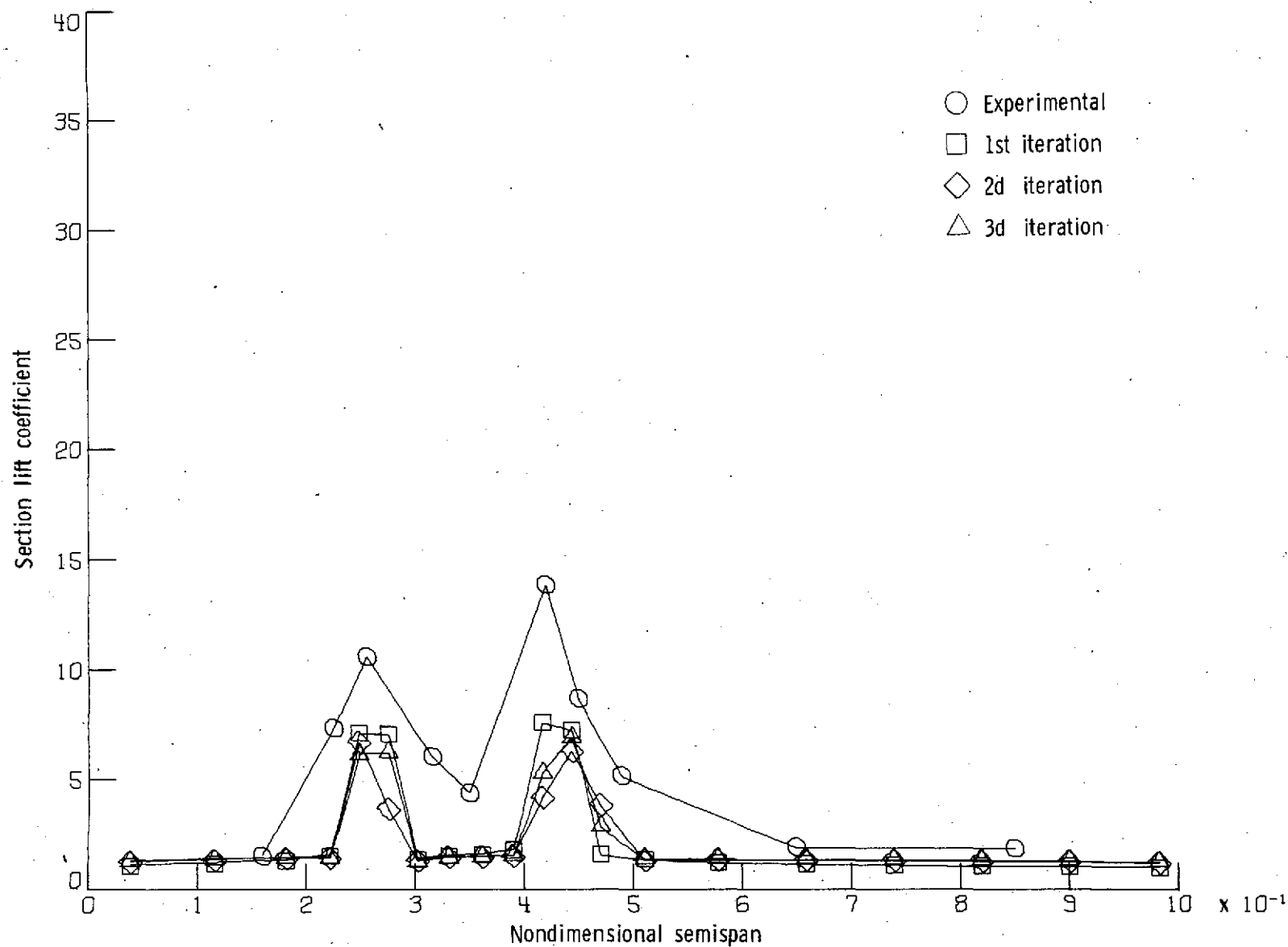
(h) Flap. $C_{\mu} = 4.0$; $\alpha = 4^{\circ}$.

Figure 22. - Continued.



(i) Flap. $C_{\mu} = 4.0$; $\alpha = 16^{\circ}$.

Figure 22. - Continued.



(j) Flap. $C_{\mu} = 4.0$; $\alpha = 24^{\circ}$.

Figure 22.- Concluded.